Department of School of Medicine and Surgery
University of Milano-Bicocca

Executive PhD Program in Neuroscience
Cycle XXXVI

Explorative and Descriptive Analysis of Differential Diagnosis with Nerve Magnetic Resonance Imaging (MRI) in Patients with Neuromuscular Diseases: Subgroup Study of Patients with Parsonage-Turner Syndrome (PTS)

Surname MAIONE Name MELANIA

Registration number 734069

Tutor: Prof. Guido Cavaletti

Co-tutor: Prof. Simonetta Gerevini

Coordinator: Prof. Rosa Maria Moresco

ACADEMIC YEAR 2024/2025

SUMMARY

ABBREVIATIONS

AI - Artificial Intelligence
AIN - Anterior Interosseous Nerve
AR - Area of the Region of Interest
CIAP - Chronic Idiopathic Axonal Neuropathy
CIDP - Chronic Inflammatory Demyelinating Polyneuropathy
CMAP - Compound Muscle Action Potentials
CMV - Cytomegalovirus
CNS - Central Nervous System
CR - Cervical Radiculopathy
CRF - Case Report Form
CSA - Cross-Sectional Area
CTL - Healthy Controls
EBV - Epstein-Barr Virus
EMG - Electromyography
FSE - Fast Spin-Echo
HIV - Human Immunodeficiency Virus
LAC - Lateral Cutaneous Nerve of the Forearm
MED - Median Value of Measurements
ML - Machine Learning
MRI - Magnetic Resonance Imaging
MRN - Magnetic Resonance Neurography
MPR - Multi-Planar Reconstruction
NCS - Nerve Conduction Studies
NSAIDs - Nonsteroidal Anti-Inflammatory Drugs
PIN - Posterior Interosseous Nerve
PNIs - Peripheral Nerve Injuries
PNS - Peripheral Nervous System
PTS - Parsonage-Turner Syndrome
ROI - Region of Interest
SNAP - Sensory Nerve Action Potentials
US - Ultrasound

INTRODUCTION

The study of neuropathies has undergone a profound evolution from its nascent stages to contemporary advancements in neurobiology and clinical practice. The historical trajectory of neuropathies is marked by significant milestones that have shaped our current understanding and management of these complex disorders.

Parsonage-Turner syndrome (PTS) is a rare neurological disorder, also known as 'acute idiopathic brachial neuritis'; the patients show acute shoulder pain and/or progressive muscle weakness and paresthesia. The causative mechanism is not fully understood but viral and autoimmune processes have been suggested to play a role. Diagnosis is made by a combination of clinical history, electromyography (EMG) results, and imaging findings. EMG may show signs of acute denervation in the distribution of the brachial plexus, with the suprascapular nerve being most frequently affected. Magnetic resonance imaging (MRI) is a sensitive tool in demonstrating signal abnormalities in the shoulder musculature that reflect denervation, but in the early acute phase, the signal intensity of the muscles may be normal on MRI. MRI is also useful to detect structural abnormalities, such as spinoglenoid and suprascapular notch masses that may compress the nerve, and to rule out more common causes of shoulder pain.

MRI has revolutionized the field of neuropathology, offering unparalleled resolution and contrast in imaging soft tissues. The evolution of MRI technology, including the development of high-field magnets, advanced imaging sequences, and functional imaging techniques, has allowed for unprecedented visualization of neuropathic lesions. MRI's ability to delineate subtle structural changes in peripheral nerves has markedly improved diagnostic capabilities and facilitated better disease management. MRI's applications in the realm of peripheral neuropathies are vast and multifaceted. Its role extends from the initial diagnosis of neuropathic conditions to monitoring disease progression and evaluating treatment efficacy. MRI enables clinicians to assess the extent of nerve damage, identify underlying causes, and guide therapeutic strategies. The integration of MRI with other diagnostic modalities, such as electrophysiological testing and biochemical assays, has further enhanced the comprehensive evaluation of neuropathic disorders.

Advancements in MRI for the Evaluation of Peripheral Neuropathies

The evolution of MRI technology has been instrumental in enhancing the diagnostic process for peripheral neuropathies. Conventional MRI, although a breakthrough at the time of its introduction, offered limited visibility of peripheral nerves due to their small size and low contrast with surrounding tissues.

MRI is instrumental in offering detailed insights into the location and pathology of neuropathies affecting large fibers. These imaging modalities can complement clinical and electrophysiological assessments. MRI has advanced with techniques like neurography, which uses T2-weighted sequences with fat suppression to evaluate nerve morphology, including nerve caliber, internal fascicular pattern, and perineurial-endoneurial fluid content. Recent technological advancements such as parallel imaging, coil design, and new pulse sequences, along with the availability of 3T MRI scanners, have led to the development of high-resolution peripheral nerve MRI. This includes 3D MRI, which allows for oblique and curved planar reconstructions, beneficial for studying deep

plexuses like the brachial and lumbosacral plexuses, which are less accessible with ultrasound (Gasparotti et al., 2017). However, the development of magnetic resonance neurography (MRN) addressed these limitations by employing T2-weighted sequences with fat suppression. This advancement allowed for detailed visualization of nerve morphology, including caliber, fascicular patterns, and the surrounding perineurial-endoneurial fluid (Lehmann et al., 2020).

CHAPTER 1

Parsonage-Turner Syndrome

1.1 The Disease

PTS, also known as neuralgic amyotrophy or brachial plexus neuritis, is a rare neurological disorder affecting peripheral nerves, characterized by the sudden onset of severe shoulder and upper arm pain, followed by significant muscle weakness or atrophy. Although identified in the mid-20th century, this condition remains a subject of ongoing research and debate regarding its pathogenesis, diagnostic strategies, and treatment protocols. The estimated incidence of PTS is between 1 and 3 cases per 100,000 people annually. The condition tends to affect men more frequently than women, with no specific age group preference. However, a bimodal distribution pattern has been observed, with peaks in young adults and those around middle age. PTS affects individuals of all races and ethnicities, indicating a worldwide distribution. While clear risk factors have not been identified, certain events are known to trigger the onset of the syndrome (Meneses do Rego & Araujo-Filho I., 2024).

Clinically, PTS presents with a sudden onset of acute pain in the shoulder area, which may radiate down the arm and hand. The pain is often described as severe, sharp, or throbbing, intense enough to disrupt sleep, and may last for days or even weeks before gradually resolving. After this initial phase, patients typically develop muscle weakness, which can progress to atrophy, as well as sensory disturbances, primarily affecting the proximal muscles of the arm.

Despite ongoing research, the exact mechanisms underlying PTS are not fully understood. It is hypothesized that PTS may result from an immune-mediated inflammatory response that affects the brachial plexus, a network of nerves responsible for controlling the shoulder and arm muscles. This autoimmune response may be triggered by viral infections, surgical procedures, vaccinations, or strenuous physical activity. Additionally, recent studies have explored the possibility of a genetic predisposition, with familial cases suggesting that certain inherited traits may increase susceptibility to nerve inflammation.

Diagnosing PTS can be challenging due to the sudden onset and variability of symptoms, which may easily be mistaken for other neurological conditions. Diagnosis is primarily clinical, based on the patient's history and physical examination findings. However, tests such as EMG and nerve conduction studies can provide essential information about nerve involvement and help rule out other potential differential diagnoses. Recent advances in imaging, particularly MRI and ultrasound, have significantly improved the ability to visualize inflammatory

changes in the brachial plexus, allowing for a more precise diagnosis (Meneses do Rego & Araujo-Filho I., 2024).

The treatment of PTS is largely symptomatic, aimed at pain relief and promoting functional recovery. In the acute phase, pain is managed with nonsteroidal anti-inflammatory drugs (NSAIDs), corticosteroids, or, in more severe cases, opioid analgesics. Once the acute pain subsides, physical therapy becomes crucial to prevent muscle atrophy and maintain joint mobility. In more severe cases with significant muscle deficits or complications, surgical intervention may be considered.

The prognosis for PTS varies widely among patients. Many experience spontaneous significant recovery, with improvement in muscle strength within the first two years of onset. However, a portion of patients may continue to experience residual muscle weakness, sensory disturbances, or chronic pain. Early intervention and targeted rehabilitation are crucial to improving long-term outcomes and enhancing quality of life (Meneses do Rego & Araujo-Filho I., 2024).

1.2 Etiology and Pathophysiology

As we said, PTS is traditionally described as a condition characterized by the sudden onset of severe, constant pain in the shoulder girdle, usually unilateral. This pain often radiates to the trapezius region, upper arm, forearm, and hand. A distinctive feature of the pain is that it is not positional, tends to worsen at night, and frequently causes sleep. Typically, no associated constitutional symptoms such as fever or fatigue are present.

PTS generally progresses through three distinct stages, each characterized by specific symptoms and clinical manifestations.

The first stage, known as the acute pain phase, is marked by the sudden onset of severe, debilitating pain that typically affects one shoulder. This pain is often described as extremely intense and can last from a few days to several weeks. The duration of this stage can significantly impact the overall recovery time: the longer the pain persists, the longer the recovery may take. During this period, the patient tends to limit the use of the affected limb due to the intensity of the pain.

In the second stage, as the pain begins to subside, muscle weakness emerges, revealing the neurological damage caused by the syndrome. This stage is characterized by weakness in the muscles of the shoulder and arm and may also lead to muscle atrophy, a loss of muscle mass due to nerve inactivity. This phase can last from 6 to 18 months, though in some cases it may extend even longer, depending on the severity of the nerve damage and the patient’s capacity for recovery.

In the third stage, the affected muscles start to regain strength and function, although the recovery process can be slow and drawn out, lasting months or even years. Some patients may fully recover muscle strength, while others may experience permanent deficits, such as reduced strength or mobility. The success of recovery largely depends on the extent of nerve damage and the timeliness of rehabilitation treatment.

The pain in PTS is almost always self-limiting, with a duration typically ranging from one to two weeks, though in rare cases, it can persist for longer periods. Muscle weakness, however, does not appear immediately but tends

to develop gradually, from a few days to several weeks after the initial onset of pain. Sensory deficits are less common but, when present, can vary in prevalence. Some studies report sensory deficits in 66% of patients, while other research indicates they occur in only a minority of cases (Feinberg & Radecki, 2010).

In many patients, the loss of strength is not immediately noticeable due to the inhibition of movement caused by debilitating pain. Additionally, muscle weakness may go unnoticed when it affects muscle groups that are difficult to assess manually, such as the serratus anterior or supraspinatus. However, within a month, the weakness typically becomes more apparent, and signs of muscle atrophy may appear. Scapular winging is a characteristic sign in cases where the long thoracic nerve, which innervates the serratus anterior, is involved. However, this sign may not be immediately recognized, especially if the physical examination is not conducted thoroughly.

Although PTS is largely based on specific clinical findings, some classic symptoms, such as constant and disabling pain lasting for 1-2 weeks, may not always be present in all cases, which can make the diagnosis more challenging and delay the initiation of appropriate treatment. Therefore, PTS should always be considered in patients presenting with acute, sudden-onset shoulder girdle pain, especially in the absence of other systemic symptoms (Feinberg & Radecki, 2010).

The exact etiology of PTS remains elusive, though current research suggests that it is often triggered by immune-mediated dysregulation. A common feature in many cases is the occurrence of a precipitating event, particularly post-infectious triggers, where the immune system appears to become dysregulated following an infection. Among the most frequently associated infections are upper respiratory tract infections, which are believed to set off an immune response that damages the peripheral nerves. Specific pathogens linked to PTS include Cytomegalovirus (CMV), Human Immunodeficiency Virus (HIV), Epstein-Barr Virus (EBV), Parvovirus B19, Campylobacter, and Yersinia. Additionally, Hepatitis E Virus has also been identified as a potential trigger, highlighting the syndrome's association with a broad range of viral and bacterial infections (Al Hinai et al., 2024).

Beyond infectious causes, research indicates that genetic and mechanical factors may also play a role in the development of PTS. A higher recurrence rate has been observed among athletes, suggesting that physical strain and mechanical stress on the nerves could act as contributing factors. Genetic predisposition is another area of growing interest, with familial cases of PTS reported, indicating that hereditary traits may influence susceptibility to nerve inflammation and dysfunction (Al Hinai et al., 2024).

1.3 Epidemiology

The epidemiology of PTS highlights both its rarity and the variability in clinical presentations. Recent studies estimate an incidence of approximately 0.34 per 1000 individuals, underscoring the uncommon nature of this condition. While earlier literature suggested a higher prevalence in men, more recent investigations have shown a slight predominance in women.

One significant aspect of PTS is its correlation with hand dominance. Most patients are right-handed, and 58%

of cases involve the dominant upper limb. This finding suggests that repetitive use or increased strain on the dominant limb may contribute to the vulnerability for developing the syndrome (Milner et al., 2016).
Additionally, a triggering event was identified in around 42% of cases, with a substantial portion of these related to surgical procedures. This supports the hypothesis that traumatic events or surgeries may play a role in the onset of PTS. However, a significant percentage of patients (29%) present without the typical neuropathic pain, reflecting the diversity and atypical nature of clinical presentations associated with the syndrome.
In terms of nerve involvement, PTS frequently manifests with involvement of the anterior interosseous nerve (AIN) or posterior interosseous nerve (PIN), highlighting a trend that does not always emerge clearly in traditional literature on PTS.
Finally, the rate of complete recovery is relatively low: only 44% of patients fully recover, with an average recovery time of approximately 10 months. These findings indicate that, compared to earlier studies that reported more favorable outcomes, the prospects for complete recovery are more complex. This emphasizes the need for greater attention to developing effective early diagnosis and treatments and long-term management strategies for PTS patients (Milner et al., 2016).

1.4 Risk Factors

PTS manifests in two primary forms: idiopathic and hereditary, each with distinct causes and mechanisms.
The *idiopathic form*, which is more common, has an unclear etiology, though several risk factors have been identified as potential triggers. Various infections (between 25% and 55%), including viral, bacterial, and parasitic, such as HIV, mumps, parvovirus B19, and SARS-CoV-2, are often linked to the syndrome's development. In addition to infections, surgical procedures and certain invasive medical interventions seem to act as potential triggers, likely due to the inflammatory or autoimmune response activated following such events. Vaccinations, though rarely, have also been associated with PTS, as seen in a few rare cases involving COVID-19 vaccines. Despite these cases, the medical community continues to emphasize that the benefits of vaccinations far outweigh the risks of complications, including PTS. Other possible triggers include physical trauma, especially in the shoulder and arm areas, as well as physiological conditions such as childbirth, which can cause significant bodily stress and contribute to the syndrome's onset. Vigorous exercise is another risk factor, likely due to mechanical stress or repeated microtrauma affecting the nerves. Lastly, pre-existing conditions such as Ehlers- Danlos syndrome, systemic lupus erythematosus, and temporal arteritis, which involve systemic inflammation or connective tissue dysfunction, seem to increase vulnerability to developing PTS (Santhakumar, 2022).
The *hereditary form* of PTS, in contrast, is linked to genetic mutations. Approximately 85% of hereditary PTS cases are associated with a variation in the SEPT9 gene, which is responsible for producing septins, proteins that play a crucial role in various cellular processes, including cell division and maintaining the cytoskeleton structure. The mutation in this gene impairs septin functionality, increasing the nerves' susceptibility to damage and inflammation. In patients with hereditary PTS, episodes of muscle weakness and atrophy tend to recur over

time, often with an earlier onset compared to the idiopathic form. Additionally, a familial predisposition to the condition has been observed, with an increased risk for family members. As a result, genetic counselling becomes an important option for families with a history of PTS (Santhakumar, 2022).

1.5 Diagnosis and Treatment

The diagnosis of PTS begins with a detailed clinical assessment of symptoms and a thorough physical examination by an experienced physician. The classic presentation includes sudden, acute shoulder pain followed by progressive muscle weakness, which directs the clinician toward a potential diagnosis of PTS. However, since PTS can manifest in atypical ways, it is essential to use specific diagnostic tools to confirm the diagnosis and identify the nerves involved (Feinberg & Radecki, 2010).

MRI allows for detailed visualization of nerves and related structures, revealing potential inflammation or structural abnormalities in the brachial plexus, which is frequently affected in PTS. This type of imaging is helpful in distinguishing PTS from other neurological conditions, such as brachial plexopathies due to compression or nerve trauma. Ultrasound may also be used to evaluate peripheral nerves, particularly those near the surface. While less detailed than MRI for deep structures, ultrasound is a quick and accessible tool useful for monitoring PTS progression or examining specific nerves in real time.

The treatment of PTS primarily focuses on managing symptoms and supporting functional rehabilitation, as there is no specific cure for the condition. Since PTS tends to resolve on its own over time, therapy aims to alleviate acute pain and prevent long-term complications such as muscle weakness and atrophy.

To further reduce pain and limit movement of the affected limb, shoulder immobilization with the use of a brace or stabilizer may be recommended. This approach helps prevent movements that could aggravate the pain.

When the pain subsides, usually after a few weeks, the focus shifts to restoring muscle function and preventing atrophy. Physical therapy becomes crucial at this stage. A physical therapist specialized in neuromuscular rehabilitation will develop a specific exercise program to improve the strength and flexibility of the affected muscles. Stretching exercises help prevent joint stiffness, while strengthening exercises aim to recover muscle strength lost due to inactivity and nerve damage.

PTS patients may also be treated with specific analgesic medications for neuropathic pain, known as co-analgesics. These include gabapentin, pregabalin, carbamazepine, and amitriptyline, which are frequently used to reduce nerve-related pain. These drugs modulate nerve signal activity and can help relieve burning or tingling sensations that some patients experience during recovery.

In more severe cases of PTS, where nerve damage is significant and functional deficits persist despite conservative therapies, it may consider surgery. Surgical options include advanced techniques such as nerve grafting, in which a healthy nerve segment is taken from another part of the body to replace the damaged nerve. Alternatively, tendon transfers may be indicated to restore muscle function in the affected areas. These procedures are generally considered only when spontaneous recovery is limited, and symptoms are debilitating.

1.6 Differential Diagnosis with Other Neuropathies

Differentiating PTS from other neuropathies is challenging due to its overlapping symptoms with various conditions such as cervical radiculopathy (CR), brachial plexopathy, diabetic neuropathy, entrapment neuropathies and other inflammatory neuropathies. While PTS presents with sudden, severe pain and localized motor deficits, it typically lacks sensory involvement, in contrast to CR, which often causes radicular pain, sensory loss in a dermatomal distribution, and weakness corresponding to the affected nerve root. Brachial plexopathy, another major consideration, shares similarities in its clinical presentation but usually results from trauma or malignancy and may involve additional nerve roots beyond those typically affected in PTS. MRI plays a key role in differentiating these conditions, with PTS showing distinct multifocal T2-weighted hyperintensities along the involved nerves, indicative of inflammation and edema, whereas CR and brachial plexopathy typically do not show these features. Diabetic neuropathy, often presenting with distal sensory and motor impairments, is less likely to mimic PTS because it affects the lower limbs and involves a more gradual onset of symptoms. However, distinguishing between diabetic amyotrophy and PTS can be difficult, particularly in patients with concurrent diabetes, as both can present with sudden severe pain and muscle weakness (Kong et al., 2023, Patel et al., 2022). Additionally, entrapment neuropathies, such as carpal tunnel syndrome, may mimic some motor features of PTS, but these typically have a chronic, insidious onset with sensory involvement, contrasting with the rapid progression and motor predominance seen in PTS. Electrophysiological studies further aid in differentiation, as PTS typically reveals axonal damage and denervation with fibrillation potentials, whereas entrapment neuropathies and radiculopathies show conduction block or root compression without significant axonal degeneration (Song et al., 2023). Recent case reports also highlight the growing recognition of immune-mediated and viral triggers, such as those seen in COVID-19, as potential etiologies for PTS, complicating the differential diagnosis with other viral or post-viral neuropathies (Huang et al., 2023, Zhang et al., 2022).

1.7 Relevance of Differential Diagnosis of Peripheral Neuropathies

The recognition of specific clinical patterns is crucial in establishing a diagnostic pathway for patients presenting with signs and symptoms of peripheral neuropathy. A complete diagnostic process requires a thorough medical history and a detailed clinical examination. Our framework identifies five main clinical patterns, each with distinct features that can guide the clinician towards an accurate and targeted diagnosis. However, it is important to note that these subtypes should not be considered rigid or mutually exclusive, as overlapping neuropathic patterns are common.

• Slowly progressive, symmetric distal, predominantly sensory neuropathy. This is the most common subtype, often associated with metabolic conditions (such as diabetes), chronic alcohol use, or neurotoxic drugs (such as chemotherapy). In these patients, a limited diagnostic process is usually sufficient unless atypical neuropathy signs emerge. In the absence of identifiable causes, the diagnosis may lean towards chronic idiopathic axonal neuropathy (CIAP), which generally has a benign course. CIAP is usually non-progressive and has a low impact

on quality of life (Lehmann et al., 2020).

• Long-standing progressive neuropathy with muscle atrophy and foot abnormalities. This pattern, characterized by predominant motor involvement, typically begins in childhood or early adulthood and may be associated with hereditary neuropathies. The patient presents with muscle atrophy and foot deformities, such as claw toes. Diagnosis should be guided by genetic testing, as these neuropathies can be linked to specific genetic mutations (e.g., Charcot-Marie-Tooth).

• Subacute onset neuropathy and/or proximal involvement. Patients in this subtype exhibit clinical signs suggesting an acquired immune-mediated condition, such as chronic inflammatory demyelinating polyneuropathy (CIDP). In these cases, a more in-depth diagnostic process, including antibody tests (anti-ganglioside, anti-MAG, etc.), is necessary. These patients often require immunosuppressive therapies, and the response to treatment can be a significant diagnostic clue (Lehmann et al., 2020).

• Rapidly progressive neuropathy with multifocal symptoms, neuropathic pain, and autonomic dysfunction. This clinical pattern may be associated with serious conditions such as vasculitis, amyloidosis, or paraneoplastic syndromes. A comprehensive set of diagnostic tests, including serological tests for inflammatory and autoimmune markers, is essential. The rapid progression of the clinical picture requires prompt intervention to prevent irreversible damage. In this context, nerve biopsy may be crucial to confirm a diagnosis of vasculitis neuropathy.

• Sensory ataxic neuropathy. This pattern is characterized by loss of proprioception and vibration sense, with relatively spared muscle strength. Conditions such as Sjögren's syndrome or paraneoplastic neuropathy should be ruled out through specific tests. A thorough family history may point to a possible hereditary cause, such as POLG1 gene mutations involved in mitochondrial disorders. The absence of sensory nerve action potentials (SNAP) with normal motor nerve action potentials is typical of this subtype (Lehmann et al., 2020).

A detailed medical history and the timeline of symptom onset are essential to framing the type of neuropathy. Most peripheral neuropathies have a chronic, progressive course (pattern #1), but acute or subacute onset may indicate inflammatory or immune-mediated neuropathies (patterns #3 to #5), such as Guillain-Barré syndrome or CIDP. The presence of skeletal deformities and muscle atrophy, as seen in pattern #2, suggests hereditary neuropathy. Signs of autonomic dysfunction, such as night sweats or tachycardia, may indicate neuropathy associated with amyloidosis or diabetes.

A neurological evaluation helps to define the involvement of different nerve fibers (motor, sensory, autonomic) and the distribution of symptoms. Most neuropathies are sensory or sensorimotor. A purely or predominantly motor pattern is observed in clinical patterns #2 and #3. It is important to differentiate neuropathies from conditions that may mimic their symptoms, such as distal myopathies or spinal muscular atrophy. The presence of autonomic symptoms is a key feature in pattern #4 and may indicate diabetic neuropathy or amyloidosis. Nerve conduction studies (NCS) and EMG are essential diagnostic tools to confirm the presence of peripheral neuropathy and differentiate between axonal and demyelinating neuropathies. Axonal neuropathies are typically recognized by the reduction of compound muscle action potentials (CMAP) and SNAP, whereas

demyelinating neuropathies show slowed nerve conduction velocities and prolonged distal motor latencies (Lehmann et al., 2020). Laboratory tests should be tailored according to the clinical pattern. In patterns #1 and #2, basic tests such as blood glucose, HbA1c, vitamin B12, and serum protein levels are usually sufficient. In pattern #3, more specific tests, such as anti-ganglioside antibodies, may be required. In pattern #4, serology for vasculitis and immune-mediated neuropathies is essential. Genetic testing is also indicated in the presence of suspected hereditary neuropathies, especially in patterns #2 and #5. Nerve biopsy is indicated in selected cases, especially when inflammatory or vasculitic neuropathy is suspected (pattern #4). Ultrasound of the nerves can be used to assess nerve thickening, characteristic of some immune-mediated or hereditary neuropathies such as CMT1A (Lehmann et al., 2020).

CHAPTER 2
Magnetic Resonance Imaging

2.1 Magnetic Resonance Imaging in Clinical and Research Contexts

Peripheral nerve pathology may occur secondary to a variety of etiologies, including mechanical entrapment, compression by external factors, trauma, infectious and inflammatory causes, neoplasms, or as a complication of surgery. Clinical evaluation often begins with a detailed history and focused physical examination and may include electrodiagnostic studies or advanced imaging. With recent innovations in MRI techniques, high-resolution MRI of peripheral nerves is possible and is often referred to as "MR neurography." MR imaging can demonstrate both primary signs of nerve injury and secondary signs such as muscle denervation.

In this research, PTS has been extensively evaluated using both qualitative and quantitative measurements. Qualitative techniques, such as the 3D Nerve Cube, assess nerve root pathology, distinguishing between unilateral and bilateral involvement. Specific imaging sequences, such as STIR (Short Tau Inversion Recovery), are used to identify edema, an indicator of inflammation, while T1-weighted imaging detects adipose infiltration and nerve root atrophy. These imaging modalities are crucial as PTS is known to have an inflammatory basis. In addition to qualitative methods, quantitative measurements also utilize the 3D Nerve Cube technique, alongside T2-weighted images (axial and coronal), to measure the cross-sectional area (CSA) of each nerve root in affected individuals. One significant advantage of MRI is its ability to detect signs of muscle denervation and nerve injury much earlier than EMG. MRI can reveal muscle edema within days of an injury, while EMG may not show significant changes until several weeks later. This early detection is vital in PTS, as it enables prompt intervention, which may lead to improved patient outcomes. Additionally, MRI’s capacity to distinguish between acute and chronic injuries further aids in tailoring appropriate therapeutic strategies (Gilcrease-Garcia et al., 2020).

The Use of MRI

Peripheral nervous system (PNS) is essential for transmitting commands from the central nervous system (CNS) to the rest of the body, including sensory organs and muscles. Peripheral nerves are organized into bundles,

protected by layers of connective tissue, such as the epineurium, perineurium, and endoneurium, which provide structure and insulation. Nerve fibers can be either myelinated, with a myelin sheath that speeds up the transmission of electrical signals, or unmyelinated, which conduct signals more slowly. One of the main strengths of MRI is its ability to precisely visualize morphological changes in peripheral nerves, thanks to its high contrast and image resolution. This is especially useful for identifying lesions such as demyelination, axonal degeneration, or inflammation, which often cannot be detected with other diagnostic tools. Moreover, MRI allows the examination of nerves located deep within tissues, such as proximal nerves (near the trunk), which are difficult to access with methods like NCS or ultrasound (Chen et al., 2019).

Familiarity with the MRI features of PTS is critical for radiologists because they may be the first to suggest the diagnosis. In a study that involved 26 patients with PTS published in 2012 by Scalf et al., it found the largest reported series describing the imaging features of PTS to date via MRI findings. The study patients included 20 males (77%) and six females (23%). The median age at diagnosis was 45 years (range, 8-77 years). Clinical symptoms were on the right side for 12 patients (46%), on the left side for 12 patients (46%), and bilateral for two patients (8%). Clinical symptoms were isolated pain, weakness, or numbness (or a combination of the three). The most common clinical presentation was pain and weakness (11 patients [42%]). Males are predominantly affected, with male-to-female ratios ranging from 2:1 to 11.5:1. Treatment was palliative and includes analgesics for pain and physical therapy for weakness.

MRI had been an important imaging tool for establishing the diagnosis of PTS, also to exclude more common causes of shoulder pain such as rotator cuff tear, impingement syndrome, or labral tear, MRI is sensitive for the detection of signal abnormalities in the shoulder girdle musculature that are related to denervation. It also provides an advantage for excluding structural abnormalities that may cause similar denervation changes in rotator cuff musculature such as a rotator cuff tear or spinoglenoid and suprascapular notch masses. In addition, MRI findings indicative of muscle atrophy, including evidence of fatty infiltration and decrease in muscle bulk, were identified more frequently when compared with previous studies. The latter findings are likely related to the relative delay between the onset of symptoms and the MRI examination.

Advantages of MRI

The key benefits of MRI encompass its safety - due to the absence of ionizing radiation - its exceptional ability to differentiate soft tissues, its capability for multi-planar imaging, and the high-quality images produced that remain unaffected by surrounding bone or air. These features render MRI an indispensable tool for diagnosing a wide array of medical conditions while providing a non-invasive alternative to other imaging techniques (Vaskovic, 2023). Otherwise, MRI plays a fundamental role in disease management, providing detailed information on function, and functioning of electrically active medical devices, leading to failures in delivering necessary therapies.

CHAPTER 3

Other Methods

3.1 Ultrasound

Peripheral nerve injuries (PNIs) present with diverse etiologies and clinical manifestations, ranging from compression and ischemia to trauma and inflammation. Accurate diagnosis and tailored treatment - ranging from conservative management to surgical intervention - require precise localization and characterization of the injury. While PNIs are more frequently observed in the upper limbs, particularly affecting the median, radial, and ulnar nerves, subtle presentations can complicate clinical assessment (Dong et al., 2023).

Ultrasound (US) has emerged as a powerful, non-invasive imaging modality in the evaluation of PNIs. Compared to MRI, ultrasound offers real-time, high-resolution visualization of superficial nerves, is more cost-effective, and avoids the need for contrast agents or sedation - making it especially advantageous in pediatric and perioperative settings. High-frequency probes allow for detailed imaging of nerve fascicles, epineurium, and perineural structures. Moreover, color and power Doppler imaging enable assessment of microvascular perfusion, which varies with the stage and severity of nerve injury.

In the context of PTS, ultrasound plays a complementary role to MRI and EMG. While MRI remains superior for evaluating deep structures and muscle denervation, ultrasound excels in identifying focal nerve swelling, neuromas, and perineural fibrosis. It can also guide interventions and monitor nerve recovery over time. In PTS, ultrasound may detect enlargement or hypoechoic changes in affected nerve roots or branches, particularly in the supraclavicular region, and can be used to assess associated muscle atrophy or fat infiltration. Quantitative ultrasound, including CSA measurements and elastography, is increasingly used to assess nerve stiffness and structural integrity. These techniques, when combined with clinical and electrophysiological data, enhance diagnostic confidence and may help differentiate PTS from other causes of brachial plexopathy.

3.2 Electromyography

A key step in the diagnostic process is EMG, which measures the electrical activity in muscles and nerves to detect signs of denervation and axonal damage, typical of PTS. This test allows the identification of abnormalities in affected muscles, even when clinical signs are not yet evident. It is important that EMG is performed meticulously, testing not only the suspected muscles but also those that might appear normal, as PTS can affect muscles asymmetrically or without clear symptoms in all involved areas (Feinberg & Radecki, 2010).

In addition to EMG, nerve conduction studies are often conducted to evaluate the function of peripheral nerves. However, since PTS primarily affects the proximal muscles of the upper limb, the results of these tests may appear normal, making it difficult to identify abnormalities in routine sensory and motor nerves. In such cases, examining specific sensory nerves, such as the lateral cutaneous nerve of the forearm (LAC), often involved in PTS, is useful. A significant decrease in the sensory amplitude of the LAC, especially when compared to the unaffected side, can provide a critical diagnostic clue. Beyond electrodiagnostic testing, advanced imaging plays a significant role in confirming PTS.

CHAPTER 4

Research Questions

4.1 Research Overview and Rationale

The proposed study adopts a descriptive analysis approach, leveraging an existing comprehensive database of patients diagnosed with neuropathies, with a final selection of those with PTS. The primary objective is to explore potential correlations among clinical variables (such as pain and muscle weakness), neurophysiological findings, and imaging findings. By integrating clinical presentation with EMG results and qualitative MRI data, the study aims to evaluate the role of MRI in both confirming and completing the diagnosis of PTS.

Particular attention will be given to detecting MRI abnormalities in muscles typically affected by PTS, such as the supraspinatus and infraspinatus. The study hypothesizes that MRI may reveal signs of disease -including muscle edema, fat infiltration, and atrophy - prior to the emergence of overt clinical symptoms, suggesting a role for MRI as a sensitive early biomarker in the disease course.

Furthermore, the study will compare MRI quantitative parameters such as CSA and signal intensity between PTS patients and healthy controls. It is hypothesized that PTS patients, especially during the acute phase, will show increased CSA and T2-weighted signal intensity in affected nerve roots and muscle groups, reflecting underlying inflammatory processes. Ultimately, the integration of clinical, neurophysiological, and imaging data, particularly MRI, is expected to improve the diagnostic accuracy of PTS.

4.2 Specific Objectives for Parsonage-Turner Syndrome

The main goal of this research is to describe the clinical and neurophysiological correlations of PTS, with a particular focus on utilizing advanced imaging techniques to identify patterns of inflammation, nerve degeneration, and muscle changes. This comprehensive exploration will leverage two key types of measurements - qualitative and quantitative - through MRI sequences specifically tailored to examine the brachial plexus.

The *qualitative analysis* of the research aims to determine the pathological status of the nerve roots using STIR sequences, T1-weighted images, and the 3D cube nerve protocol. By systematically analyzing these qualitative aspects, the research aims to construct a detailed picture of the pathological changes occurring in the nerve roots, providing a basis for further investigations.

The *quantitative analysis* focuses on the nerve roots using the 3D Cube Nerve protocol, enabling a comparison of anatomical and pathological differences between PTS patients and healthy controls, as well as variability within the PTS patient population.

By combining these qualitative and quantitative measurements, the study aims to achieve following objectives:

- to identify specific patterns of nerve involvement, distinguishing between unilateral and bilateral pathology to understand how PTS manifests differently among patients;
- to correlate imaging findings with clinical outcomes, establishing relationships between

neurophysiology, imaging results, and clinical symptoms such as pain, muscle weakness, and functional impairment;

- to compare PTS patients with healthy controls using quantitative metrics of CSA and T2 values to examine differences between the two groups, elucidating physiological changes specific to PTS and revealing potential diagnostic markers.

In conclusion, this research aims to demonstrate that the combined use of advanced imaging techniques, such as the 3D Cube Nerve, can significantly enhance the understanding of the anatomical and functional changes associated with PTS, complementing and enhancing initial outcomes from clinic and EMG assessments. These qualitative and quantitative measurements are expected to offer valuable insights into the pathology of the condition and represent a crucial step toward more accurate, early diagnosis and monitoring.

4.3 Expected Clinical Applications

The expected clinical applications of this research are poised to bring substantial advancements in the diagnosis, monitoring, and treatment of PTS. By leveraging advanced MRI techniques such as the 3D Cube Nerve, it will be able to obtain a more detailed and accurate understanding of the structural and inflammatory changes in the affected nerve roots. This could refine current diagnostic practices, allowing for earlier and more precise detection compared to traditional methods like EMG and clinical assessments.

The integration of both qualitative and quantitative imaging measurements - such as CSA and T2 values - into the diagnostic process offers a comprehensive framework that complements clinical and neurophysiological evaluations. This approach not only enhances diagnostic accuracy but also enables more effective monitoring of disease progression and assessment of treatment response, using objective imaging markers rather than relying only on symptomatic reports.

Ultimately, this research holds promise not only for improving diagnosis and monitoring but also for shaping the future of PTS treatment and enhancing patient care through more individualized and data-driven approaches.

CHAPTER 5

Materials and Methods

5.1 Study Design: Description of the PTS Database and Healthy Controls with Measurements

A subgroup of neuroinflammatory pathologies was selected from a comprehensive database for in-depth analysis, focusing specifically on 54 observations related to PTS. After quality checks, one case was excluded due to inconsistencies between MRI and clinical data, and two follow-up records were merged with their corresponding initial entries. The final dataset includes 51 unique, retrospectively collected observations of PTS patients recorded between 2019 and 2024 at Papa Giovanni XXIII Hospital in Bergamo, Italy.

To support the analysis, a detailed Case Report Form (CRF) was developed to gather essential baseline characteristics, including demographic data (gender, age, race), clinical onset, and diagnostic information from

EMG and MRI records, such as test dates. This structured documentation enables accurate correlation between clinical findings and imaging results, contributing to a clearer understanding of the patient cohort.

The control group consists of 25 retrospectively collected observations from the same hospital and time frame. These individuals underwent MRI scans for unrelated conditions but were confirmed to have no neurological or muscular disorders. Their inclusion provides a reliable baseline for comparison with the PTS group, particularly in evaluating differences in quantitative MRI parameters. Careful selection and health status verification of these controls enhance the validity and reliability of the study's findings.

The primary analysis involves both qualitative and quantitative measurements to identify pathological characteristics of affected nerve roots and determine differences between PTS patients and healthy controls.

In the first phase, the 3D Cube Nerve tool is used to identify pathological nerve roots and evaluate whether the pathology is unilateral or bilateral. Detailed anatomical alterations of nerve roots associated with PTS are anticipated, specifically:

- identification of pathological nerve roots: utilizing the advanced 3D Cube Nerve protocol, this analysis systematically identifies pathological nerve roots in PTS patients, determining whether the pathology is unilateral or bilateral;
- evaluation of edema: T2-weighted STIR imaging in axial and coronal planes highlights edema within nerve roots and surrounding tissues, confirming PTS as an inflammatory condition;
- assessment of fat infiltration and atrophy: T1-weighted fast spin-echo (FSE) images in axial and coronal planes assess fat infiltration and muscular atrophy. PTS patients are expected to show muscle and tissue atrophy, indicating chronic nerve damage from prolonged denervation.

The qualitative phase provides a basis for understanding anatomical and pathological alterations in PTS patients, emphasizing inflammation's importance.

The second phase involves quantitative evaluation using the 3D Cube Nerve to measure specific nerve root parameters. Significant differences between PTS patients and healthy controls are expected:

- size of nerve roots: increased CSA in PTS patients' nerve roots compared to controls may indicate nerve inflammation, supporting structural changes in nerve roots associated with PTS;
- T2 Parameters: T2 measurements, the area of the region of interest (AR) and the median value (MED), are expected to show significant variations between PTS patients and healthy controls, suggesting differences in nerve tissue composition and hydration affecting pain function and sensation.

An exploratory quantitative analysis compares pathological and non-pathological nerve roots in PTS patients, aiming to elucidate differences and signals of inflammatory involvement even in normal-appearing nerve roots. Recent literature highlights the importance of understanding these distinctions for insights into PTS inflammatory processes (Smith et al., 2023; Johnson & Lee, 2022). Significant differences in CSA and T2 relaxation times between pathological and non-pathological nerve roots are anticipated, with increased CSA indicating edema and inflammation in affected roots, while non-pathological roots show normative values.

Elevated T2 values suggest ongoing edema in affected roots.

A well-defined control group of 25 healthy observations is pivotal for research integrity, providing a benchmark for assessing unique MRI findings associated with PTS and laying the groundwork for effective diagnostic and therapeutic approaches. In addition, exploring further analysis of a third cohort of individuals with inflammatory neuropathies alongside PTS patients and healthy controls could offer valuable insights into quantitative MRI differences, enhancing understanding of pathophysiological mechanisms and improving diagnostic accuracy. This systematic approach also lays the groundwork for future longitudinal and comparative studies within the broader context of neuroinflammatory disorders, potentially leading to standardized diagnostic criteria and ultimately supporting improved clinical decision-making and patient outcomes.

5.2 Data Collection: Clinic and Neurophysiological Assessments

The clinical records of patients were gathered from their medical records, which included details from prior assessments and consultations. This process involved a thorough review of documentations related to each patient's previous visits, capturing pertinent information that could provide insights into their condition. In addition to the historical data, specific signs and symptoms reported by the patients on the day of their MRI examination were also recorded. This real-time data collection is crucial, as it helps establish a clear picture of the patient's clinical presentation at the time of imaging.

Furthermore, EMG studies were carried out in close coordination with the onset of symptoms and the MRI procedures. Specifically, EMG and MRI were performed respecting the period of ~3 months from each other and ~6 months starting from the onset of patient's symptoms/signs and the execution of the exams. This quite simultaneous approach allowed for a more comprehensive assessment of the patients' neurological and muscular conditions, ensuring that the results of both diagnostic methods could be analyzed in conjunction to provide a more thorough understanding of the underlying pathologies.

An integrated diagnostic approach is essential when evaluating the timing of symptom onset in PTS. The scheduling of EMG and MRI plays a critical role, as early assessments may be less reliable due to the evolving nature of the syndrome. Since both EMG and MRI findings can change over time, aligning these studies with the clinical timeline is key to improving diagnostic accuracy. By correlating EMG and MRI results, the study aims to deepen the understanding of PTS pathophysiology. The inclusion of detailed clinical records, prompt symptom reporting, and synchronized EMG testing strengthens the dataset and enhances the reliability of the analysis.

5.3 Methods

MRI Machine for MRI Image Acquisition

Image quality plays a pivotal role in achieving the most accurate diagnoses for patients, particularly in complex cases involving neurological conditions. The MRIs performed in this study utilized advanced imaging technologies that significantly enhance diagnostic capabilities. Specifically, the MRIs conducted from 2019 to 2022 were carried out on a 3 Tesla GE MRI machine. This high-field strength MRI system provides enhanced

signal- to-noise ratios, allowing for greater detail and clarity in the images produced. Then, there was a transition to using the 1.5 Tesla GE MRI machine later in the study period.

The superior image quality obtained from these GE MRI machines is crucial not only for diagnosing PTS but also for monitoring disease progression and evaluating treatment efficacy. High-resolution images allow clinicians to visualize subtle changes in nerve structures and surrounding tissues, which can be indicative of inflammatory processes or nerve degeneration.

In summary, the combination of advanced MRI technology and high-quality imaging significantly enhances the diagnostic process. By employing both the 3 Tesla and 1.5 Tesla GE MRI machines, this research capitalizes on the strengths of each system, ensuring comprehensive and detailed imaging that is essential for accurately diagnosing and managing neuromuscular diseases such as PTS.

Protocol for MRI Image Acquisition

Each individual both control group and the PTS group underwent MRI of the brachial plexus or shoulder, depending on the clinical suspicion of the cause of the pathologic process.

In 2022, the hospital implemented a standardized protocol for MRI image acquisition specifically tailored for the brachial plexus. This protocol was designed to enhance the consistency and quality of imaging, ensuring that all relevant anatomical structures are captured in detail. By establishing a uniform approach, it aimed to minimize variability in the imaging process and improve the reliability of our diagnostic outcomes.

The protocol outlines specific guidelines regarding patient positioning, the selection of MRI sequences, and the parameters for image acquisition. It also emphasizes the importance of using advanced techniques to optimize visualization of nerve structures, including high-resolution imaging and appropriate contrast settings. This comprehensive guideline will provide valuable insights into the methodology employed, ensuring that all team members are aligned in their approach to imaging the brachial plexus.

Nerve Root Alterations Evaluation

To evaluate nerve root alterations associated with PTS using MRI, specific sequences are particularly effective:

- STIR Sequence, excellent for detecting edema in the nerve roots. It highlights areas of inflammation and helps identify acute changes, which are critical in diagnosing PTS;
- T1-weighted Images, useful for assessing chronic changes, such as fat infiltration and muscle atrophy. T1-weighted images can reveal atrophy in muscles innervated by affected nerve roots, indicating long-term denervation;
- 3D Cube Nerve Protocol, advanced imaging technique provides high-resolution images of the brachial plexus and can accurately depict the specific nerve roots involved in PTS. It helps visualize both acute and chronic changes in the nerve roots;
- T2-weighted Image can also be beneficial for identifying edema and other changes in the nerve roots and surrounding tissues. T2-weighted images provide additional context regarding the extent of inflammation.

Generally, the edema reflects active inflammation, a hallmark of PTS. Radiologists evaluates the extent and distribution of edema to determine the severity of the inflammatory process. All limb-girdle muscles were thoroughly examined for signs of edema, fat infiltration, and atrophy. Specifically, shoulder girdle muscles (Pectoralis Major, Pectoralis Minor, Subclavius, Serratus Anterior, Deltoid), shoulder girdle posterior muscles (Trapezius, Latissum Dorsi, Levator Scapula, Rhomboid Major, Rhomboid Minor, Teres Major, Teres Minor), rotation cuff muscles (Supraspinatus, Infraspinatus, Subscapularis), arm posterior muscles (Triceps, Anconeus), arm anterior muscles (Brachialis, Coracobrachialis), neck lateral muscles (Scalene Muscle Anterior, Medial and Posterior) were evaluated bilaterally for the presence of edema following the edema score signal, categorized on a scale from 0 to 3 as follows: *grade 0*, no edema detected, normal appearance of the tissue; *grade 1*, mild edema, slight signal intensity changes noted, but not significantly impacting overall tissue structure; *grade 2*, moderate edema, clear signal intensity changes with some evidence of swelling or structural alteration in the tissue; *grade 3* severe edema, significant signal intensity changes with marked swelling, likely associated with extensive tissue involvement or injury (Mercuri, E., Talim, B., Moghadaszadeh, B., et al. 2002). The evidence of muscle fat infiltration and atrophy, especially in muscles innervated by affected nerve roots, such as the supraspinatus and infraspinatus, indicates chronic denervation and helps assess the long-term impact of nerve damage. All limb-girdle muscles were specifically assessed for fat infiltration using the adapted Mercuri score, which quantifies the extent of fat replacement in the muscle tissue: *grade 0*, normal appearance; *grade 1*, "moth-eaten" appearance, with numerous discrete areas of increased intensity with beginning confluence; *grade 2A*, late moth-eaten appearance with numerous discrete areas of increased intensity with beginning confluence, comprising less than 30% of the volume of the individual muscle; *grade 2B*, late moth-eaten appearance with numerous discrete areas of increased intensity with beginning confluence comprising 30%-60% of the volume of the individual muscle; *grade 3*, washed out appearance with muscle replaced but still present at the periphery; *grade 4*, end-stage appearance by increased intensity of connective tissue and fat, with only a rim of fascia and neurovascular structures distinguishable (Mercuri, E., Talim, B., Moghadaszadeh, B., et al. 2002). Atrophy was assessed in the limb-girdle muscles and recorded as either present or absent based on the imaging findings for the same muscle groups. This evaluation is crucial for understanding the extent of muscle degeneration associated with PTS. By systematically documenting the presence or absence of atrophy, we can gain valuable insights into the progression of the disease and its impact on muscle integrity. This information not only aids in clinical diagnosis but also enhances our ability to monitor changes over time, informing patient management.

Descriptive statistics for categorical variables were presented as frequencies and percentages, providing a clear overview of the distribution of these variables within the study population. For quantitative variables, we calculated the mean and standard deviation, which allowed for an understanding of central tendency and variability. Given the small sample size, comparisons related to pain and functional impairment were conducted using Fisher's exact test. This statistical method is particularly suitable for small sample sizes as it evaluates the significance of the association between two categorical variables without assuming a normal distribution.

We established a significance threshold at 5% ($p < 0.05$), meaning that any p-value below this threshold would indicate a statistically significant difference, warranting further examination of the underlying relationships.

5.4 Acquisition for Qualitative Measurements and Analysis

The study cohort comprises a well-defined population, enabling precise demographic and clinical profiling. Males constitute the majority (80.4%), with females representing 19.6%. The mean age is 51.9 years (SD ±15.9), indicating a heterogeneous age distribution. Ethnically, the sample is predominantly Caucasian (96.1%), with a minority of Middle Eastern origin (3.9%).

Laterality analysis reveals a near-equitable distribution: 41.2% of cases involve the right side, 39.2% the left, and 19.6% present bilateral involvement. Clinically, nociceptive symptoms are the most prevalent, reported in 70.6% of patients, followed by functional deficits in 52.9%, underscoring the syndrome's impact on quality of life and motor performance.

Electrophysiological assessment via EMG demonstrates a high incidence of neurogenic impairment (80.4%), with additional findings including denervation activity (19.6%), and isolated cases of bilateral PESS, paralysis, electrical silence, and motor unit remodeling. These findings reflect varying degrees of axonal damage and reinnervation processes. MRI analysis corroborates the inflammatory etiology of PTS, with 92.0% of patients exhibiting imaging features consistent with neuroinflammation. Non-specific and trauma-related findings were each observed in 4.0% of cases.

This multidimensional dataset - integrating demographic, clinical, neurophysiological, and radiological parameters - provides a comprehensive characterization of PTS within the studied cohort. **Table 1** synthesizes these findings, highlighting the predominance of male patients, the centrality of pain as a presenting symptom, and the outcomes at EMG and MRI findings.

Table 1 – Patients' Characteristics

No. of patients	51
Gender, n (%)	
Female	10 (19.6)
Male	41 (80.4)
Age, mean (SD)	51.9 ± 15.9
Race, n (%)	
Caucasian	49 (96.1)
Middle Eastern	2 (3.9)
Side, n (%)	
Right	21 (41.2)
Left	20 (39.2)
Both	10 (19.6)
Clinical Onset, n (%)	
Pain	36 (70.6)
Functional Impairment	27 (52.9)
EMG, n (%)	
EMG Neurogenic Impairment	41 (80.4)

EMG Denervation Activity	10 (19.6)
EMG Bilateral Pess	1 (2.0)
EMG Paralysis	1 (2.0)
EMG Absence of electrical activity	1 (2.0)
EMG Motor Unit remodeling	3 (5.9)
MRI Onset, n (%)	
Not specific	2 (4.0)
Inflammatory	46 (92.0)
Trauma	2 (4.0)

Note: Baseline characteristics - Descriptive statistics for categorical variables are presented as frequencies and percentages, whereas for quantitative variables, both the mean and standard deviation were calculated. This approach ensures a comprehensive overview of the data, allowing for a clear understanding of the distribution and central tendencies within the studied population.

Qualitative MRI assessments in PTS focused on detecting and characterizing pathological alterations of the brachial plexus, particularly involving the C5-C8 nerve roots and, when applicable, the upper, middle, and lower primary trunks. Radiologists evaluated signs of nerve root swelling or signal abnormalities, which are critical for confirming PTS diagnosis.

High-resolution bilateral imaging of the entire brachial plexus and limb-girdle musculature was performed using a dedicated 40-minute MRI protocol. This protocol employed a large field of view in both coronal and axial planes to capture both shoulders simultaneously, enabling direct comparison and detection of asymmetries, including potential bilateral involvement. Axial images were acquired in a neutral orientation, extending from the skull base to the cervicothoracic junction, allowing detailed visualization of nerve roots and adjacent structures. Coronal images spanned from the posterior paraspinal region to the pectoralis muscles, facilitating evaluation of limb-girdle muscles for signs of atrophy or fat infiltration - markers of chronic denervation.

This imaging strategy enhances diagnostic accuracy by correlating structural abnormalities with clinical symptoms. The use of multi-planar reconstruction (MPR) further improves visualization, enabling detailed assessment in axial, coronal, and sagittal planes. Each plane offers unique diagnostic value: axial views provide cross-sectional detail of nerve roots; coronal views reveal the course of the plexus and muscle involvement; sagittal views clarify spatial relationships between nerve roots, vessels, and soft tissues. Advanced post-processing software allows for high-resolution reconstructions, adjustable in angle and slice thickness, to highlight specific anatomical or pathological features.

5.5 Acquisition for Quantitative Measurements and Analysis

The second analysis focused on quantifying pathological changes in the brachial plexus among 51 patients with PTS. For each nerve root from C5 to C8, CSA in mm^2, T2 signal intensity, with AR in mm^2 and MED, were measured bilaterally. These parameters were then compared to a control group of 25 age- and gender-matched healthy individuals, using the same imaging metrics. An intra-cohort exploratory analysis was subsequently performed within the PTS group, comparing MRI-derived metrics between roots classified as pathological and those unaffected. This allowed for a more granular assessment of disease-specific alterations, even within the

same individual.

Table 2 summarizes the baseline characteristics of the study population (N=76), comprising 51 PTS patients and 25 healthy controls. The mean age across the cohort was 50.0 years (SD ±16.6), ranging from 14 to 83 years. The median age was 52 years [IQR: 39–62]. Healthy controls had a slightly lower mean age of 46.5 years (SD ±18.1), while the PTS group averaged 51.9 years (SD ±15.9). Gender distribution revealed a predominance of male participants (76.3%), with 80.4% of the PTS group being male, compared to 72.0% in the control group. Female representation was 23.7% overall, with 19.6% in the PTS group and 28.0% among controls.

Table 2 – Demographic Characteristics

	Total	**Healthy Control Subjects**	**Patients with Disease (PTS)**
No. of Subjects	76	25	51
Age at MRI imaging* (years)	50.0 ± 16.6 (14-83) [52, 39-62]	46.5±18.1 (18-83) [46, 32-56]	51.9± 15.9 (14-78) [53, 46-63]
Gender, n (%)			
Female	18 (23.7)	7 (28.0)	10 (19.6)
Male	58 (76.3)	18 (72.0)	41 (80.4)

Note - * Results are reported as means ± standard deviation, with the range in round brackets. Results in squared brackets are median and interquartile range.

Quantitative measurements were performed using the 3D Cube Nerves MRI sequence, which is particularly effective for three-dimensional and volumetric evaluations. Starting from the sagittal plane of the image, the C5 root was identified, and subsequent roots were analyzed before transitioning to the axial plane to initiate measurements. As the analysis progressed from the C5 root to the C8 root, the axial plane was adjusted to align with the spinal column's orientation.

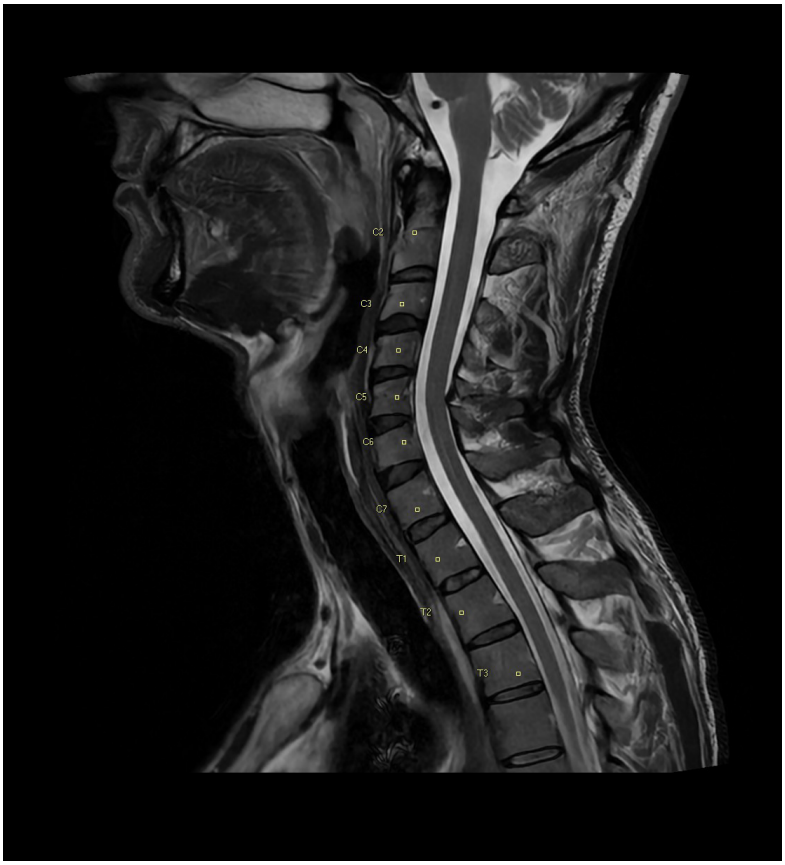

Figure 1 – Sagittal image from MRI in 3D Cube Nerves, to count the nerve roots to analyze.

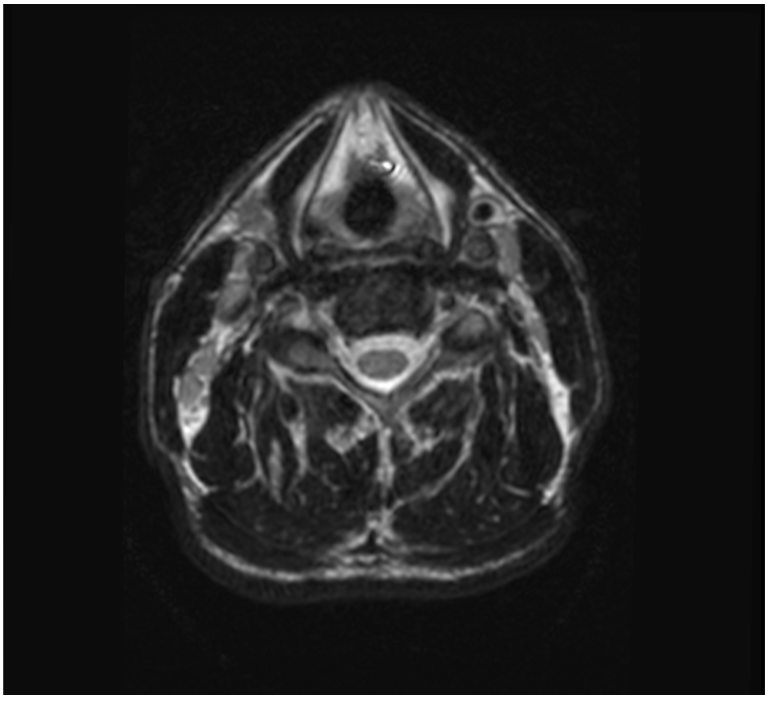

Figure 2 – Axial image from MRI in 3D Cube Nerves, to start the quantitative measurements of the nerve roots to analyze.

For the intensity measurements (AR and MED), a region of interest (ROI) was manually delineated, beginning 15 mm (±2 mm) from the exit of the foramen, to standardize the measurements. The diameter of each root was measured as CSA, also at 15 mm (±2 mm), ensuring consistency across all assessments. This meticulous process was applied to all roots from C5 to C8, encompassing both sides of the brachial plexus, right and left.

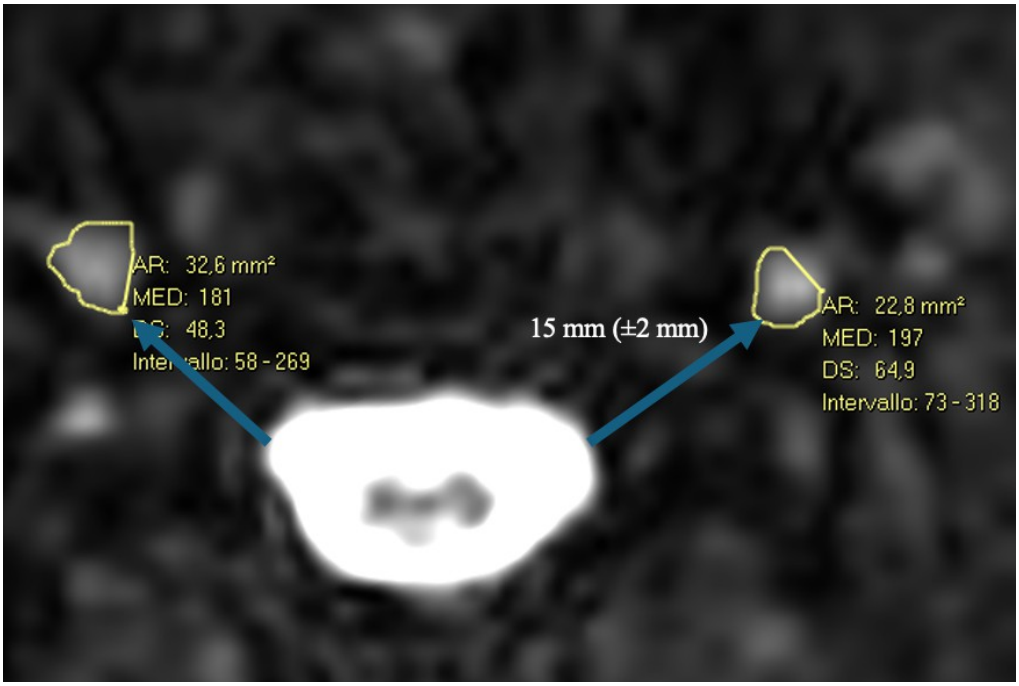

Figure 3 – Axial image from MRI in 3D Cube Nerves, with quantitative measurements of the nerve roots to analyze in CSA and T2-weighted intensity signal (AR and MED). In this case, the observed measurements is C5 roots of a patient with PTS: right pathologic root compared with the left not pathologic.

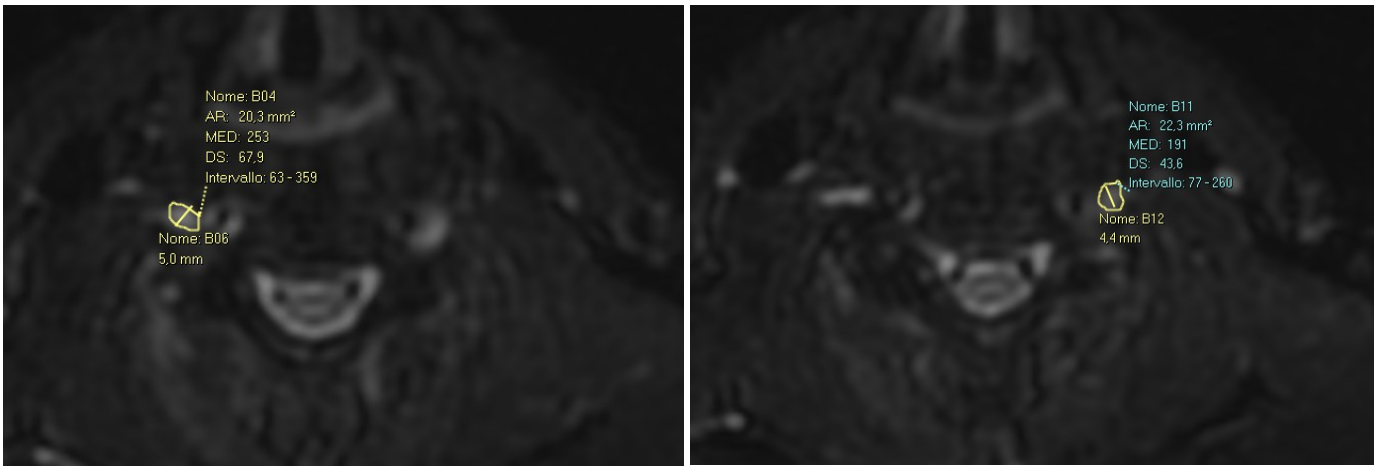

Figure 4 – Axial images from MRI in 3D Cube Nerves, with quantitative measurements of the nerve roots to analyze in CSA and T2-weighted intensity signal (AR and MED). In this case, the observed measurements combined the CSA (mm) = 5.0 mm with the AR and MED measurements.

Quantitative variables are presented as mean ± standard deviation, alongside the range (minimum-maximum), median, and interquartile range (IQR: 25th–75th percentile). Categorical variables are reported as frequencies and percentages. To compare demographic characteristics between patients with PTS and healthy controls (CTL), the Mann-Whitney U test or Fisher's exact test was employed, depending on whether the variables were quantitative or categorical. The decision to utilize a non-parametric approach for quantitative variables was based on the results of the Shapiro-Wilk test, which assessed normality in the data distribution. For the comparisons regarding nerve root diameter (mm) and intensity (mm²) for ROI between patients with PTS and healthy subjects, a hierarchical linear model was utilized to account for the repeated measures design (patient -

side - root). This model was selected due to the nested structure of the data, which encompassed multiple levels of grouping: groups (PTS vs. CTL), side (left vs. right), and nerve root (C5, C6, C7, and C8). Employing a hierarchical model is crucial in such contexts, as it effectively addresses variability at each grouping level and accurately models' relationships between the groups to yield more precise estimates of effects. In this analysis, the model was configured with the patient group, side, and nerve roots treated as fixed effects, while individual patients were incorporated as a random effect. This choice was made to account for variability in nerve root characteristics among individuals, which may not be directly explained by the differences among groups, sides, or roots. The hierarchical model is particularly adept at managing correlations between measurements within the same group - such as patients or nerve roots - and ensures that dependencies in the data are appropriately considered. Consequently, this approach facilitates more reliable conclusions regarding the factors influencing the results while accommodating the complex structure of the data. The final model included predictors for group (PTS vs. healthy subjects), root (C5, C6, C7, C8), side (left vs. right), and two interaction terms (group-root and group-side). These interaction terms were crucial for identifying any potential differences in associations between the groups that might be influenced by the root or the side. Post-hoc analyses were conducted utilizing both contrasts with Bonferroni correction and margins. The contrasts were specifically aimed at directly comparing levels of categorical variables, particularly examining differences between patients with PTS and healthy subjects, across the different nerve roots (C5, C6, C7, and C8), and between the left and right sides, including the interaction terms. Margins were calculated to provide adjusted predicted means for each group and condition (e.g., side or nerve root), offering a comprehensive overview of average effects. The analysis of these margins is visually represented in accompanying graphs. Additionally, a subgroup analysis was conducted using the same hierarchical linear model to differentiate between pathological and non-pathological nerve roots in patients with PTS. In this instance, the variable "group" was replaced with a variable indicating the condition of the nerve root (pathological vs. non-pathological). This approach has the advantage of reducing the influence of selection bias and confounding factors within the sample.

5.6 Informed Consent to Research

All participants - both patients and healthy controls - provided written informed consent prior to undergoing MRI examinations. This process ensured that individuals, or their legal representatives, were fully apprised of the potential risks associated with exposure to electromagnetic fields and the administration of contrast agents.

Informed consent represents a core ethical requirement in clinical research, safeguarding participant autonomy and reinforcing transparency in the researcher-participant relationship. It ensures that individuals are adequately informed about the study's objectives, procedures, and associated risks, thereby enabling voluntary and informed participation.

The consent documentation included the following key elements:

- Procedural information: A detailed explanation of the MRI protocol, including duration, equipment specifications, and preparatory instructions.

- Risk disclosure: Clear communication of potential risks related to electromagnetic exposure and contrast media, allowing participants to make risk-benefit assessments.
- Data protection and usage: Authorization for the use of anonymized data for scientific and educational purposes, with assurances of compliance with Italian privacy legislation (DL 196/2003) and the EU General Data Protection Regulation (GDPR 2016/679/EU).

Beyond regulatory compliance, the informed consent process reinforces the ethical integrity of the study. It promotes participant trust, facilitates broader engagement in research, and supports the reproducibility and credibility of scientific findings. Moreover, strict adherence to data protection standards ensures confidentiality and mitigates concerns related to data security - an increasingly critical consideration in contemporary biomedical research.

CHAPTER 6

Results

6.1 Description of PTS Group Population

The descriptive analysis of the PTS cohort starts with key demographic and clinical insights, particularly regarding age distribution, symptomatology, and laterality of nerve involvement (**Tables 1-3**). The mean age of patients was 51.9 years (SD ±15.9), consistent with literature indicating that PTS predominantly affects individuals in midlife, typically between 30 and 70 years of age, with a peak incidence around 50 years (van Alfen & van Engelen, 2006). This age range corresponds to increased susceptibility to immune-mediated mechanisms, post-infectious syndromes, and trauma-related neuropathies - recognized triggers of PTS. Specifically, the study identified two cases where the clinical onset of symptoms was associated with a traumatic event. This observation underscores a critical aspect of PTS: its potential to manifest following trauma. PTS is often characterized by sudden, severe shoulder pain and subsequent muscle weakness, which can easily be mistaken for a straightforward muscle injury or strain. This misdiagnosis is particularly concerning, as the symptoms of PTS may initially present similarly to those of common musculoskeletal injuries, leading to delays in proper diagnosis and treatment. The relationship between trauma and the onset of PTS is well documented in the literature, highlighting that individuals may experience an inflammatory response in the brachial plexus after a significant physical impact or injury. Pain was the most frequently reported symptom, followed by muscle weakness (hyposthenia), muscle wasting (hypotrophy), and functional deficits - findings consistent with the clinical profile of brachial plexopathies.

Laterality analysis revealed that 80.4% of patients exhibited unilateral involvement, aligning with the classical presentation of PTS as a focal neuropathy affecting one side of the brachial plexus. Bilateral involvement was observed in 19.6% of cases, a less common but clinically significant variant. Notably, bilateral symptoms were more prevalent among patients under 55, suggesting a possible age-related variation in disease expression or immune reactivity. This observation may reflect a more aggressive inflammatory phenotype in younger

individuals, potentially leading to bilateral plexus involvement. Alternatively, it may indicate differences in neuromuscular recovery dynamics or systemic immune activation. These findings underscore the importance of age-stratified analysis in understanding disease progression and tailoring therapeutic strategies.

Table 3 – Side of Nerve Roots per Gender and Age Range

			Gender				Age Range				
	Overall (n = 51)		**Female (n = 10)**		**Male (n = 41)**	**p-value**	**< 55 years (n = 27)**		**≥ 55 years (n = 24)**		**p-value**
Side											
Right	21	(41.2)	5	(50.0)	16	(39.0)	0.816	10	(37.0)	11	(45.8)	0.510
Left	20	(39.2)	4	(40.0)	16	(39.0)		10	(37.0)	10	(41.7)	
Both	10	(19.6)	1	(10.0)	9	(22.0)		7	(25.9)	3	(12.5)	
Unilateral vs. Bilateral											
Unilateral	41	(80.4)	9	(90.0)	32	(78.0)	0.664	20	(74.1)	21	(87.5)	0.300
Bilateral	10	(19.6)	1	(10.0)	9	(22.0)		7	(25.9)	3	(12.5)	

Note: Results are reported as relative frequencies and percentages, sample size = 51 cases.

At the *nerve root level* (**Table 4**), the data reveals that C6 is the most commonly affected root, with involvement observed in 61.3% of patients on the right side and 56.7% on the left. This aligns with expectations, as C6 is a key component of the upper trunk of the brachial plexus, which is frequently impacted in PTS. Damage to the C6 nerve root typically results in weakness in the shoulder and arm muscles, particularly affecting the deltoid and biceps, which are essential for arm abduction and flexion. The symmetrical involvement of C6 across both sides suggests that the underlying pathology may not exhibit a strong lateral bias but rather indicates a generalized vulnerability of this nerve root. However, the role of gender in the manifestation of PTS symptoms remains an area of ongoing research. While some studies suggest that males may have a higher incidence of PTS, there is evidence indicating that females may experience a distinct pattern of nerve root involvement or symptom progression, although these findings are not always consistent across different populations. The observed gender difference in C5 involvement is due to the small sample that has been considered for our purpose and could be related to a variety of factors, such as physiological or anatomical predisposition in females, rendering the C5 nerve root more susceptible to inflammation or damage. Potential anatomical differences, such as variations in muscle mass, body composition, or hormonal influences, may contribute to the differential impact on nerve roots in PTS between genders. We will discuss on chapter 7 the bias connected to the gender difference discovered in our results.

Table 4 – Nerve Roots

			Gender				Age Range				
	Overall		Female		Male	p-value	< 55 years		≥ 55 years		p-value
Right											
C5	9	(29.0)	4	(66.7)	5	(20.0)	0.043	5	(29.4)	4	(28.6)	1.000
C6	19	(61.3)	4	(66.7)	15	(60.0)	1.000	10	(58.8)	9	(64.3)	1.000
C7	13	(41.9)	3	(50.0)	10	(40.0)	0.676	7	(41.2)	6	(42.9)	1.000
C8	15	(48.4)	3	(50.0)	12	(48.0)	1.000	10	(58.8)	5	(35.7)	0.285
T1	4	(12.9)	1	(16.7)	3	(12.0)	1.000	2	(11.8)	2	(14.3)	1.000
Left											
C5	13	(43.3)	3	(60.0)	10	(40.0)	0.628	5	(29.4)	8	(61.5)	0.138
C6	17	(56.7)	3	(60.0)	14	(56.0)	1.000	7	(41.2)	10	(76.9)	0.071
C7	13	(43.3)	2	(40.0)	11	(44.0)	1.000	8	(47.1)	5	(38.5)	0.721
C8	10	(33.3)	2	(40.0)	8	(32.0)	1.000	7	(41.2)	3	(23.1)	0.440
T1	2	(6.7)	1	(20.0)	1	(4.0)	0.310	1	(5.9)	1	(7.7)	1.000

Note: Results are reported as relative frequencies and percentages; sample size of 51 patients with PTS.

As shown in **Table 5**, the upper trunk of the brachial plexus is affected in 20.6% of cases on the right side and 13.3% on the left, with no significant differences observed based on age or gender. Research indicates that PTS typically affects one side of the body (unilateral), with no consistent preference for the right or left side. Some studies showed a right-sided involvement, suggesting a slight predominance on the right side. However, this is not a universal finding, and other studies have reported varying results. For instance, some literature suggests that the left arm may be more frequently affected. However, the condition can affect either side, and no definitive pattern has been established. Age and gender do not appear to have a significant impact on the laterality of the syndrome (Milner et al. 2016). Further research with larger sample sizes is needed to better understand these aspects of PTS.

The simultaneous involvement of both the upper and lower trunks aligns with established patterns in brachial plexus neuropathies, as supported by existing literature. The symmetrical nature of trunk involvement indicates a consistent pattern of damage throughout the brachial plexus, highlighting the slightly increased vulnerability of the upper trunk to injury in PTS; this vulnerability might be related to the anatomy of the brachial plexus, with the upper trunk (C5-C6 roots) being more superficial and exposed in the neck area (Chhabra et al., 2013). This finding reinforces the notion that upper brachial plexus involvement is a common characteristic in neuropathic disorders, as documented in previous studies.

Table 5 – Nerve Trunk

			Gender					Age Range				
	Overall		Female		Male		p-value	< 55 years		≥ 55 years		p-value
Right												
Upper Primary Trunk	7	(20.6)	1	(16.7)	6	(21.4)	1.000	3	(16.7)	4	(25.0)	0.681
Middle Primary Trunk	1	(3.2)	0	(0.0)	1	(4.0)	1.000	1	(5.9)	0	(0.0)	1.000
Lower Primary Trunk	4	(12.9)	1	(16.7)	3	(12.0)	1.000	4	(23.5)	0	(0.0)	0.107
Left												
Upper Primary Trunk	4	(13.3)	0	(0.0)	4	(16.0)	1.000	2	(11.8)	2	(15.4)	1.000
Middle Primary Trunk	4	(13.3)	0	(0.0)	4	(16.0)	1.000	2	(11.8)	2	(15.4)	1.000
Lower Primary Trunk	3	(10.0)	0	(0.0)	3	(12.0)	1.000	2	(11.8)	1	(7.7)	1.000

Note: Results are reported as relative frequencies and percentages; sample size of 51 patients with PTS.

An examination of *edema* across limb-girdle muscle groups (**Table 6**; see Appendix) stratified by age (<55 years and ≥55 years) highlights the subscapularis and deltoid muscles as particularly affected. The subscapularis, a key component of the rotator cuff responsible for internal shoulder rotation, shows a significantly higher prevalence of edema in females ($p = 0.013$), suggesting a potential significance of this gender difference based on the sample size analyzed.

Edema in the subscapularis is indicative of acute inflammation, often associated with early-stage PTS, particularly when nerve roots C5 and C6 - responsible for its innervation - are involved. This inflammation can result in severe pain and impaired internal rotation.

The deltoid muscle, essential for arm abduction, exhibits edema in 19.4% of patients on the right side, with slightly lower involvement on the left. This finding is consistent with axillary nerve involvement, commonly affected in PTS. Deltoid edema correlates with functional limitations, particularly in overhead activities, and reflects the frequent impairment of the C6 root and axillary nerve. Although right-sided involvement is marginally higher, the bilateral pattern suggests that PTS may affect both sides, especially in severe or early-onset cases.

An analysis of fat infiltration across limb-girdle muscle groups (**Table 7**; see Appendix), stratified by gender and age (<55 years and ≥55 years), identifies the rotator cuff muscles as key indicators of chronic muscle degeneration, typically following prolonged nerve injury in PTS.

Among these, the infraspinatus muscle shows notable involvement, particularly on the left side, where fat infiltration is more pronounced. Although the supraspinatus and subscapularis also exhibit fatty changes - affecting 19.4% and 16.1% of patients on the right side, respectively - the infraspinatus stands out for its consistent left-sided predominance. While statistical analysis does not reveal significant differences by age or gender, the asymmetrical pattern observed in the infraspinatus may suggest a subtle lateralization in the degenerative process. Functionally, the infraspinatus is critical for external shoulder rotation and contributes significantly to joint stability. Chronic denervation of this muscle, often due to injury of the C5 and C6 nerve roots, leads to progressive replacement of muscle fibers with adipose tissue - a hallmark of chronic neuropathies such as PTS. This fat infiltration reflects irreversible muscle atrophy and is associated with persistent weakness

and reduced range of motion, particularly in external rotation.

The higher frequency of left-sided infraspinatus involvement may point to a mild asymmetry in disease progression, although the current sample size limits definitive conclusions. Importantly, the absence of significant gender- or age-related differences in fat infiltration contrasts with earlier findings on muscle edema, where female predominance was noted in the subscapularis. This suggests that chronic muscle degeneration in PTS is more closely related to the duration and severity of nerve injury than to demographic variables. However, it is conceivable that with a larger sample size, more nuanced variations in how different populations experience fat degeneration could emerge.

An analysis of muscle *atrophy* across limb-girdle groups (**Table 8**; see Appendix), stratified by gender and age (<55 years and ≥55 years), reveals that on the right side, the serratus anterior shows a low overall prevalence of atrophy (3.2%), with a higher rate in females (16.7%). However, this difference lacks statistical significance ($p = 0.194$), suggesting that any gender-related pattern could be not robust. Similarly, the deltoid muscle presents an atrophy rate of 12.5%, more frequent in males (15.4%), but again without statistical significance ($p = 0.566$). Among the rotator cuff muscles, the supraspinatus exhibits the highest atrophy rate (25.0%), particularly in females (33.3%). Despite this apparent trend, the p-value (0.625) indicates no significant gender difference. Age-related data show that 35.7% of patients aged ≥55 years exhibit supraspinatus atrophy, compared to 16.7% in younger individuals, suggesting a possible age-related progression of muscle degeneration. On the left side, similar patterns emerge. Atrophy is observed in the pectoralis major, pectoralis minor, and serratus anterior (3.3% each), with no significant gender differences. The deltoid shows a slightly higher prevalence (6.7%), particularly among older patients. In the rotator cuff, both the supraspinatus and infraspinatus show notable atrophy (20.0% each), mirroring the trends seen on the right. However, these differences are not statistically significant.

These findings underscore the rotator cuff - especially the supraspinatus and infraspinatus - as key sites of muscle atrophy in PTS because more involved in previous edema and fat processes of the disease. While some muscles appear more vulnerable, the absence of significant gender differences suggests that factors such as the duration and severity of nerve injury may be more influential than demographic variables. The observed increase in atrophy among older patients points to age as a potential modifier of disease progression and recovery capacity.

Correlation in roots involvement based on EMG and MRI

Table 9 presents a comparative analysis of nerve root involvement (C5-C8) as assessed by EMG and MRI. The matrix format allows for direct comparison of findings across both modalities, highlighting cases where the same root is concurrently identified as pathological by EMG and MRI. A detailed examination reveals that the C5 and C6 nerve roots are most frequently involved. Specifically, C5 shows concurrent abnormalities in 18 cases across both EMG and MRI. MRI also identifies C5 involvement in 16 cases when paired with C6, while involvement decreases markedly with C7 (8 cases) and C8 (4 cases). The C6 nerve root demonstrates the highest frequency of involvement. EMG detects abnormalities in 25 cases when paired with C5 and in 28 cases when

assessed independently. MRI findings mirror this pattern, with 25 and 28 cases respectively, confirming C6 as a central site of pathology in PTS. In contrast, involvement of C7 is moderate, with EMG showing 17 cases with C5 and 19 with C6, but fewer with C7 (11) and C8 (5). The C8 root is the least affected, with EMG identifying 14 cases with C5 and 16 with C6, and MRI showing similar values (14, 16, 11, and 9 for C5–C8, respectively).

These findings underscore the predominant role of C5 and C6 in PTS-related nerve damage, with strong concordance between EMG and MRI results. The consistency across modalities reinforces the diagnostic value of combining both techniques for accurate root-level assessment.

Table 9 – Nerve Involvement at EMG and MRI respectively

		EMG			
		C5	**C6**	**C7**	**C8**
MRI	**C5**	18	16	8	4
	C6	25	28	14	6
	C7	17	19	11	5
	C8	14	16	11	9

Descriptive analysis reveals that a substantial proportion of patients report pain (70.6%) and functional impairment (52.9%) during clinical evaluation (**Table 1**). To explore the relationship between these symptoms and nerve involvement, we analyzed EMG and MRI findings in relation to the presence or absence of pain and functional deficits, as summarized in **Table 10**. The table provides a detailed overview of nerve root involvement (C5-C8) in the cohort of 51 patients, categorized by symptomatology.

Looking before at the *laterality*, the right-side involvement was observed in 21 patients (41.2%), with 17 reporting pain (47.2%) and 4 without (26.7%). Although pain was more prevalent in this group, the difference was not statistically significant ($p = 0.079$). Functional impairment was reported by 14 patients (51.9%) versus 7 (29.2%) without impairment ($p = 0.273$). The left side involvement was present in 20 patients (39.2%), with 15 (41.7%) experiencing pain and 5 (33.3%) not. Functional impairment was reported by 9 (33.3%) patients, while 11 (45.8%) did not report deficits. Among the bilateral cases (10 patients, 19.6%), 6 (60%) reported pain and 4 (40%) did not. Functional impairment was noted in 4 patients (14.8%), while 6 (25%) reported no impairment.

The *EMG results* indicate substantial involvement of various nerve roots:

• C5: Overall involvement was noted in 38 patients (74.5%). Among those with pain, 26 (72.2%) showed involvement, while 12 (80%) without pain did as well ($p = 0.730$). This suggests that C5 involvement is prevalent regardless of pain presence.

• C6: This nerve root had the highest involvement at 42 patients (82.4%). Here, the pain group showed 30 (83.3%) with involvement compared to 12 (80%) in the no pain group, yielding a p-value of 1.000. This indicates no significant difference.

• C7 and C8: C7 involvement was observed in 23 patients (45.1%), with pain seen in 15 (41.7%) and 8 (53.3%) without pain (p = 0.542). C8 showed similar patterns, with 12 patients (23.5%) overall, where 10 (27.8%) had pain, and 2 (13.3%) did not (p = 0.470). Again, no significant differences were evident.

The *MRI findings* reflected a similar lack of significant correlation between symptoms and nerve involvement:

• C5: MRI indicated 20 patients (39.2%) had C5 involvement, with 14 (38.9%) of those experiencing pain and 6 (40%) without (p = 1.000).

• C6: MRI findings for C6 showed involvement in 32 patients (62.7%). Among the pain group, 25 (69.4%) was involved, whereas 7 (46.7%) did not, resulting in p-value of 0.203, indicating no significant association.

• C7 and C8: For C7, 22 patients (43.1%) were involved, with 16 (44.4%) in the pain group and 6 (40%) without (p = 1.000). C8 involvement was noted in 20 patients (39.2%), with a slight majority (16 or 44.4%) reporting pain compared to 4 (26.7%) without (p = 0.348).

These findings confirm that C5 and C6 are the most frequently involved nerve roots in PTS, as detected by both EMG and MRI. However, no statistically significant associations were found between nerve involvement and the presence of pain or functional impairment. This suggests that nerve pathology may be present regardless of symptom severity, highlighting the complex and variable clinical presentation of PTS.

The lack of correlation between objective findings and subjective symptoms points to the influence of additional factors - such as individual pain thresholds, compensatory neuromuscular mechanisms, and symptom duration - in shaping patient experience and functional outcomes.

Table 10 – Nerve Characteristics by EMG and MRI, at Clinics

	Total	Pain (n = 36)	No Pain (n = 15)	p-value	Functional Impairment (n = 27)	No Functional Impairment (n = 24)	p-value
Side							
Right	21 (41.2)	17 (47.2)	4 (26.7)	0.079	14 (51.9)	7 (29.2)	0.273
Left	20 (39.2)	15 (41.7)	5 (33.3)		9 (33.3)	11 (45.8)	
Both	10 (19.6)	4 (11.1)	6 (40)		4 (14.8)	6 (25)	
EMG C5	38 (74.5)	26 (72.2)	12 (80)	0.730	20 (74.1)	18 (75)	1.000
EMG C6	42 (82.4)	30 (83.3)	12 (80)	1.000	22 (81.5)	20 (83.3)	1.000
EMG C7	23 (45.1)	15 (41.7)	8 (53.3)	0.542	11 (40.7)	12 (50)	0.580
EMG C8	12 (23.5)	10 (27.8)	2 (13.3)	0.470	6 (22.2)	6 (25)	1.000
MRI C5	20 (39.2)	14 (38.9)	6 (40)	1.000	10 (37)	10 (41.7)	0.780
MRI C6	32 (62.7)	25 (69.4)	7 (46.7)	0.203	18 (66.7)	14 (58.3)	0.575
MRI C7	22 (43.1)	16 (44.4)	6 (40)	1.000	13 (48.1)	9 (37.5)	0.573
MRI C8	20 (39.2)	16 (44.4)	4 (26.7)	0.348	11 (40.7)	9 (37.5)	1.000

Note: Results are reported as relative frequencies and percentages, sample size of 51 patients.

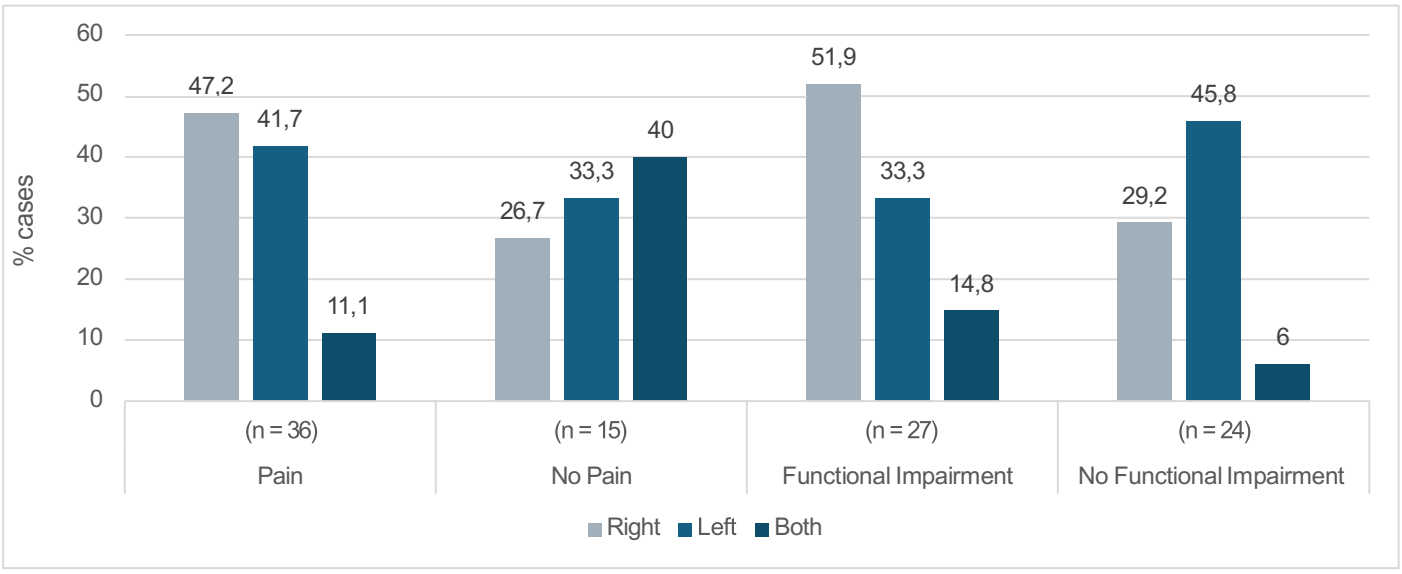

Figure 5: note - Graphic of the table 10, Group Population with PTS – Side Nerve Root matched with Clinic and EMG outcomes.

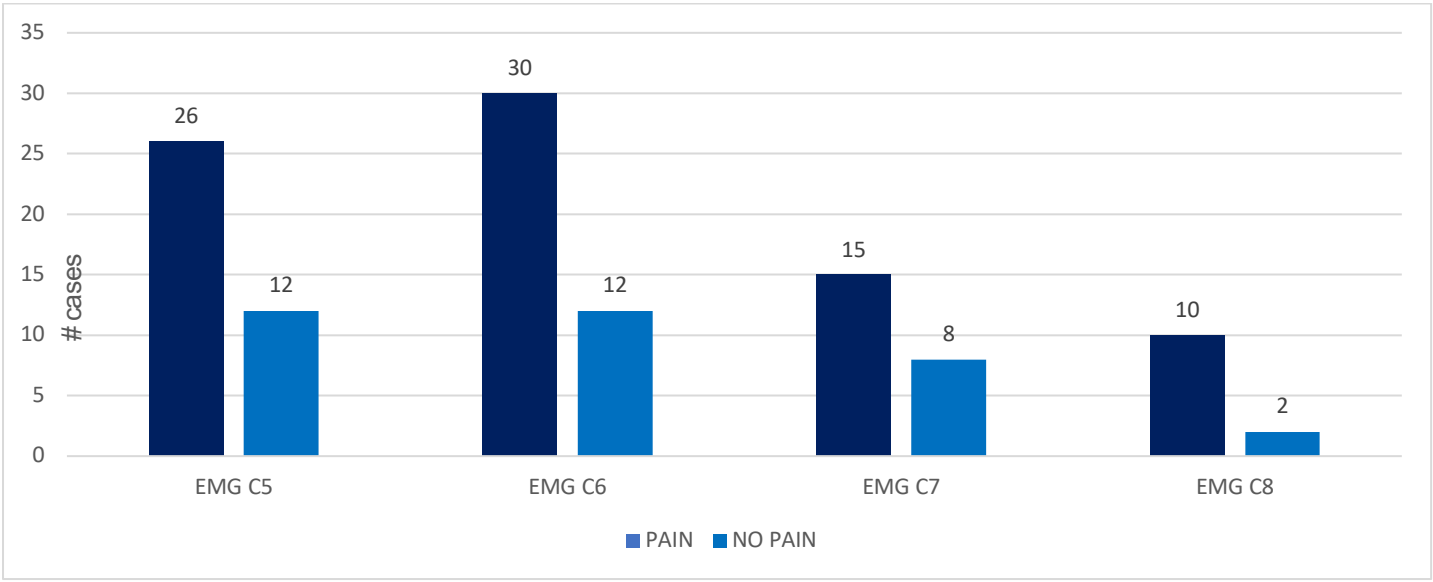

Figure 6: note - Graphic of the table 10, Pathologic Nerve Root at EMG with PAIN or NOT (#)

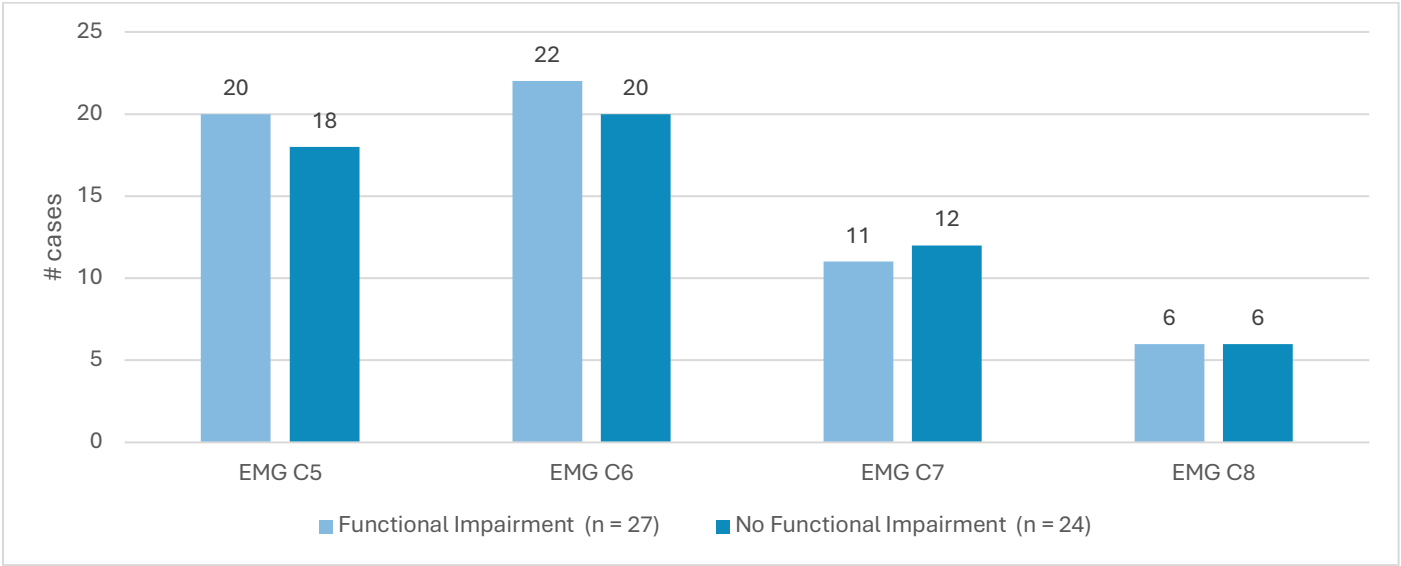

Figure 7: note - Graphic of the table 10, Pathologic Nerve Root at EMG with IMPAIRMENT or NOT (#)

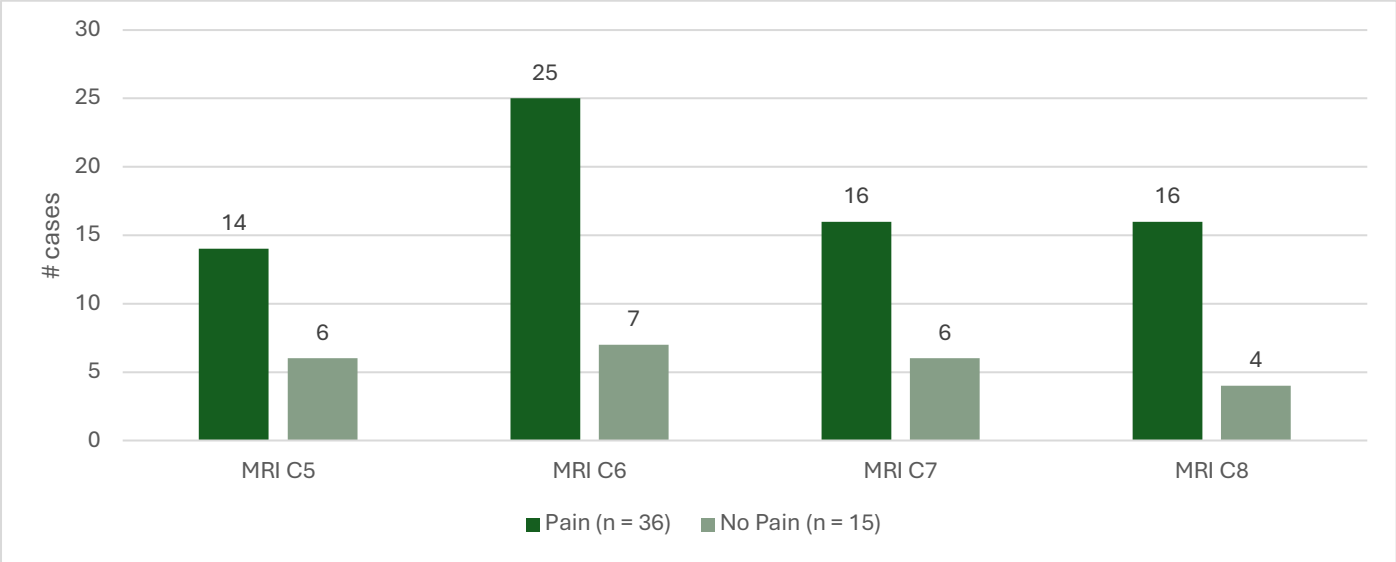

Figure 8: note - Graphic of the table 10, Pathologic Nerve Root at MRI with PAIN or NOT (#)

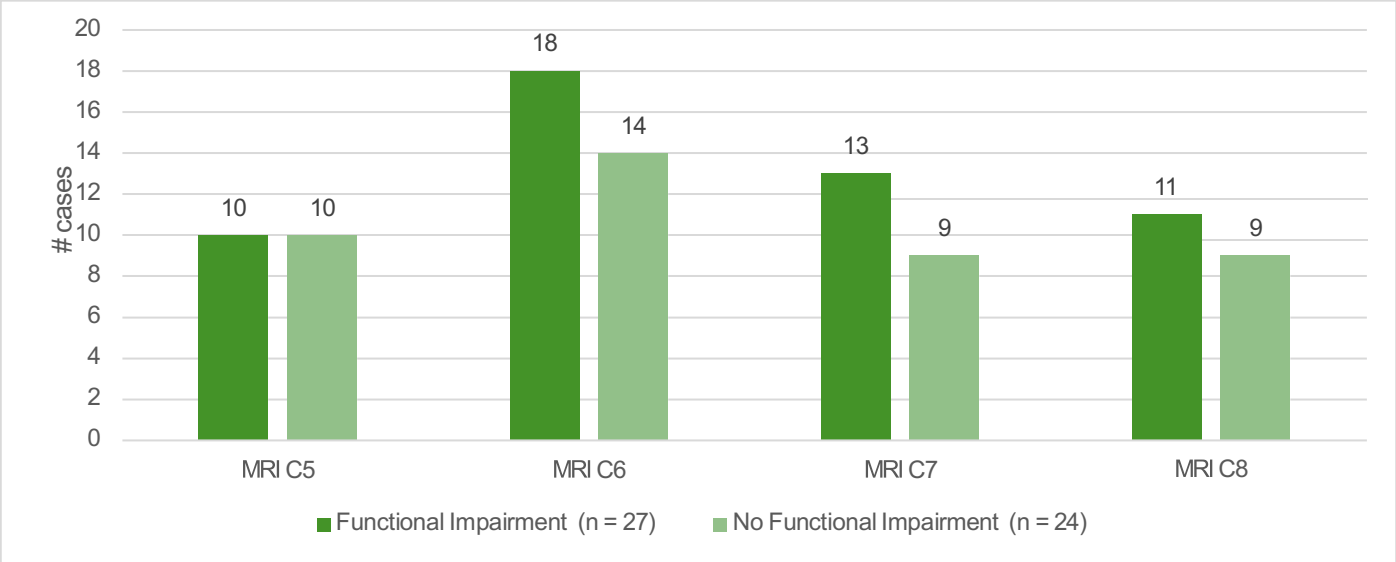

Figure 9: note - Graphic of the table 10, Pathologic Nerve Root at MRI with IMPAIRMENT or NOT (#)

MRI findings correlated with clinics

To better understand the muscular alterations underlying PTS, we analyzed MRI findings across various muscle groups, focusing on edema, fat infiltration, and atrophy, and correlated these with the presence or absence of pain and functional impairment.

Edema: Patterns and Clinical Associations

As shown in **Table 11** (see Appendix), most patients exhibited Grade 0 edema, indicating no visible inflammation. However, the analysis focused on Grades 1 and above, which reflect active or residual inflammatory processes.

- Pectoralis major and minor: Both muscles showed minimal involvement, with only 2% of patients presenting Grade 1 or 2 edema. No cases of Grade 3 or 4 were observed, suggesting limited inflammatory activity in these muscles.
- Subclavius: Similarly, only 2% of patients exhibited Grade 2 edema, reinforcing the notion that anterior shoulder girdle muscles are less frequently affected in symptomatic PTS.
- Serratus anterior: Showed slightly higher variability, with 11.8% of patients presenting Grade 1 and 2% with Grade 2 edema. However, no statistically significant correlation with pain or functional impairment was found.
- Deltoid: Demonstrated a broader distribution, with 23.5% of patients showing Grade 1 and 15.7% Grade 2 edema. Although not statistically significant, this variability may reflect underlying subclinical pathology and warrants further investigation.
- Trapezius: Notably, 11.8% of patients had Grade 1 and 5.9% had Grade 2 edema. A statistically significant association with pain was observed ($p = 0.026$), suggesting that even mild edema in this muscle may contribute to symptomatology.
- Latissimus dorsi: No edema was detected, indicating this muscle may serve as a reference for unaffected tissue in this cohort.
- Supraspinatus and infraspinatus: These muscles showed the highest incidence of edema, with 29.4% and 27.5% of patients exhibiting Grade 1 edema, respectively. Importantly, infraspinatus edema was significantly associated with pain ($p = 0.018$), highlighting its potential role in the clinical presentation of PTS.

The presence of mild to moderate edema (Grades 1-2) in specific muscles - particularly the trapezius and infraspinatus - suggests a meaningful link between localized inflammation and clinical symptoms such as pain and functional impairment. These findings support the hypothesis that muscle-specific inflammatory responses contribute to the heterogeneity of PTS presentations.

Fat Infiltration: Distribution and Clinical Correlation

Table 12 (see Appendix) presents the distribution of fat infiltration across shoulder girdle and arm muscles, categorized by the presence of pain and functional impairment, using a grading scale from 0 to 4 (including

subgrades 2A and 2B).

- Pectoralis major and minor: Minimal fat infiltration was observed, with only 3.9% of patients classified as Grade 2A. No higher grades were reported. There were no significant associations with pain ($p = 0.506$) or functional impairment ($p = 1.000$).
- Subclavius: Showed low involvement (2% in Grade 2A), with no significant differences based on symptoms ($p = 1.000$).
- Serratus anterior: 5.9% of patients were classified as Grade 2A. Again, no significant correlation with pain or impairment was found ($p = 1.000$).
- Deltoid: Displayed greater variability, with 7.8% in Grade 1 and 11.8% in Grade 2A. However, these findings were not statistically significant for pain ($p = 0.218$) or functional impairment ($p = 0.523$).
- Trapezius: 5.9% of patients showed Grade 1 infiltration, without significant associations (pain: $p = 0.203$; impairment: $p = 0.595$).

Among the rotator cuff muscles, the supraspinatus stood out: 21.6% of patients exhibited Grade 1 and 5.9% Grade 2A infiltration. A statistically significant association with pain was found ($p = 0.001$), suggesting a potential link between fat infiltration and symptom severity. The infraspinatus and subscapularis showed moderate infiltration (15.7% each in Grade 1), but without significant correlations. No fat infiltration was observed in the triceps, brachialis, or coracobrachialis, indicating these muscles were unaffected.

Fat infiltration was generally low across most muscles, with the supraspinatus being the only muscle showing both higher infiltration rates and a significant correlation with pain. This suggests a potential role in the pathophysiology of PTS-related discomfort.

Atrophy: Prevalence and Symptom Association

Table 13 (see Appendix) details muscle atrophy findings, comparing patients with and without pain and functional impairment.

- In the pectoralis major and minor muscles, atrophy was observed in 7.8% of patients. However, no statistically significant differences were found between patients with and without pain ($p = 1.000$), suggesting that atrophy in these muscles may not be directly linked to symptom severity.
- The subclavius muscle showed a low prevalence of atrophy, affecting only 2% of the cohort. This finding was consistent across symptomatic and asymptomatic individuals, with no significant association with pain ($p = 1.000$).
- For the serratus anterior, atrophy was present in 7.8% of patients, but notably, no cases were recorded among those without pain. Despite this trend, the difference did not reach statistical significance ($p = 0.307$), indicating that the observed variation may not be clinically meaningful.
- The deltoid muscle exhibited a higher prevalence of atrophy, affecting 21.6% of patients. Interestingly, the condition was slightly more frequent among those without pain, although the difference was not statistically significant ($p = 0.711$), suggesting that deltoid atrophy may occur independently of pain

perception.

- In the trapezius muscle, atrophy was identified in 5.9% of patients, with no significant differences between symptomatic and asymptomatic groups (p = 1.000). Similarly, no atrophy was observed in the latissimus dorsi or rhomboid muscles, indicating these regions were spared in this cohort.
- Among the rotator cuff muscles, the supraspinatus demonstrated the highest rate of atrophy, affecting 41.2% of patients. A statistically significant difference was found between those with pain (30.6%) and those without (66.7%) (p = 0.028), suggesting a potential link between supraspinatus atrophy and the presence of pain, possibly reflecting different stages of disease progression or compensatory mechanisms. The infraspinatus and subscapularis muscles were also commonly affected, with atrophy rates of 29.4% and 25.5%, respectively. However, neither showed a significant correlation with pain status, indicating that their involvement may not directly influence symptom expression.
- In the triceps, atrophy was observed in 3.9% of patients, with no significant differences between groups. The brachialis muscle showed a low overall prevalence (2%), with a slightly higher rate among patients reporting pain (6.7%), though this difference was not statistically significant (p = 0.294).
- Finally, in the scalene muscles - including the anterior, medial, and posterior groups - atrophy was present in 2% of patients for each subgroup. These cases were exclusively observed in individuals with functional impairment, yet the association did not reach statistical significance (p = 0.294).

While atrophy was observed in several muscle groups, only the supraspinatus showed a statistically significant association with pain. Most other muscles exhibited similar atrophy rates regardless of symptom presence, suggesting that muscle atrophy in PTS may not consistently correlate with clinical symptoms in all cases analyzed.

EMG findings correlated with MRI

In this study, all patients underwent EMG assessment prior to MRI, enabling a sequential diagnostic approach. This methodology allowed for a direct comparison between neurophysiological and radiological findings. By integrating EMG results with MRI data, it aimed to better characterize the patterns of nerve involvement and their clinical correlates. This combined analysis enhances our understanding of the pathophysiological mechanisms underlying PTS and may refine the interpretation of imaging findings in light of functional nerve assessments. The correlations between EMG and MRI findings, along with their relationship to clinical presentations, are summarized in **Table 14**, offering an overview of how these diagnostic modalities complement each other in the context of PTS.

Table 14 – Nerve characteristics by EMG Findings

	EMG Neurogenic Impairment			EMG Denervation Activity		
	Yes (n = 41)	No (n = 10)	p-value	Yes (n = 10)	No (n = 41)	p-value
Side						
Right	17 (41.5)	4 (40)	1.000	5 (50)	16 (39)	0.816
Left	16 (39)	4 (40)		4 (40)	16 (39)	
Both	8 (19.5)	2 (20)		1 (10)	9 (22)	
EMG C5	31 (75.6)	7 (70)	0.701	7 (70)	31 (75.6)	0.701
EMG C6	34 (82.9)	8 (80)	1.000	9 (90)	33 (80.5)	0.667
EMG C7	19 (46.3)	4 (40)	1.000	7 (70)	16 (39)	0.154
EMG C8	11 (26.8)	1 (10)	0.417	4 (40)	8 (19.5)	0.218
MRI C5	17 (41.5)	3 (30)	0.721	2 (20)	18 (43.9)	0.280
MRI C6	27 (65.9)	5 (50)	0.470	5 (50)	27 (65.9)	0.470
MRI C7	19 (46.3)	3 (30)	0.483	4 (40)	18 (43.9)	1.000
MRI C8	18 (43.9)	2 (20)	0.280	4 (40)	16 (39)	1.000

Note: Results are reported as relative frequencies and percentages. N/A: Statistical Test Not Applicable

Table 14 presents a comparative analysis of neurogenic impairment and denervation activity across cervical nerve roots (C5–C8), assessed through EMG. The data are visualized using two variables representing neurogenic impairment and denervation activity at EMG compared with laterality and EMG/MRI findings.

When examining *side involvement*, the distribution was relatively balanced. Among patients with neurogenic impairment, 41.5% had right-sided involvement, 39% left-sided, and 19.5% bilateral. These proportions were nearly identical in patients without impairment (40%, 40%, and 20%, respectively), with no significant differences ($p = 1.000$ for all comparisons). Among patients without denervation activity were also balanced between the two sides.

In the analysis with *neurogenic impairment*, the most frequently involved roots on EMG were C5 and C6, with 31 and 34 cases respectively. MRI findings similarly showed a high frequency of involvement at C6 (27 cases). Despite these trends, statistical analysis revealed no significant differences between patients with and without neurogenic impairment (all p-values > 0.05), indicating that the observed distributions may not reflect clinically meaningful distinctions.

In the *analysis of denervation* activity, EMG again highlighted C5 and C6 as the most commonly affected roots. While EMG C7 showed a lower p-value (0.154), suggesting a possible trend toward significance, it did not meet the conventional threshold ($p < 0.05$). MRI findings were more evenly distributed across roots, and no statistically significant associations were observed.

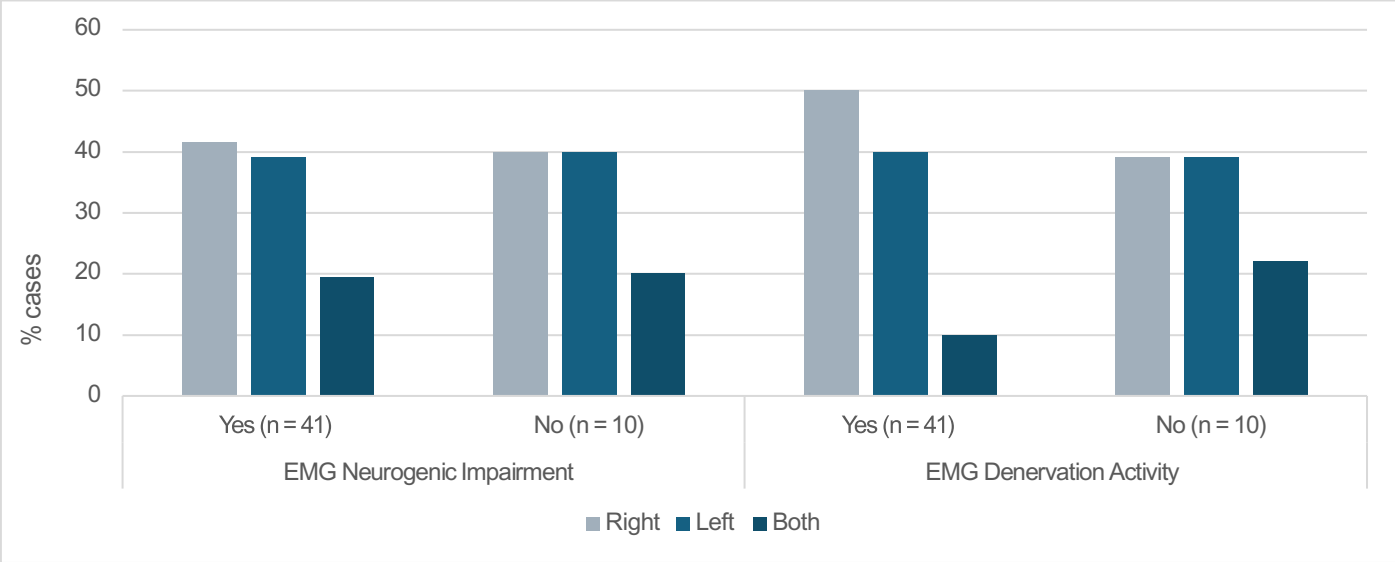

Figure 10: Note - graphic of the table 14, Nerve Characteristics from EMG Findings – Pathologic Side

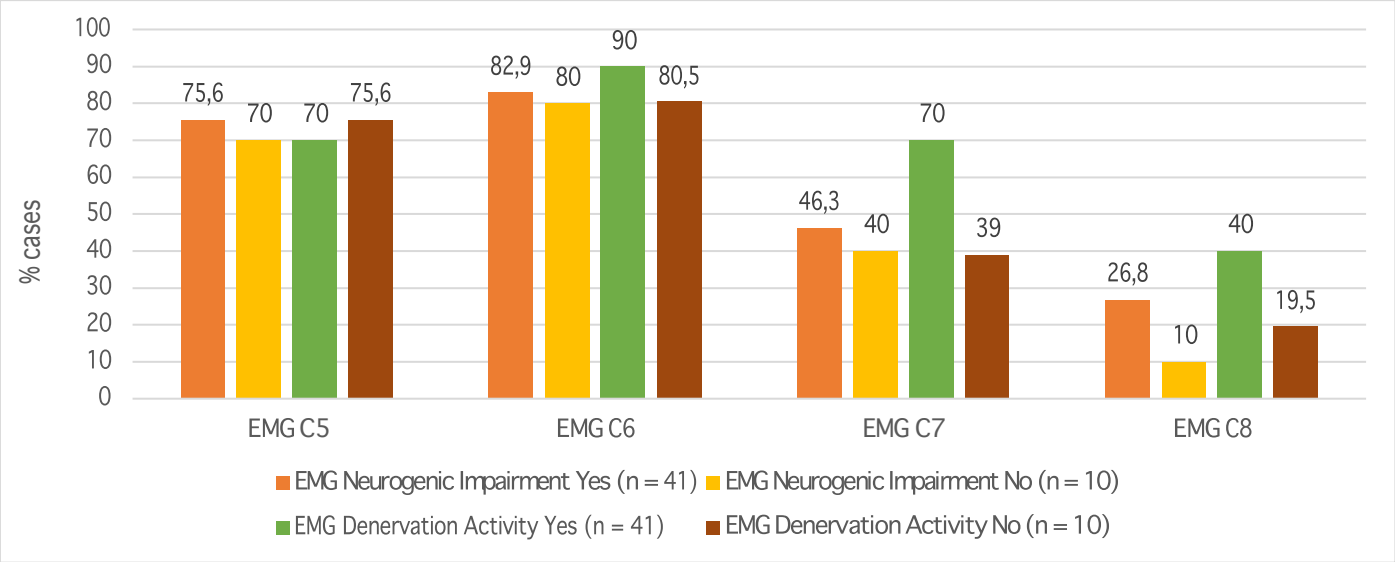

Figure 11: Note - Graphic of the table 14, Nerve Characteristics from EMG Findings at EMG

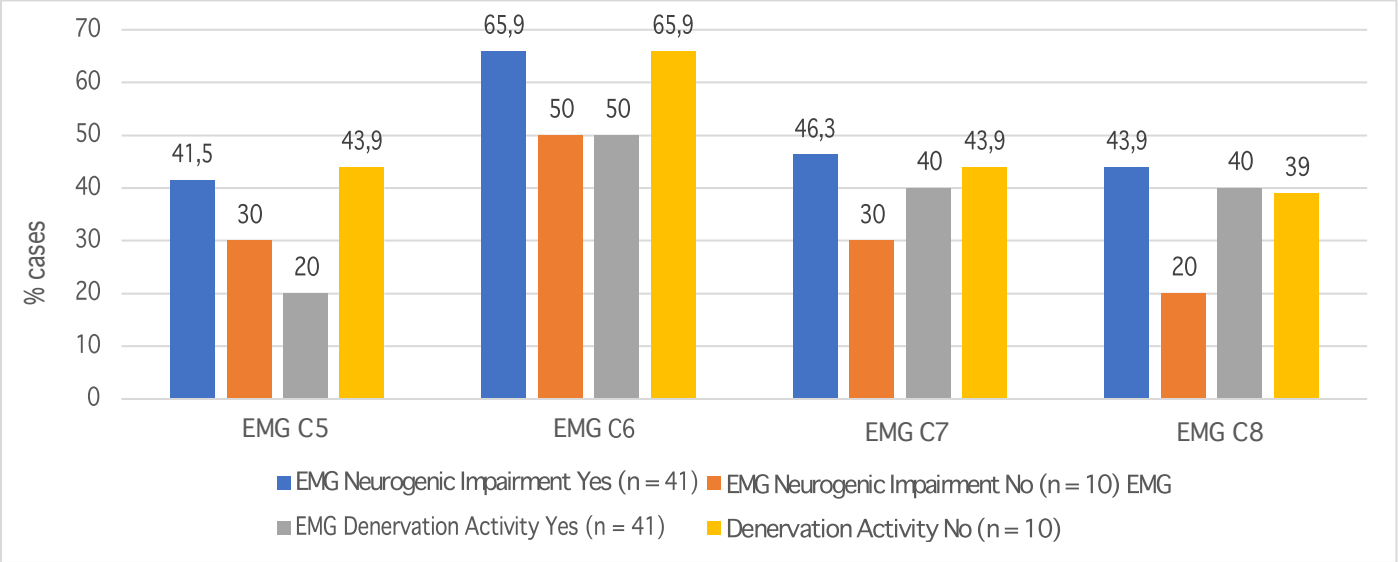

Figure 12: Note - Graphic of the table 14, Nerve Characteristics from EMG Findings at MRI

Correlation Between EMG and MRI Findings

Although trends were observed linking EMG-detected neurogenic impairment and denervation activity with MRI abnormalities across cervical nerve roots, none of these associations reached statistical significance. Specifically, no significant differences emerged between patients with and without neurogenic impairment regarding the side of involvement (right, left, or bilateral), suggesting that laterality does not substantially influence the presence of EMG abnormalities.

When analyzing individual nerve roots, a consistently higher proportion of patients with neurogenic impairment showed abnormalities on both EMG and MRI - particularly at C5, C6, C7, and C8 - compared to those without impairment. For instance, EMG abnormalities at C6 were present in 82.9% of impaired patients versus 80% of non-impaired, while MRI abnormalities at the same root were observed in 65.9% versus 50%, respectively. Similarly, C8 involvement was more frequent in the impaired group on both EMG (26.8% vs. 10%) and MRI (43.9% vs. 20%). Despite these numerical differences, all p-values exceeded the threshold for statistical significance ($p > 0.05$), likely due to the limited sample size, particularly in the non-impaired subgroup.

Overall, while EMG and MRI consistently identified C5 and C6 as the most frequently involved roots - consistent with the typical pattern of cervical radiculopathy - none of the comparisons between impaired and non-impaired groups reached statistical significance. These findings suggest that although certain trends are evident, further investigation with larger sample sizes may be necessary to clarify the clinical relevance of these observations.

MRI finding correlated with EMG

Given the predominance of neurogenic impairment and partially of denervation activity observed in the EMG findings of patients with PTS, it is essential to explore how these electrophysiological alterations correspond to

structural muscle changes on MRI: edema, fat infiltration, and atrophy.

Edema – **Table 15** (see Appendix) presents an analysis of edema distribution across various muscle groups in 51 patients, 41 of whom exhibited EMG-confirmed neurogenic impairment with denervation activity, and 10 without.

- In the pectoralis major and minor, nearly all patients with neurogenic impairment exhibited Grade 1 or 2 edema (2.4% each), with no cases of Grades 3 or 4. A similar pattern was observed in the subclavius, where 2.4% showed Grade 2 edema, again without higher-grade involvement.
- The serratus anterior showed greater variability: 9.8% of patients with neurogenic impairment had Grade 1 edema and 2.4% had Grade 2. Interestingly, 20% of patients without impairment also exhibited Grade 1 edema, suggesting that mild edema in this muscle may occur independently of neurogenic changes.
- In the deltoid, 22% of patients with neurogenic impairment had Grade 1 edema and 17.1% had Grade 2. The non-impaired group showed a similar but slightly lower distribution. The trapezius showed edema in 14.6% (Grade 1) and 7.3% (Grade 2) of impaired patients, while no edema was observed in the control group, suggesting a stronger association with neurogenic pathology.
- The latissimus dorsi was unaffected in all patients. In the levator scapulae, 2.4% of impaired patients showed Grade 2 edema, with no cases in the control group.
- For the rhomboid major and minor, Grade 1 edema was observed in 4.9% and 2.4% of impaired patients, respectively. Interestingly, one patient in each muscle group from the non-impaired cohort also showed Grade 1 edema. The teres major and minor followed a similar trend, with a few cases of Grade 1 edema only in the impaired group.
- The supraspinatus muscle showed the highest incidence: 29.3% of impaired patients had Grade 1 edema and 19.5% had Grade 2. The infraspinatus followed closely, with 29.3% at Grade 1 and 14.6% at Grade 2. These findings suggest a strong correlation between neurogenic impairment and edema in the rotator cuff.
- In the subscapularis, 26.8% of impaired patients had Grade 1 edema, with minimal higher-grade involvement. The triceps showed Grade 1 edema in 9.8% and Grade 2 in 2.4% of impaired patients, with slightly lower rates in the control group.
- No edema was observed in the anconeus, brachialis, or coracobrachialis muscles in either group. The scalene muscles showed a few cases of Grade 1 edema among impaired patients, though overall incidence was low.

Although most patients presented with no edema (Grade 0), Grades 1 and 2 were notably more frequent among those with EMG-confirmed neurogenic impairment. This trend was particularly evident in the shoulder girdle

and rotator cuff muscles, suggesting a potential pathophysiological link.

Fat Infiltration – **Table 16** (see Appendix) provides a detailed assessment of fat infiltration in shoulder girdle muscles among all cases. Grade 0 findings dominate across all muscle groups, with minimal occurrences of higher grades.

- In the pectoralis major and minor, 95.1% of patients with neurogenic impairment and 100% of those without show Grade 0 infiltration. Only 4.9% of impaired patients exhibit Grade 2A, with no statistically significant difference between groups ($p = 1.000$). The subclavius follows a similar pattern: 97.6% at Grade 0 and 2.4% at Grade 2A in the impaired group ($p = 1.000$).
- The serratus anterior shows 92.7% of impaired patients at Grade 0 and 7.3% at Grade 2A, again without significant group differences ($p = 1.000$). In the deltoid, 78% of impaired patients are at Grade 0 and 14.6% at Grade 2A. Despite this slight increase, the difference remains statistically non-significant ($p = 0.544$).
- In the trapezius, 92.7% of impaired and 90% of non-impaired patients are at Grade 0, with 7.3% of the impaired group at Grade 1 ($p = 1.000$). Both the latissimus dorsi and levator scapulae show no fat infiltration in any patient (100% at Grade 0), rendering statistical comparison unnecessary.
- The rhomboid major shows 97.6% at Grade 0 and 2.4% at Grade 2A in the impaired group, while the rhomboid minor remains entirely unaffected (100% at Grade 0 in both groups). No significant differences are observed.
- Among rotator cuff muscles, the supraspinatus shows 68.3% at Grade 0 and 7.3% at Grade 2A in the impaired group ($p = 0.541$). The infraspinatus mirrors this distribution (68.3% at Grade 0), with additional lower-grade involvement ($p = 0.121$). The subscapularis shows 73.2% at Grade 0 and 17.1% at Grade 1 ($p = 0.616$), again without significant differences.
- Muscles of the arm and neck - including the triceps, anconeus, brachialis, and scalene - show no fat infiltration in any patient (100% at Grade 0), with no group differences.

Across all examined muscle groups, fat infiltration is minimal and predominantly limited to Grades 1 and 2A. The vast majority of patients, regardless of EMG neurogenic status, exhibit Grade 0 infiltration. Statistical analyses consistently reveal no significant differences between groups, suggesting that neurogenic impairment does not substantially influence fat infiltration in the studied muscles. Further research may be warranted to explore other muscle groups or mechanisms potentially involved.

Atrophy – **Table 17** (see Appendix) presents the analysis for a comparative evaluation of atrophy prevalence across muscle groups among all cases with EMG-confirmed neurogenic impairment and without.

- In the pectoralis major and minor, atrophy is rare, observed in 7.3% of impaired and 10% of non-impaired patients ($p = 1.000$), with no evidence of denervation-related atrophy. The subclavius shows

atrophy in 2.4% of impaired patients and none in the control group (p = 1.000). The serratus anterior shows slightly higher involvement (9.8% in the impaired group), but again, no significant difference is found (p = 0.573).

- The deltoid exhibits a more notable prevalence: 24.4% of impaired patients show atrophy compared to 10% of controls (p = 0.428). In the trapezius, atrophy is present in 4.9% of impaired and 10% of non-impaired patients (p = 0.488). The latissimus dorsi shows no atrophy in either group.
- In the levator scapulae, atrophy is observed in 2.4% of impaired and 10% of non-impaired patients (p = 0.357). The rhomboid major and minor show no atrophy in any patient. Similarly, the teres major and minor show low prevalence (2.4% in impaired vs. 10% in non-impaired), with no significant differences (p = 0.357).
- Among rotator cuff muscles, the supraspinatus shows the highest atrophy rates: 41.5% in the impaired group and 40% in the control group (p = 1.000). The infraspinatus shows atrophy in 24.4% of impaired and 50% of non-impaired patients (p = 0.135). The subscapularis follows a similar trend (24.4% vs. 30%, p = 0.701), with no significant group differences.
- In the triceps, atrophy is seen in 2.4% of impaired and 10% of non-impaired patients (p = 0.357). The anconeus and coracobrachialis show no atrophy in either group. The brachialis shows atrophy in 2.4% of impaired patients only (p = 1.000).
- The scalene muscles (anterior, medial, posterior) show no atrophy in the impaired group, while 10% of non-impaired patients exhibit atrophy in each (p = 0.196), again without statistical significance.

Overall, muscle atrophy is relatively infrequent across most muscle groups, with the deltoid and supraspinatus showing the most notable involvement in patients with neurogenic impairment. However, statistical analysis reveals no significant differences between groups, suggesting that EMG-confirmed neurogenic impairment does not consistently correlate with increased atrophy in the studied muscles.

MRI Results of the visual inspection of subscapularis muscles with clinics associated:

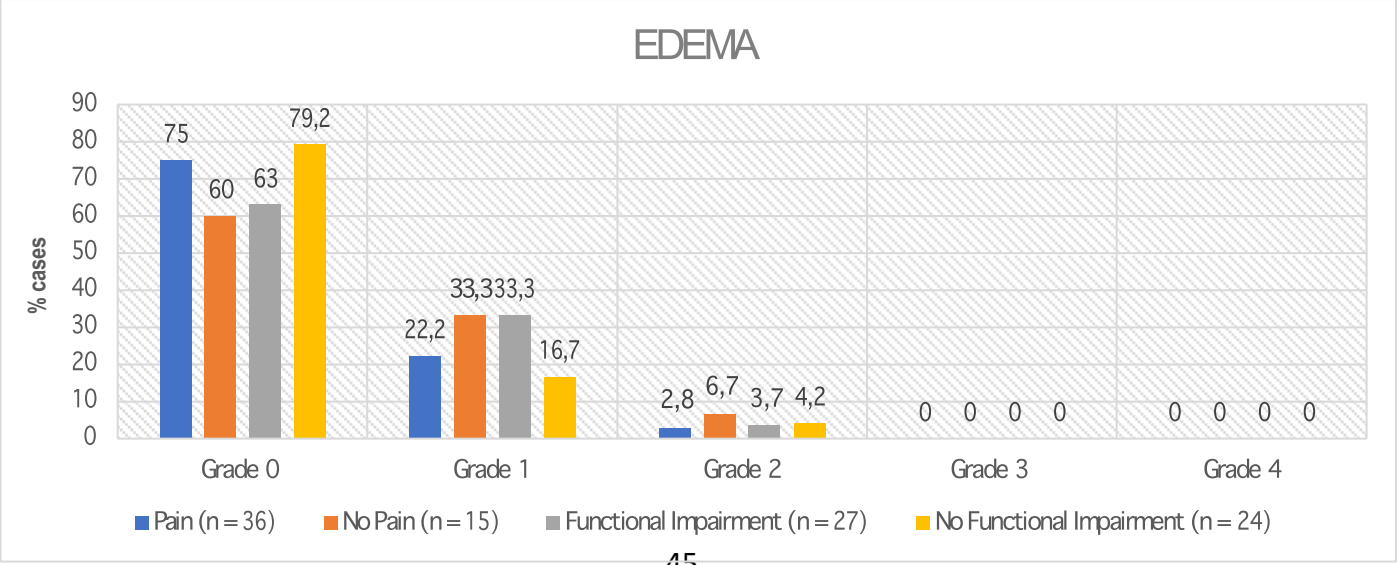

Figure 13: Note - Graphic part of the Table 15, at MRI: 29.4% of PTS with Edema: 25 % with PAIN and 37 % with functional impairment

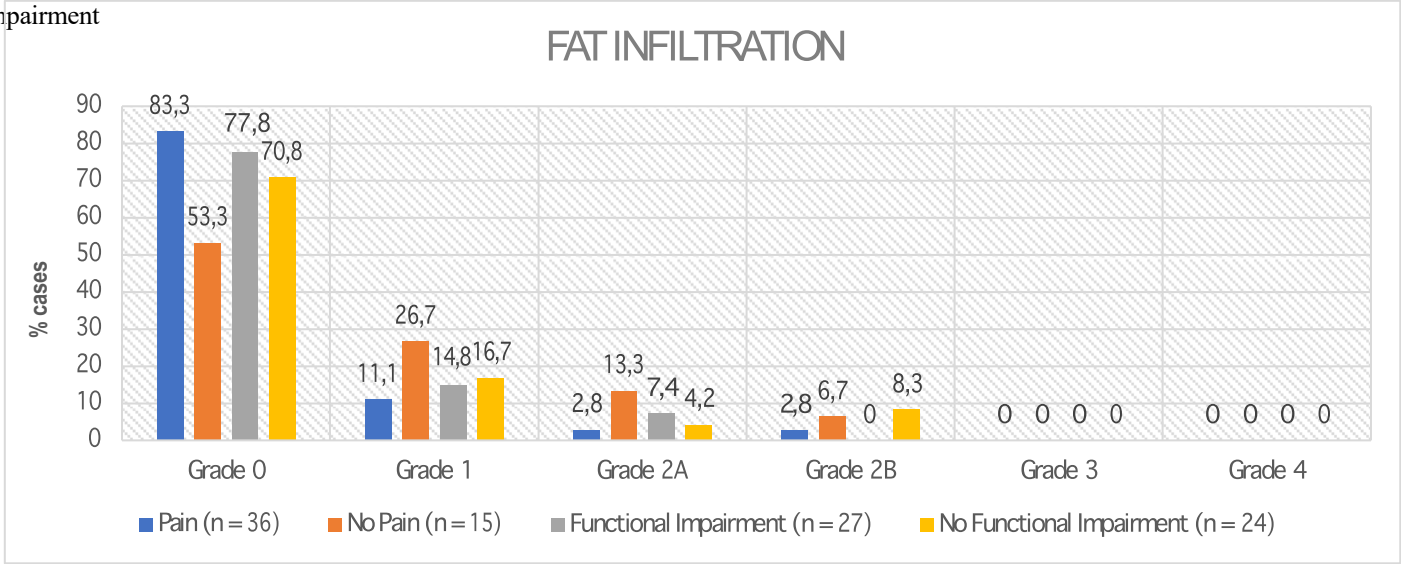

Figure 14: Note - Graphic part of the Table 16, at MRI: 31% of PTS with Fat Infiltration: 25 % with PAIN and 33.3 % with functional impairment

MRI Results of the visual inspection of supraspinatus muscles with clinics associated:

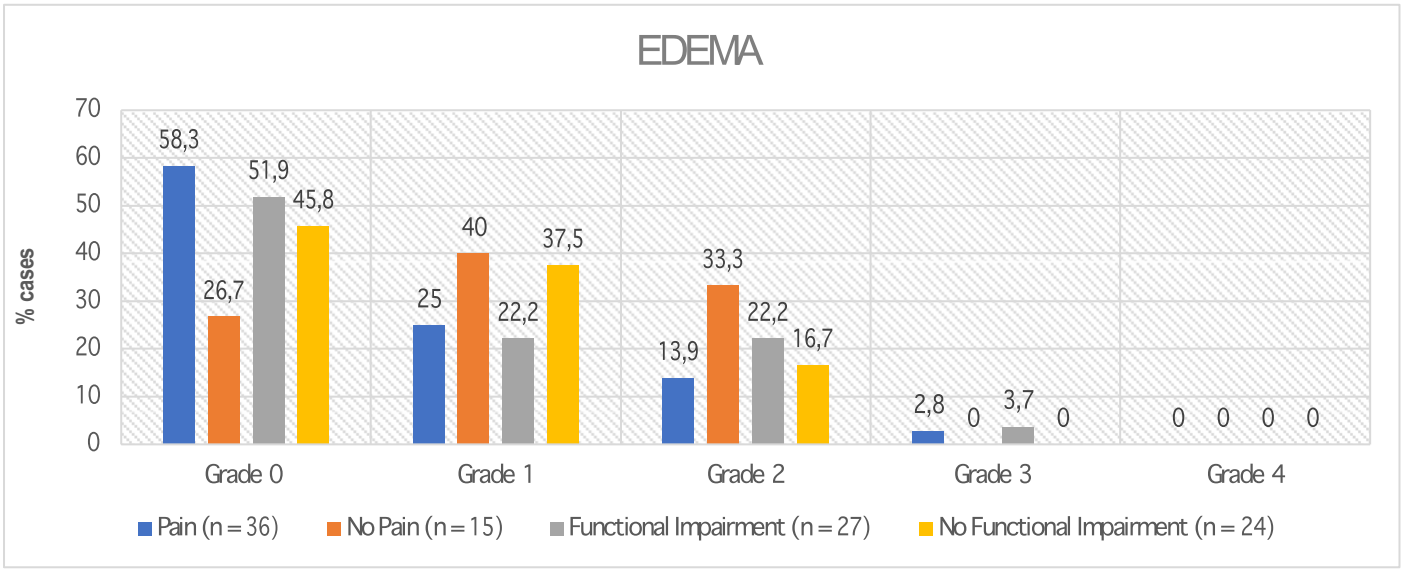

Figure 15: Note - Graphic of the table 15, at MRI: 51% of PTS with Edema: 41.9 % with PAIN and 48.1 % with functional impairment

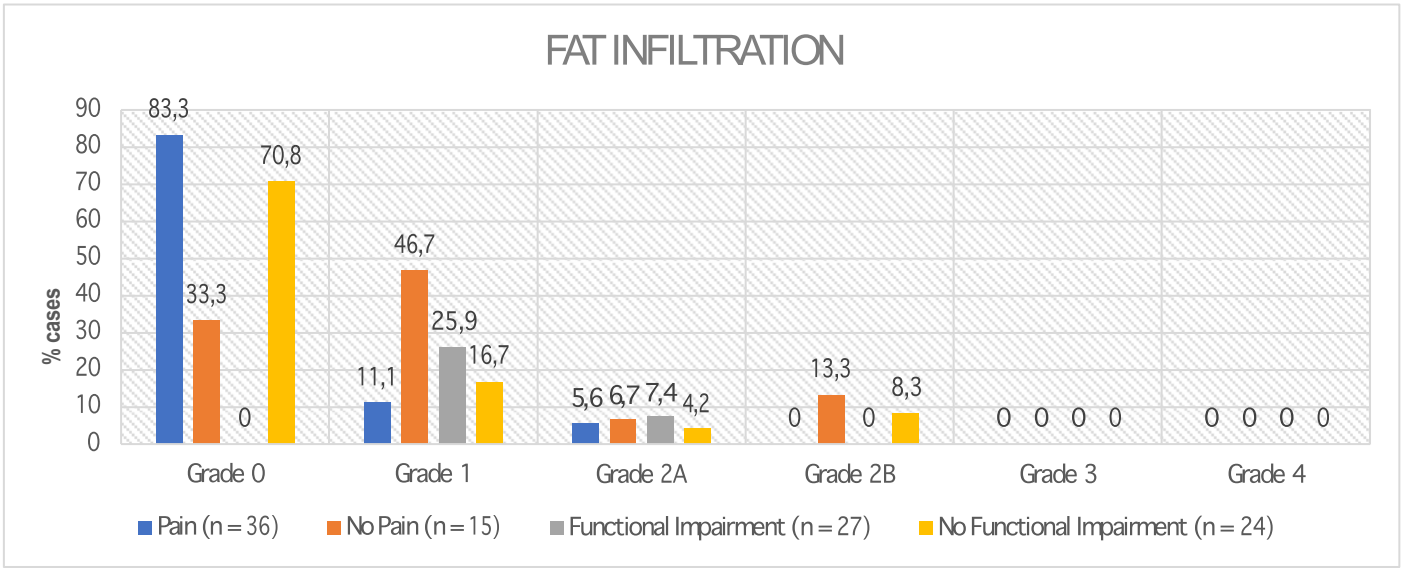

Figure 16: Note – Graphic of the Table 16, at MRI: 33.3% of PTS with Fat Infiltration: 16.7 % with PAIN and 33.3 % with functional impairment

MRI Results of the visual inspection of infraspinatus muscles with clinics associated:

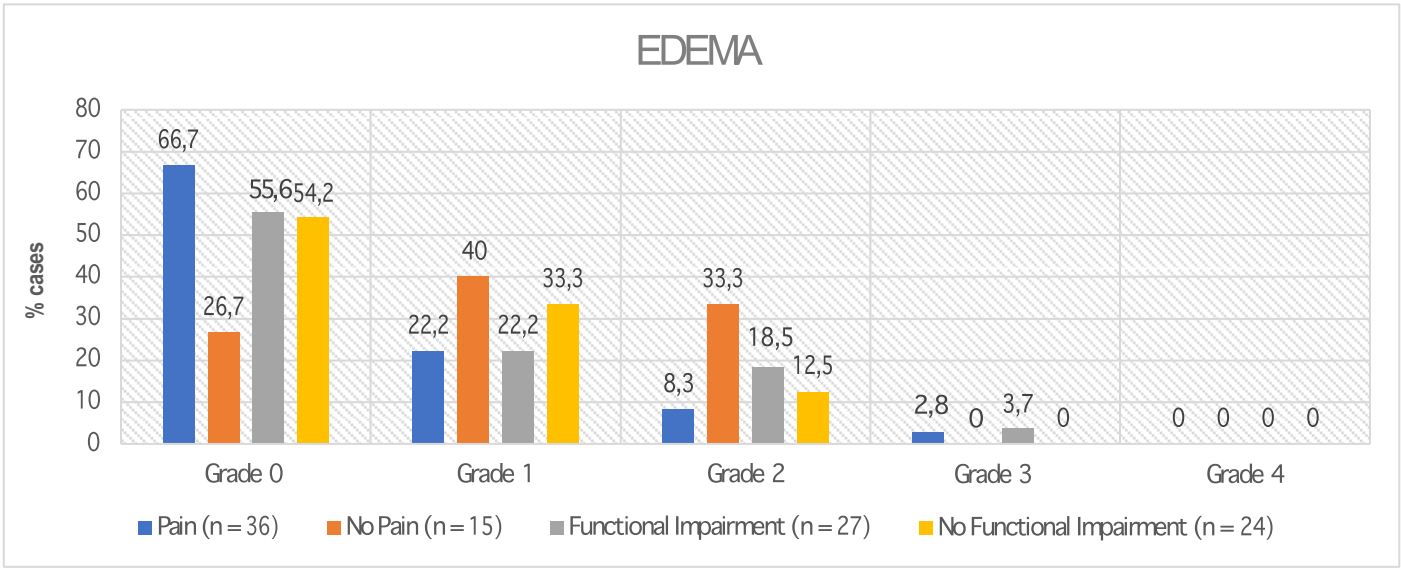

Figure 17: Note – Graphic of the table 15, at MRI: 45.1% of PTS with Edema: 33.3 % with PAIN and 44.4 % with functional impairment

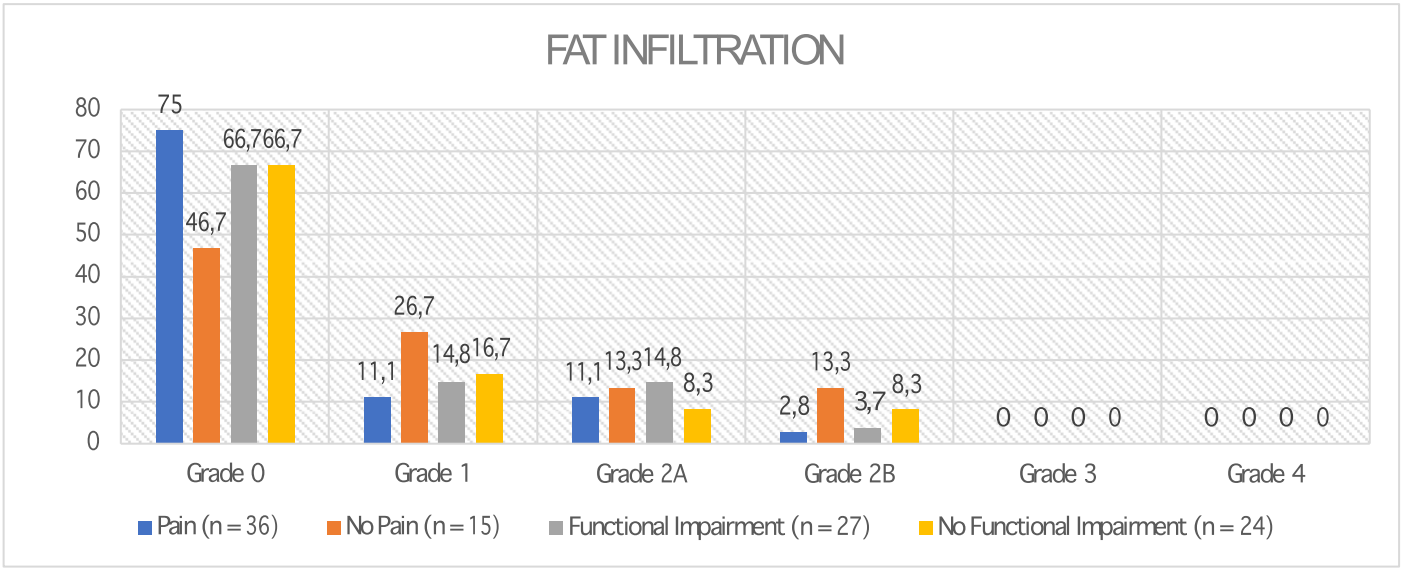

Figure 18: Note – Graphic of the table 16, at MRI: 25.5% of PTS with Fat Infiltration: 16.7 % with PAIN and 22.2 % with functional impairment

MRI Results of the visual inspection of *subscapularis, supraspinatus and infraspinatus* muscles with clinics associated:

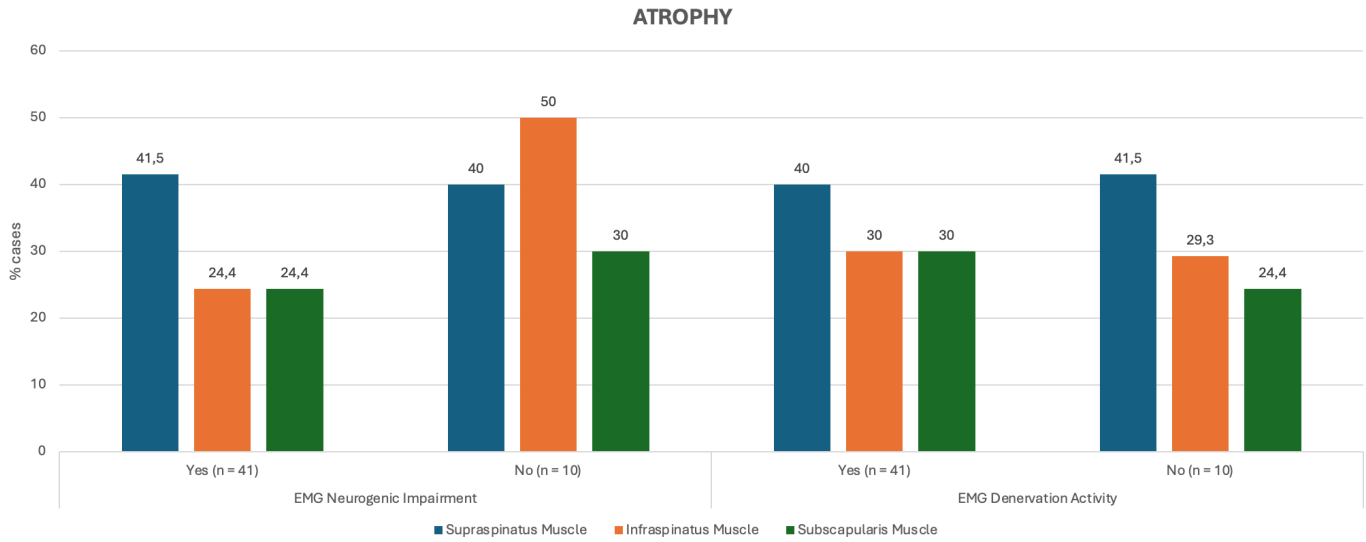

Figure 19: Note – Graphic of the table 17, at MRI: 58.8% of PTS with Atrophy: 69.4 % with PAIN and 55.6 % with functional impairment

6.2 Analysis of Nerve Changes on Quantitative Measurements

In the evaluation of nerve alterations associated with PTS, quantitative imaging measurements offer critical insights into the extent and nature of nerve involvement. It is important to note that the findings presented are based on the specific sample analyzed; further studies with larger cohorts are necessary to validate and expand upon these results.

The analysis focused on the C5, C6, C7, and C8 nerve roots, evaluating both CSA and T2 relaxation times to assess structural alterations. CSA provides an estimate of nerve root size, with enlargement indicating potential inflammation and reduction suggesting atrophy or degeneration. T2 relaxation times are particularly sensitive to changes in tissue composition, with elevated values often reflecting edema or chronic pathological changes. These metrics enable direct comparison between patients with PTS and a matched control group of healthy individuals.

A total of 76 subjects participated in the study, comprising 23.7% females and 76.3% males, with a mean age of 50 ± 16.6 years. Comparative analysis between PTS patients and healthy controls revealed no statistically significant differences in age or gender distribution (see **Table 2**), supporting the validity of group comparisons. Among the PTS cohort (**Table 18**), 122 pathological nerve roots were identified and analyzed. Of these, 52.5% were located on the left side and 47.5% on the right, suggesting a slight lateral predominance that warrants further investigation. The C6 nerve root was the most frequently affected (32.8%), followed by C7 (23%), C8 (22.1%), and C5 (22.1%). The predominance of C6 involvement aligns with existing literature, likely due to its anatomical vulnerability within the brachial plexus.

These findings provide valuable insights into the anatomical distribution of nerve involvement in PTS. The frequent involvement of the C5-C8 roots, particularly C6, underscores the importance of targeted imaging and

electrodiagnostic evaluation in these regions.

6.3 Results of Differential Diagnosis

This database analysis aims to compare imaging parameters between patients with PTS and healthy control subjects. The primary objective is to identify and characterize morphological and signal alterations in cervical nerve roots, as visualized through MRI, to better understand the structural impact of PTS. An exploratory sub-analysis was conducted within the PTS cohort, comparing pathological nerve roots (those exhibiting imaging or clinical signs of disease) to non-pathological roots. This approach was designed to elucidate the extent of nerve involvement and its clinical implications.

The analysis focused on three key MRI-derived parameters: CSA, indicative of nerve root swelling or atrophy; AR, reflecting changes in nerve root shape; MED, associated with tissue composition, including edema or fat infiltration.

Comparison between patient with PTS and healthy subjects

PTS patients exhibited significantly larger nerve root diameters compared to controls, suggesting structural alterations consistent with inflammatory or degenerative processes. This enlargement was symmetrical, with no significant differences between right and left nerve roots, indicating a systemic rather than localized pattern of involvement. All examined nerve roots (C5-C8) were similarly affected, reinforcing the notion of a diffuse pathological process in PTS (see **Table 18**). A hierarchical linear model was employed to analyze ROI measurements, revealing significant differences in nerve root morphology between PTS patients and healthy controls. The model demonstrated a statistically significant increase in nerve root diameter among PTS patients ($F = 104.76$, $p < 0.001$), strongly rejecting the null hypothesis.

		Total (n = 76)			Healthy Subjects (CTL) (n = 25)			Patients with PTS (PTS) (n = 51)		
		CSA (mm)	AR (mm²)	MED	CSA (mm)	AR (mm²)	MED	CSA (mm)	AR (mm²)	MED
C5	Right	3.3±0.9 (2-5.4) [3,2.7-3.7]	17.9±7.5 (9.7-40.8) [15.4,12.6-21.3]	151.5±68.3 (68-387) [138,104-158.5]	2.8±0.4 (2-3.4) [2.9,2.4-3]	14.4±3.3 (9.7-22.3) [14.4,11.7-16.3]	131±41.8 (68-215) [123,101-153]	4.4±0.7 (3.2-5.4) [4.5,3.9-5.1]	25.9±8.3 (15.1-40.8) [24.6,19-29.8]	197.9±93.4 (86-387) [153,137-283]
	Left	3.2±0.8 (1.9-4.9) [3.1,2.6-3.9]	15.7±5.7 (7.2-35.5) [13.8,11.9-18.4]	148±59.4 (52-365) [141,106.5-178]	2.7±0.4 (1.9-3.3) [2.7,2.4-3]	12.8±2.6 (7.2-19.8) [12.8,11.7-13.8]	129.4±42.1 (52-213) [124,100-161]	4.1±0.7 (2.7-4.9) [4.2,3.5-4.7]	20.5±6.3 (11.5-35.5) [19.5,17-22.1]	178.9±71.6 (102-365) [164,117-215]
C6	Right	3.9±0.9 (2.3-5.6) [3.6,3-4.6]	24.6±9.8 (9-49.1) [21.7,17.3-31.2]	183.4±60.4 (94-370) [175,139-212]	3.2±0.5 (2.3-4.4) [3.3,2.9-3.5]	18.6±4.8 (9.9-31.2) [18.5,15.2-20.5]	167.6±44.6 (99-280) [156,133-201]	4.7±0.7 (3.2-5.6) [4.9,4.2-5.2]	32.1±9.1 (9-49.1) [31.5,27.2-38.7]	203.2±72 (94-370) [180,161.5-256.5]
	Left	3.6±0.8 (2.1-5.3) [3.4,3-4]	21.8±8.5 (8.5-45.7) [20.4,15.3-25.9]	181.9±57.2 (81.3-325) [182.5,132-220.5]	3.1±0.4 (2.1-4) [3.1,2.8-3.3]	17.5±4.6 (8.5-25.6) [16.5,14.7-20.6]	175.2±54.5 (81.3-275) [170,131-211]	4.3±0.7 (3.3-5.3) [4.1,3.7-4.9]	27.4±9.3 (11.2-45.7) [28.2,18.6-34]	190.7±61 (87-325) [194,146-239]
C7	Right	3.7±1 (2-6.4) [3.3,3-4.3]	24.3±10.6 (10.1-54.4) [22.9,14.7-31]	189.4±61 (85-348) [187,148-211]	3.1±0.5 (2-4.9) [3,2.9-3.2]	19.1±6.4 (10.1-31.7) [20.3,13.3-23.3]	172.4±46.7 (101-316) [173,136-205]	4.8±0.8 (3.3-6.4) [4.7,4.2-5.5]	34.3±10.1 (17.3-54.4) [34.2,27.7-37.4]	222.2±73.1 (85-348) [216,170-276]
	Left	3.8±1 (2.1-6.1) [3.6,3-4.5]	23.7±9 (10-44.2) [24,16.4-29]	188.4±52.8 (87-297) [183,150-222]	3.2±0.6 (2.1-4.5) [3.1,2.8-3.5]	19.2±6.3 (10-31.4) [18.7,14.1-25.7]	177.4±48.2 (87-285) [181,144-204]	4.8±0.6 (3.7-6.1) [4.9,4.4-5.2]	31.7±7.3 (19-44.2) [32.2,26.2-36.7]	208±56.6 (114-297) [203.5,163-250]
C8	Right	3.7±0.9 (2.1-5.6) [3.7,3-4.5]	25.6±9.7 (10.7-49.8) [25,17.2-31.1]	186.2±63.3 (72-309) [184,136-245]	3.2±0.6 (2.1-4.2) [3.2,2.9-3.6]	20.5±5.9 (10.7-32.9) [19,16.1-25.4]	174.5±63.1 (72-300) [172,117-219]	4.7±0.5 (3.8-5.6) [4.7,4.5-4.9]	34.6±8.5 (19.6-49.8) [34.2,28.3-41.1]	207.2±60.3 (130-309) [203,155-245]
	Left	3.7±1 (2.2-6.4) [3.3,3.1-4.5]	24.5±10 (10.7-50.5) [22.3,18.1-31.9]	185.8±61.8 (88-366) [180,137-217]	3.2±0.4 (2.2-3.9) [3.1,3-3.4]	20±6.2 (10.7-36.2) [19.5,15.3-22.3]	172.9±47.3 (88-253) [165,137-206]	4.9±0.9 (3.2-6.4) [4.9,4.5-5.5]	34±9.9 (16.9-50.5) [34.8,26.1-39.8]	212.5±80.4 (116-366) [186,149-289.5]

Diameter (mm)

* Results are reported as means ± standard deviation, with the range in round brackets. Results in squared brackets are median and interquartile range.

Table 18 – Brachial Nerve Root Diameter, Area and Signal Intensity – Controls vs. PTS*

In detail, a closer examination of nerve *root diameters* (CSA) in patients PTS reveals a consistent and notable enlargement when compared to healthy individuals (**Figure 20**). This increase is evident on both the right and left sides and spans multiple cervical levels, suggesting a widespread structural alteration rather than a localized issue. For instance, the C5 nerve root in PTS patients measured approximately 4.4 mm on the right and 4.1 mm on the left, whereas in healthy controls, the corresponding values were significantly smaller-around 2.8 mm and 2.7 mm, respectively. This trend continues with the C6 nerve root, where diameters reached 4.7 mm on the right and 4.3 mm on the left in the PTS group, compared to just over 3 mm in controls. The pattern remains consistent at the C7 level, with PTS patients showing diameters of 4.8 mm on both sides, while controls averaged just above 3 mm. Similarly, the C8 nerve root was enlarged in PTS patients, measuring 4.7 mm on the right and 4.9 mm on the left, in contrast to 3.2 mm in the control group on both sides.

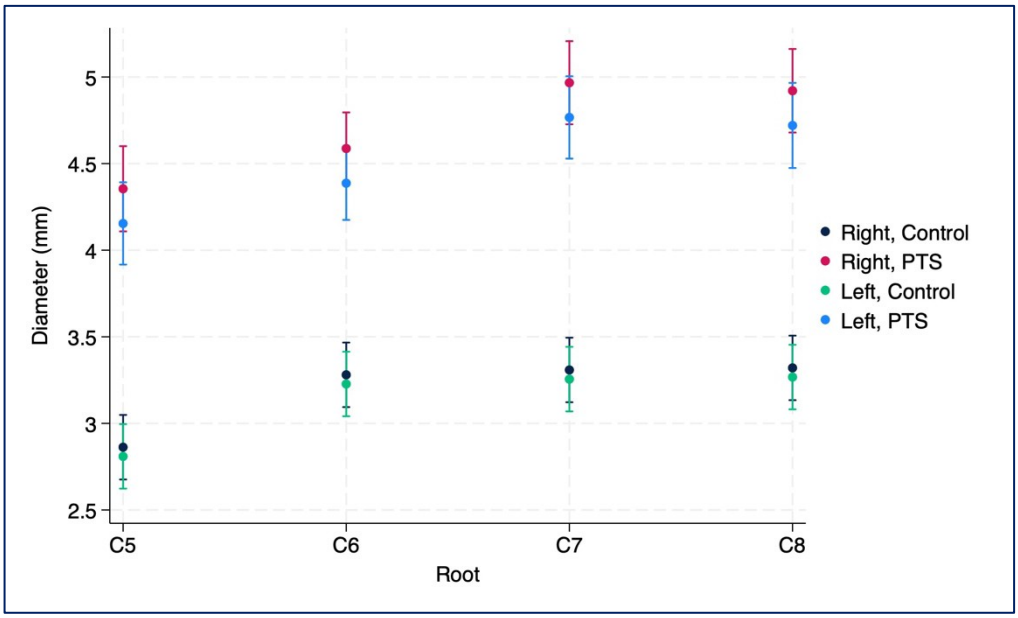

Figure 20: Scatter plot with 95% CI (vertical bars) of Nerve Root Diameter across Group, Roots, and Sides – Adjusted predicted means – Diameter (mm) – Comparison between PTS vs. CTL

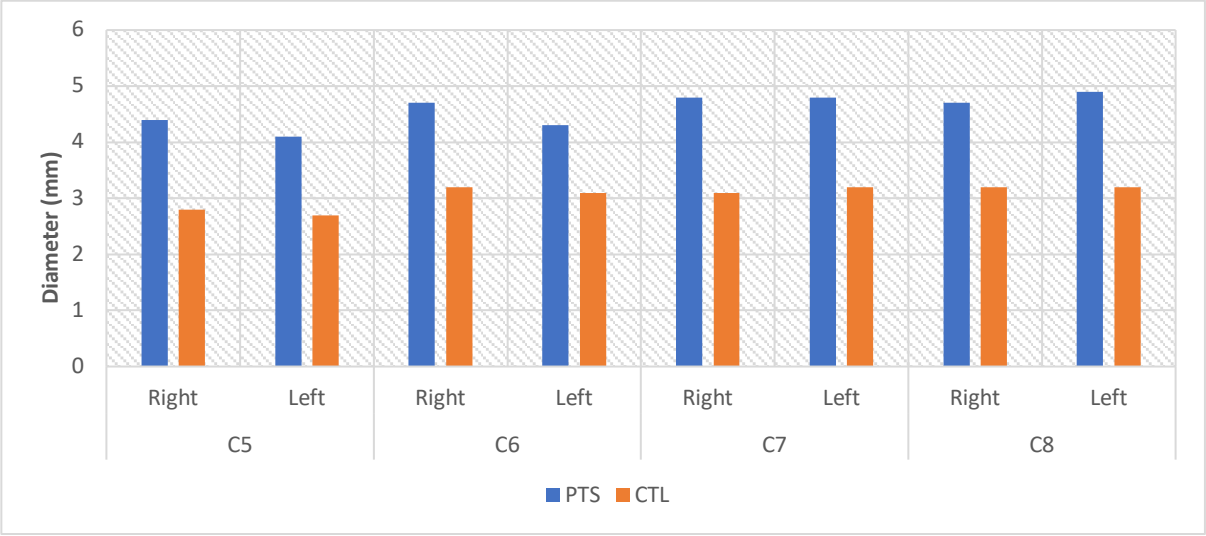

Figure 21: Note – Graphs displayed as histograms derived from the previous scatter plot: in C5 [right side - PTS: 4.4±0.7 mm, CTL: 2.8±0.4 mm; left side – PTS: 4.1±0.7 mm, CTL: 2.7±0.4 mm], in C6 [right side - PTS: 4.7±0.7 mm, CTL: 3.2±0.5 mm; left side – PTS: 4.3±0.7 mm, CTL: 3.1±0.4 mm], in C7 [right side - PTS: 4.8±0.8 mm, CTL: 3.1±0.5 mm; left side – PTS: 4.8±0.6 mm, CTL: 3.2±0.6 mm], and C8 [right side - PTS: 4.7±0.5 mm, CTL: 3.2±0.6 mm; left side – PTS: 4.9±0.9 mm, CTL: 3.2±0.4 mm]

A similar trend was observed in the analysis of nerve *root area* (AR), where patients with PTS exhibited significantly larger values compared to healthy controls. Statistical analysis confirmed this difference, with a robust main effect of group on nerve root area: $F(1,76) = 32.13$, $p < 0.001$. This enlargement was consistent across both right and left sides. Further analysis revealed a significant interaction between group and nerve root level ($F(1,76) = 11.62$, $p = 0.009$), indicating that the magnitude of difference varied depending on the specific nerve root. Notably, the C7 and C8 roots demonstrated the most pronounced increases in area, as illustrated in **Figure 22**. Post-hoc comparisons provided additional insight. On the right side, the C7 nerve root area in PTS patients measured 34.3 ± 10.1 mm², compared to 19.1 ± 6.4 mm² in controls. On the left, the values were 31.7 ± 7.3 mm² in PTS patients versus 19.2 ± 6.3 mm² in healthy individuals. The C8 nerve root followed a similar pattern: on the right, 34.6 ± 8.5 mm² in PTS patients versus 20.5 ± 5.9 mm² in controls; on the left, 34.0 ± 9.9 mm² versus 20.0 ± 6.2 mm², respectively.

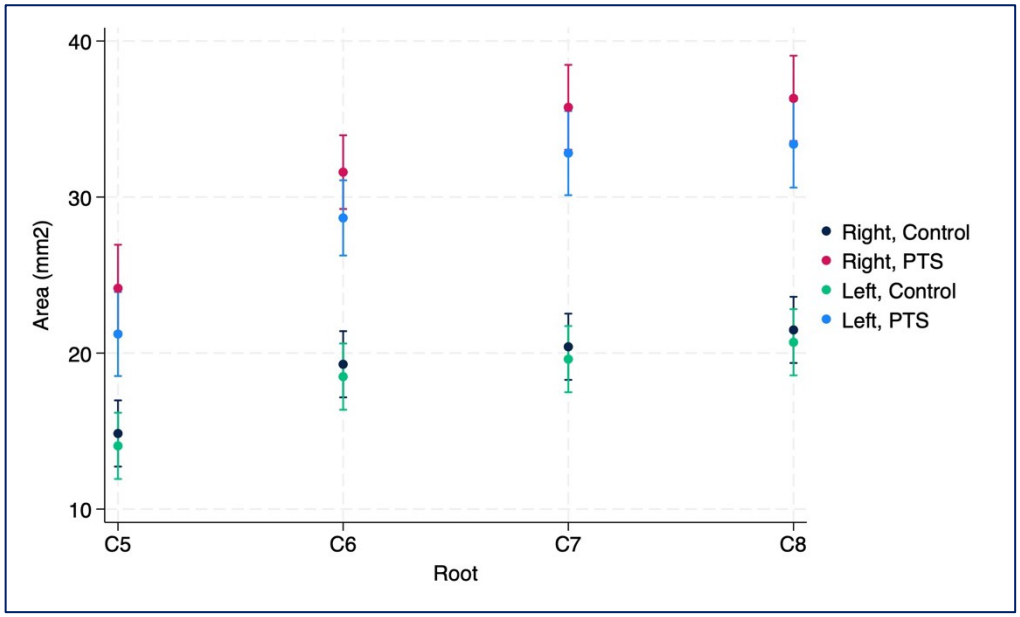

Figure 22: Scatter plot with 95% CI (vertical bars) of Nerve Root Area across Group, Roots, and Sides – Adjusted predicted means – Area (mm^2) – Comparison between PTS vs. CTL

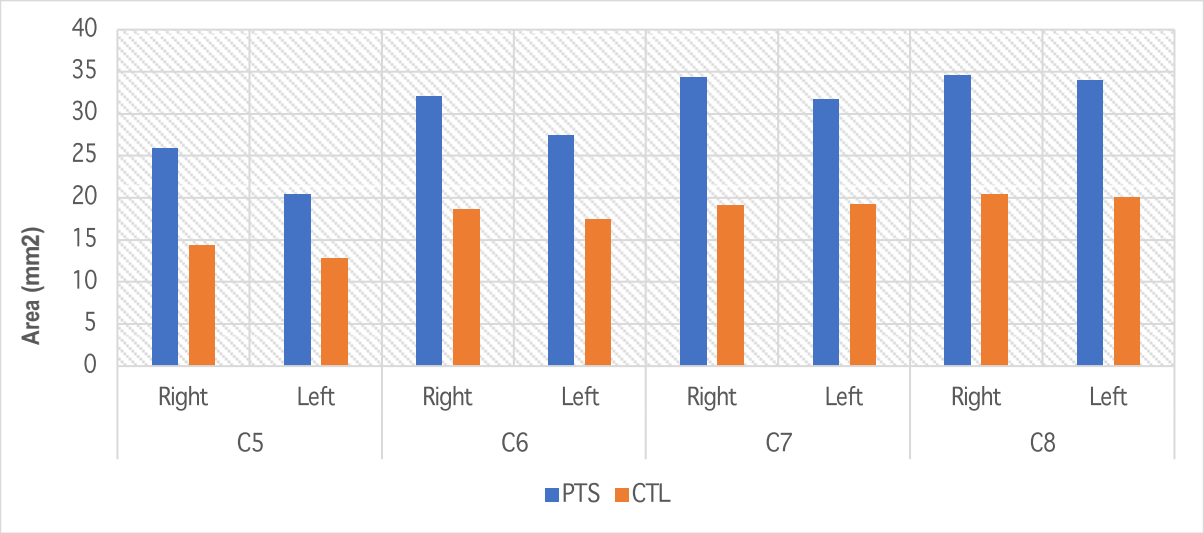

Figure 23: Note – Graphs displayed as histograms derived from the previous scatter plot: The post-hoc analysis showed that the nerve root areas of C7 and C8 were significantly higher in patients with PTS than in healthy subjects (C7 right: PTS: 34.3±10.1 mm2, CTR: 19.1±6.4 mm2; C7 left: PTS: 31.7±7.3 mm2, CTL: 19.2±6.3 mm2; C8 right: PTS: 34.6±8.5 mm2, CTL: 20.5±5.9 mm2; C8 left: PTS: 34±9.9 mm2, CTL:20±6.2 mm2].

Patients diagnosed with PTS exhibited significantly elevated *T2 signal intensity* (MED) values across cervical nerve roots when compared to healthy controls. Statistical analysis confirmed this difference, with a strong main effect of group: $F(1,76) = 24.92$, $p < 0.001$. This increase was consistent across both sides and all examined nerve roots, indicating a widespread alteration in tissue characteristics.

A more detailed analysis of individual nerve roots further highlighted these differences. For the C5 nerve root, PTS patients showed mean T2 signal intensities of 197.9 ± 93.4 on the right and 178.9 ± 71.6 on the left, compared to 131.0 ± 41.8 and 129.4 ± 42.1, respectively, in healthy controls. The C6 root followed a similar trend, with PTS patients recording 203.2 ± 72.0 on the right versus 167.6 ± 44.6 in controls. The C7 nerve root demonstrated even more pronounced differences: 222.2 ± 73.1 on the right and 208.0 ± 56.6 on the left in PTS patients, compared to 172.4 ± 46.7 and 177.4 ± 48.2 in controls. Finally, for the C8 root, signal intensity in the PTS group reached 207.2 ± 60.3 on the right, while controls averaged 174.5 ± 63.1. These findings, illustrated in **Figure 24**, underscore the diffuse and bilateral nature of T2 signal alterations and highlight the importance of T2 signal intensity as a potential biomarker for assessing the extent of nerve involvement in PTS.

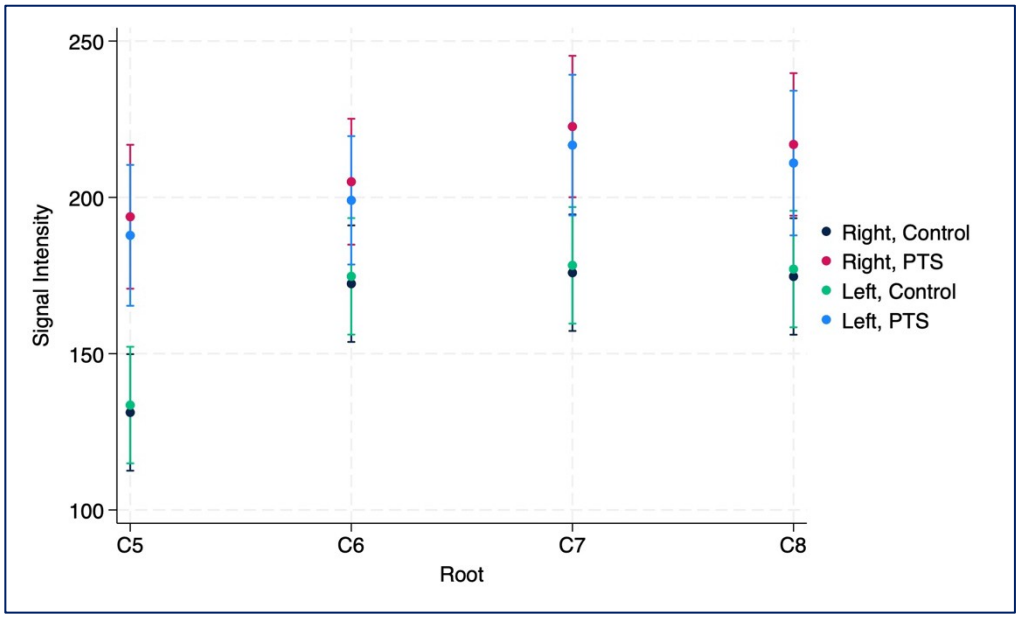

Figure 24: Scatter plot with 95% CI (vertical bars) of Nerve Root Signal Intensity across Group, Roots, and Sides - Adjusted predicted means - Signal Intensity - Comparison between PTS vs. CT

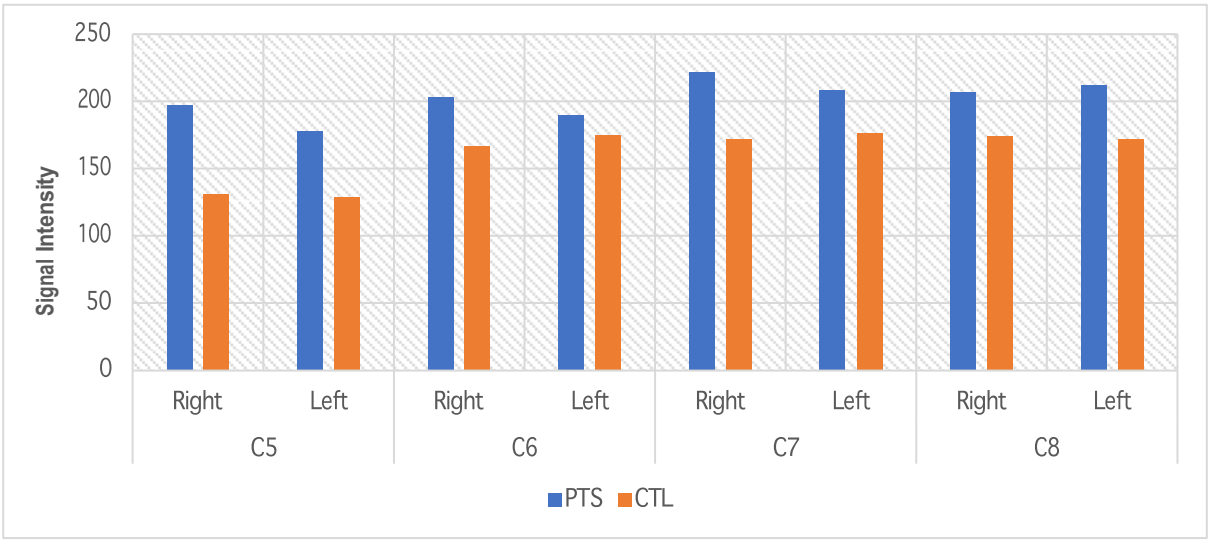

Figure 25: Note - Graphs displayed as histograms derived from the previous scatter plot: [right side - PTS: 197.9±93.4, CTL:131±41.8; left side - PTS: 178.9±71.6, CTL: 129.4±42.1], in the right C6 [PTS: 203.2±72, CTL:167.6±44.6], in the right and left C7 [right side - PTS: 222.2±73.1, CTL:172.4±46.7; left side – PTS: 208.0±56.6, CTL: 177.4±48.2], and in the right C8 [PTS: 207.2±60.3, CTL:174.5±63.1].

Comparison between health and pathological nerve roots within patients with PTS

As part of the investigation, a subgroup analysis was conducted to differentiate between the measurements of pathological and non-pathological nerve roots within the cohort of patients diagnosed with PTS. This analysis included an evaluation of 412 individual nerve roots, offering a dataset for identifying measurable anatomical differences.

The results demonstrated a statistically significant increase in the *diameter* of pathological nerve roots compared to non-pathological ones. This difference was supported by statistical evidence [F(1,51) = 11.44, p = 0.001], indicating a substantial effect size. These findings suggest that nerve roots affected by PTS are not only clinically distinguishable but also present quantifiable morphological changes detectable by MRI (**Table 19**).

		Total Nerve Roots (n = 412)			Non-Pathological Nerve Roots (no PTS) (n = 290)			Pathological Nerve Roots (PTS) (n = 122)		
		CSA (mm)	AR (mm^2)	MED	CSA (mm)	AR (mm^2)	MED	CSA (mm)	AR (mm^2)	MED
C5	Right	4±0.8 (2.4-5.6) [3.9,3.4-4.5]	21.3±7.9 (7.9-40.8) [20,15.6-26.6]	178.5±77.4 (66-387) [158,121-209]	3.8±0.7 (2.4-5.6) [3.9,3.4-4.3]	20±7.3 (7.9-38.7) [19.5,14.6-25.2]	173±72.7 (66-375) [164,120-197]	4.4±0.7 (3.2-5.4) [4.5,3.9-5.1]	25.9±8.3 (15.1-40.8) [24.6,19-29.8]	197.9±93.4 (86-387) [153,137-283]
	Left	3.9±0.6 (2.4-5.3) [4,3.5-4.3]	20.7±6.2 (7.3-35.5) [20.3,17-23.5]	169.6±55.6 (77-365) [158,127-211]	3.9±0.6 (2.4-5.3) [3.9,3.5-4.2]	20.7±6.3 (7.3-32.8) [20.3,16.3-25.3]	165.7±48.8 (77-261) [150,127-211]	4.1±0.7 (2.7-4.9) [4.3,3.6-4.7]	20.5±6.1 (11.5-35.5) [20.1,17.1-21.8]	178±69.3 (102-365) [164,128.5-205]
C6	Right	4.3±0.8 (2.6-7) [4.3,3.8-4.8]	26.9±9.5 (9-49.1) [26.1,20.9-31.8]	203.4±69.6 (94-426) [198,154-240]	4.1±0.8 (2.6-7) [4.1,3.4-4.5]	23.3±8.1 (11.3-47.7) [22.6,18-27.5]	203.6±69.2 (97-426) [199,151-225]	4.7±0.7 (3.2-5.6) [4.9,4.2-5.2]	32.1±9.1 (9-49.1) [31.4,27.1-38.7]	203.2±72 (94-370) [180,161.5-256.5]
	Left	4.2±0.6 (2.9-5.9) [4.3,3.8-4.5]	25±8.3 (10.9-45.7) [23.8,18.6-31.6]	200.8±69.2 (26.2-409) [191,159-239]	4.2±0.7 (2.9-5.9) [4.3,4-4.5]	23.2±7.3 (10.9-37) [22.8,18.2-28.9]	212.6±67.3 (106-409) [191,168-271]	4.3±0.7 (3.3-5.3) [4.3,3.7-4.9]	27.7±9.1 (11.2-45.7) [29.2,20.4-33.5]	182.5±69.8 (26.2-325) [186,134.5-231.5]
C7	Right	4.3±0.8 (2.7-6.4) [4.3,3.9-4.8]	28.3±9.2 (12-54.4) [28,20.3-34.2]	220.1±67.2 (85-406) [215,177-268]	4.1±0.7 (2.7-5.7) [4.1,3.7-4.5]	26.2±7.9 (12-45.2) [25.6,19.5-32]	219.4±66 (90-406) [214,179-258]	4.8±0.8 (3.3-6.4) [4.7,4.2-5.5]	34.3±10.1 (17.3-54.4) [34.2,27.7-37.4]	222.2±73.1 (85-348) [216,170-276]
	Left	4.4±1 (2.9-8.8) [4.3,3.8-4.5]	26.4±7.3 (12.3-47.2) [26.2,21.8-30.3]	208±63.3 (50.5-415) [200,163-247]	4.2±1 (2.9-8.8) [4,3.8-4.4]	24.3±6.4 (12.3-47.2) [23.4,21.2-27.3]	212.4±61.6 (135-415) [199,170-243]	4.8±0.6 (3.7-6.1) [4.8,4.4-5.2]	31.3±7.1 (19-44.2) [30.6,26.2-36.7]	197.5±68.1 (50.5-297) [201,150-250]
C8	Right	4.4±0.6 (3.2-6) [4.3,3.9-4.8]	30.1±8.6 (16.2-49.8) [28.4,22.4-37.3]	220.5±75.5 (103-440) [203.5,163-276]	4.3±0.6 (3.2-6) [4.2,3.9-4.6]	28.3±8.1 (16.2-45) [27.1,21.8-35.2]	225.7±80.8 (103-440) [204,163.5-281.5]	4.7±0.5 (3.8-5.6) [4.7,4.5-4.9]	34.6±8.5 (19.6-49.8) [34.2,28.3-41.1]	207.2±60.3 (130-309) [203,155-245]
	Left	4.3±0.8 (2.8-6.4) [4.3,3.8-4.7]	27.5±9.8 (12.7-51.1) [26.1,20.5-34.5]	213.9±68.1 (98-409) [196,169-257]	4.1±0.6 (2.8-5.7) [4.2,3.7-4.3]	24.9±8.1 (12.7-51.1) [24.8,18.6-29.2]	215.7±65.4 (98-409) [203,175-253]	5±1 (3.2-6.4) [5,4.5-5.6]	35.2±10.5 (16.9-50.5) [35,26.6-42.1]	208.5±78.3 (116-366) [180,161-284]

* Results are reported as means ± standard devia3on, with the range in round brackets. Results in squared brackets are median and interquarle range.

Table 19 - Brachial Nerve Root Diameter, Areas and T2 Signal Intensity - Comparison between pathological and non- pathological nerve roots in patients with PTS*

Post-hoc analysis revealed that pathological nerve roots in patients with PTS exhibited significantly larger diameters compared to non-pathological roots in individuals without the condition. This enlargement was consistent across multiple cervical levels (**Figure 26**).

For the C5 nerve root, PTS patients showed diameters of 4.4 ± 0.7 mm on the right and 4.1 ± 0.7 mm on the left, compared to 3.8 ± 0.7 mm and 3.9 ± 0.6 mm, respectively, in non-PTS individuals. A similar pattern was observed at C6, where the right-side diameter in PTS patients was 4.7 ± 0.7 mm, versus 4.1 ± 0.8 mm in controls. The C7 nerve root also demonstrated significant enlargement in the PTS group, with diameters of 4.8 ± 0.8 mm on the right and 4.8 ± 0.6 mm on the left, compared to 4.1 ± 0.7 mm and 4.2 ± 1.0 mm in the non-PTS group. At C8, the trend persisted: PTS patients had diameters of 4.7 ± 0.5 mm (right) and 5.0 ± 1.0 mm (left), while non-PTS individuals measured 4.3 ± 0.6 mm and 4.1 ± 0.6 mm, respectively.

Despite these significant differences in absolute values, the analysis did not reveal statistically significant differences between sides or among the various nerve roots within groups. This suggests a uniform pattern of nerve root involvement in PTS, rather than localized or asymmetric changes.

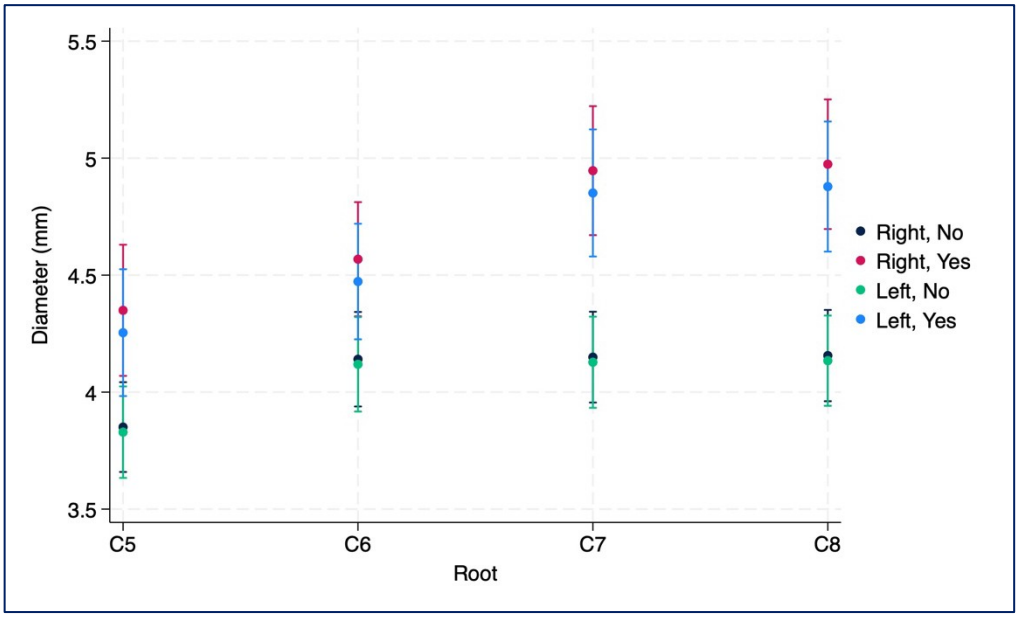

Figure 26: Scatter plot with 95% CI (vertical bars) of Nerve Root Diameter across Group, Roots, and Sides - Adjusted predicted means - Diameter (mm) - Comparison between pathological (Yes) and non-pathological roots (No) in patients with PTS

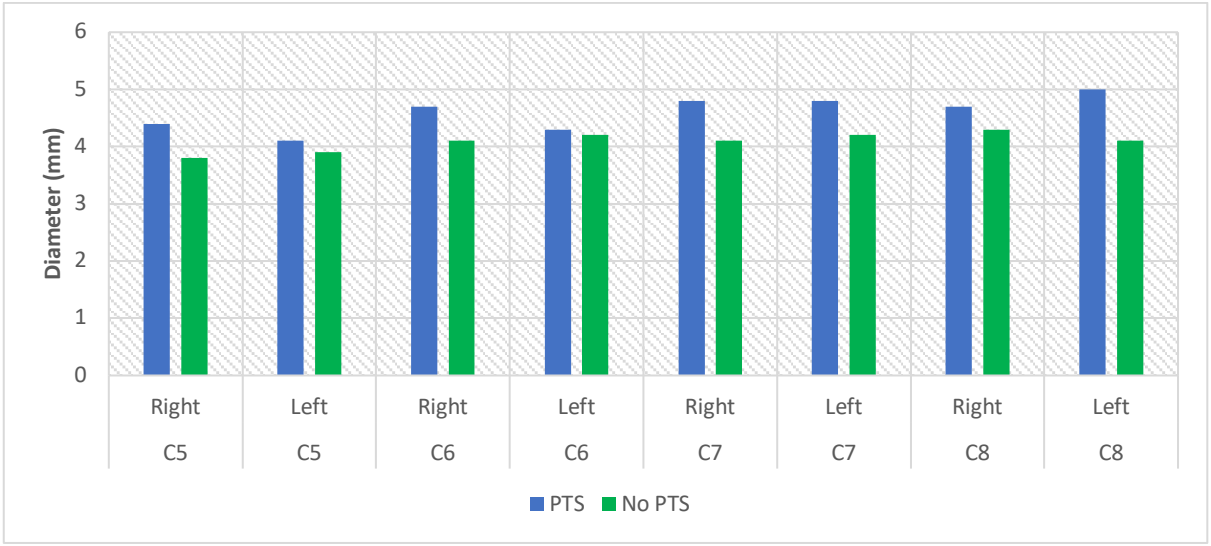

Figure 27: Note - Graphs displayed as histograms derived from the previous scatter plot: post-hoc analysis showed that diameter were significantly higher in pathological C5 nerve roots (PTS right: 4.4±0.7 mm; PTS left: 4.1±0.7 mm; No PTS right: 3.8±0.7 mm; No PTS left:3.9±0.6 mm), right C6 nerve root (PTS right: 4.7±0.7 mm; no PTS right: 4.1±0.8 mm), C7 nerve roots (PTS right: 4.8±0.8 mm; PTS left: 4.8±0.6 mm; no PTS 4.1±0.7 mm; no PTS 4.2±1 mm) and C8 nerve roots (PTS right 4.7±0.5 mm; PTS left: 5±1 mm; no PTS 4.3±0.6 mm; no PTS 4.1±0.6 mm).

The analysis of nerve *root area* revealed no statistically significant overall difference between pathological and non-pathological roots ($F(1,51) = 2.97$, $p = 0.0847$). However, a significant interaction between nerve root level and pathology status was identified ($F(1,51) = 19.04$, $p = 0.001$), indicating that specific roots - particularly C6, C7, and C8 - exhibited significantly larger areas in patients with PTS compared to non-PTS individuals. For the C6 nerve root, PTS patients showed a right-side area of 32.1 ± 9.1 mm², notably larger than the 23.3 ± 8.1 mm² observed in controls. On the left side, the area measured 27.7 ± 9.1 mm² in PTS patients versus 23.2 ± 7.3

mm² in non-PTS individuals. The C7 nerve root followed a similar pattern. On the right, PTS patients had an area of 34.3 ± 10.1 mm², compared to 26.2 ± 7.9 mm² in controls. On the left, the values were 31.3 ± 7.1 mm² for PTS and 24.3 ± 6.4 mm² for non-PTS. For the C8 nerve root, the right-side area in PTS patients was 34.6 ± 8.5 mm², compared to 28.3 ± 8.1 mm² in controls. On the left, the difference was even more pronounced: 35.2 ± 10.5 mm² in PTS patients versus 24.9 ± 8.1 mm² in non-PTS individuals.

These findings suggest that while overall differences in nerve root area may not reach statistical significance, specific cervical roots - particularly C6 through C8 - are significantly enlarged in PTS. Moreover, these roots also show clear distinctions when compared to C5, which did not exhibit similar enlargement in either group. This pattern, illustrated in **Figure 28**, highlights the selective vulnerability of lower cervical roots in PTS and underscores the importance of root-specific analysis in both diagnosis and monitoring.

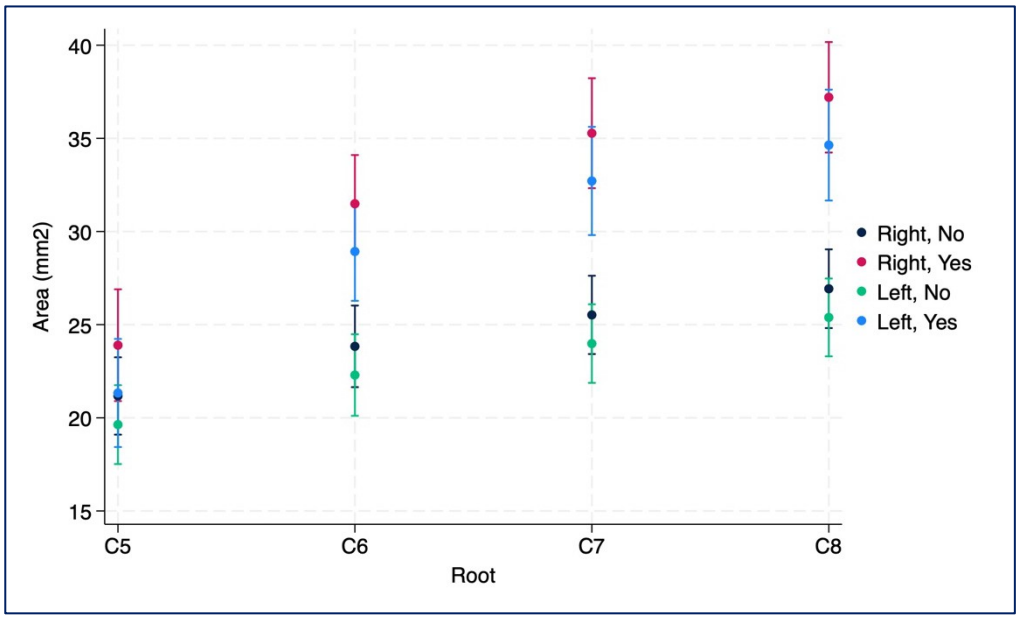

Figure 28: Scatter plot with 95% CI (vertical bars) of Nerve Root Area across Group, Roots, and Sides - Adjusted predicted means - Area (mm^2) –-Comparison between pathological (Yes) and non-pathological roots (No) in patients with PTS

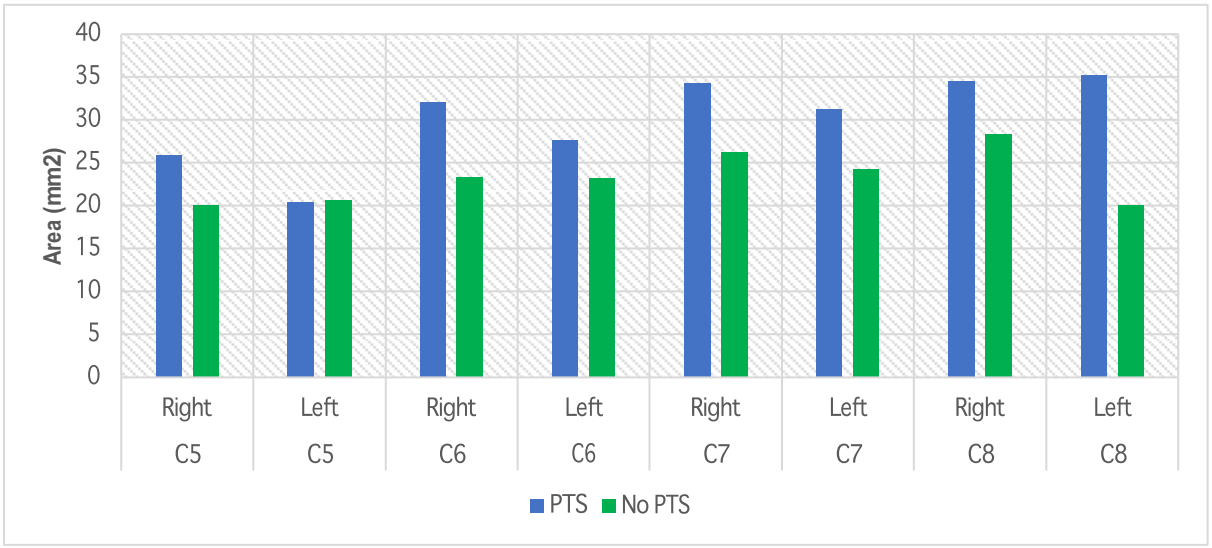

Figure 29: Note - Graphs displayed as histograms derived from the previous scatter plot: [C6 right: PTS: 32.1±9.1 mm2, non-PTS: 23.3±8.1 mm2; C6 left: PTS 27.7±9.1 mm2, non-PTS: 23.2±7.3 mm2; C7 right: PTS: 34.3±10.1 mm2, non- PTS: 26.2 ±7.9 mm2; C7 left: PTS 31.3±7.1 mm2, non- PTS: 24.3±6.4 mm2; C8 right: PTS: 34.6±8.5 mm2, non- PTS: 28.3±8.1 mm2; C8 left: PTS 35.2±10.5 mm2, non-PTS: 24.9±8.1 mm2]

The analysis of *T2 signal* intensity revealed no statistically significant differences between pathological and non-pathological nerve roots within the PTS patient group. Despite the presence of clear morphological alterations - such as CSA - in affected roots, the T2 signal intensity remained comparable across both pathological and non-pathological roots.

This finding suggests that, while structural changes are evident in PTS, the tissue characteristics reflected by T2 signal intensity do not vary significantly within the same patient population. As a result, T2 signal intensity may have limited utility as a standalone marker for assessing the severity or extent of nerve involvement in PTS. These results underscore the complexity of interpreting imaging biomarkers in this condition and highlight the need for a multimodal approach that integrates morphological, functional, and clinical data for accurate diagnosis and monitoring (see **Figure 30**).

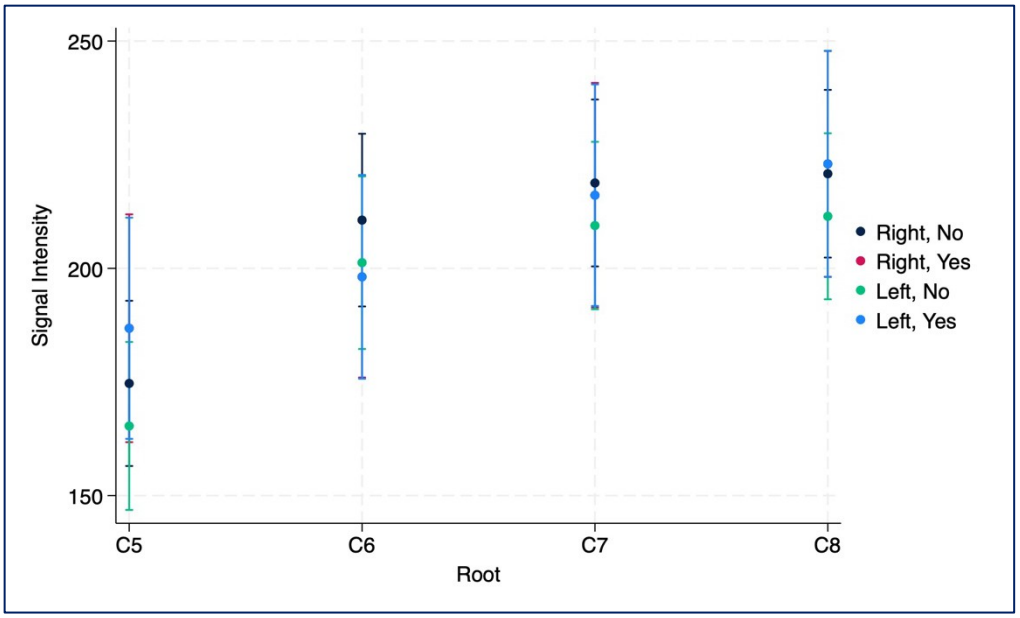

Figure 30: Scatter plot with 95% CI (vertical bars) of Nerve Root Signal Intensity across Group, Roots, and Sides – Adjusted predicted means – Signal Intensity – Comparison between pathological (Yes) and non-pathological roots (No) in patients with PTS.

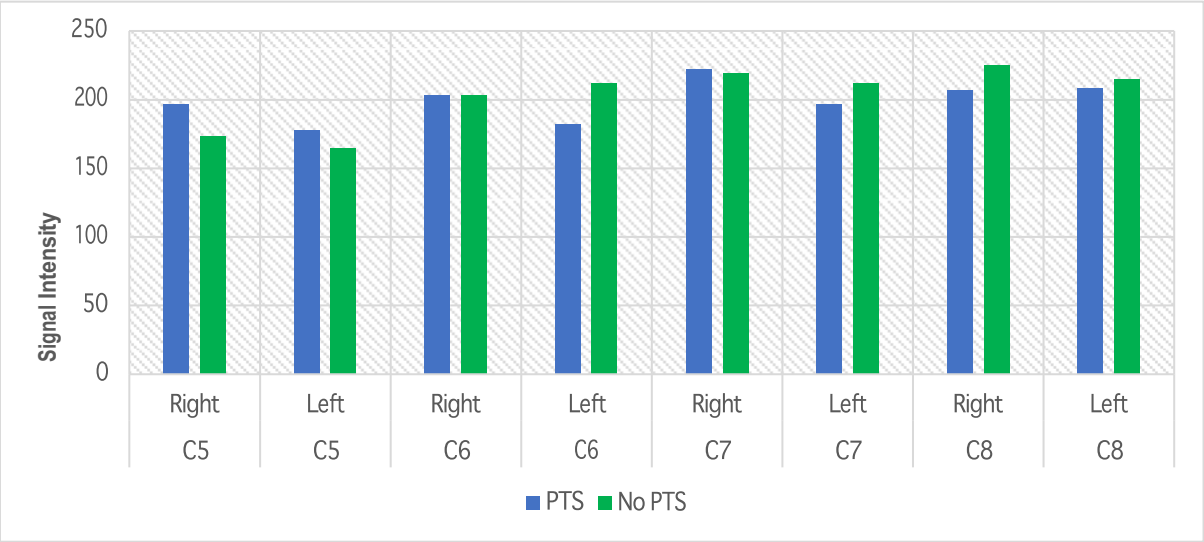

Figure 31: Note – Graphs displayed as histograms derived from the previous scatter plot: with regard to T2 signal intensity, there were no statistically significant differences between pathological and non-pathological nerve roots.

CHAPTER 7

Discussion

7.1 Interpretation of Results

Understanding the multifaceted nature of PTS requires a comprehensive approach that integrates clinical presentations, imaging data, and demographic factors. In this analysis, the synthesis of both qualitative and quantitative findings reveals the intricate relationship between these components.

7.1.1 Qualitative results

Imaging analysis revealed significant structural alterations in the affected nerve roots and adjacent musculature in patients with PTS, including signs of edema, fat infiltration, and muscle atrophy. These findings closely align with the clinical presentation of PTS, particularly the hallmark symptoms of pain and muscle weakness, reinforcing the well-established link between structural damage and functional impairment. This correlation between imaging abnormalities and clinical symptoms is well-documented in the literature. For example, van Alfen and van Engelen (2006) emphasized the critical role of early MRI in detecting the extent of nerve root involvement, which is essential for timely diagnosis and management. Similarly, Latham et al. (2013) demonstrated that MRI findings - such as nerve root edema and muscle atrophy - correlate with symptom severity. Kline et al. (2019) further highlighted the complementary role of MRI and EMG, with MRI capturing structural changes and EMG providing insight into functional deficits, particularly during the acute phase of the disease. Together, these modalities enhance diagnostic accuracy, support disease monitoring, and inform therapeutic decision-making.

Demographic analysis of the study population revealed a predominance of middle-aged males, with a mean age of 51.9 years (see chapter 6.1). This observation is consistent with prior studies reporting peak PTS incidence

between the ages of 30 and 70 (van Alfen & van Engelen, 2006; Kline et al., 2019). The age distribution suggests that age-related physiological changes - such as hormonal shifts, immune modulation, or cumulative musculoskeletal stress - may contribute to increased susceptibility. Van Alfen and van Engelen (2006) identified the 40-60 age range as the most common period for disease onset, while Naganawa et al. (2018) reported a higher incidence in males, particularly in their fifth and sixth decades, suggesting a potential gender predisposition, though the underlying mechanisms remain unclear. These demographic patterns underscore the importance of considering age and sex as potential risk factors in the clinical evaluation of suspected PTS, which may aid in early recognition and tailored management strategies.

Pain was the most frequently reported initial symptom, affecting 70.6% of the analyzed cohort. This finding is consistent with previous studies that identify pain - particularly in the shoulder or upper arm - as a common early manifestation of PTS (Hughes et al., 2011; Barron et al., 2016; Juel et al. 2014) noted that pain often precedes motor deficits by several days to weeks, serving as a potential early warning sign. However, not all patients report pain at onset. Some may underrecognize or deprioritize it, focusing instead on the sudden onset of muscle weakness. Willard et al. (2015) observed that many patients attribute early symptoms to benign causes such as muscle strain, which can delay diagnosis. This highlights the need for clinicians to maintain a high index of suspicion for PTS, even in the absence of acute pain, particularly when unexplained shoulder or arm weakness is present (Beghi et al., 2017). The integration of clinical findings - such as pain and weakness - with imaging modalities like MRI and EMG is essential for accurate diagnosis and prognosis. As emphasized by Gouveia et al. (2019), early identification of structural and functional changes can prevent long-term disability and guide appropriate therapeutic interventions.

A high prevalence of unilateral symptoms was observed in the study cohort, with 80.4% of patients exhibiting symptoms confined to one side of the body (see **Table 3**). This finding is consistent with the classical presentation of PTS, which is typically characterized by unilateral neuropathic manifestations. The predominance of unilateral involvement supports the hypothesis that PTS arises from localized inflammatory or traumatic insults to the brachial plexus (van Alfen & van Engelen, 2006; Gouveia et al., 2019). The anatomical configuration of the brachial plexus, particularly its exposure to mechanical and immunological stressors, renders it especially susceptible to such localized processes (Kline et al., 2019). Recent literature continues to reinforce this asymmetrical pattern. Mallet et al. (2021) reported that the vast majority of PTS cases are unilateral, with bilateral presentations being rare and typically associated with systemic conditions such as autoimmune or inflammatory disorders. Fazio et al. (2022) further observed that unilateral involvement is often associated with a higher incidence of acute pain in the early phase, followed by progressive muscle weakness. These findings underscore the importance of early recognition and targeted intervention, particularly on the affected side. The rarity of bilateral involvement highlights the localized nature of PTS and supports current clinical strategies that focus on managing inflammation, pain, and muscle atrophy unilaterally (Beghi

et al., 2017; Hughes et al., 2011).

Qualitative MRI analysis in this study revealed a higher frequency of structural alterations - such as edema and inflammation - at the C6 nerve root. This observation aligns with previous research identifying C6 as one of the most commonly affected roots in PTS (van Alfen & van Engelen, 2006; Kline et al., 2019). The C5-C7 roots, which form the upper trunk of the brachial plexus, are particularly vulnerable to inflammatory processes due to their anatomical positioning and biomechanical exposure (Gouveia et al., 2019).

Interestingly, those results than can be in contrast of what we identified in the quantitative analysis, which objectively measures nerve root areas, showed that C7-C8 have significantly larger areas than C6, both in the PTS group and in healthy controls. This may indicate that, despite the evident qualitative alteration at the C6 level, the C7-C8 roots have an intrinsically larger size, and/or respond to pathological processes with a more evident and measurable volumetric increase. Furthermore, studies have consistently demonstrated that C7 and C8 nerve roots exhibit larger diameters and cross-sectional areas compared to C6 nerve roots (Tanaka N et al. 2000).

As previously noted in chapter, the significant prevalence of C5 nerve root involvement in female patients - accompanied by a statistically significant gender difference - raises important questions regarding potential anatomical and physiological predispositions. While this study's sample may reflect inherent demographic biases, emerging literature supports the hypothesis that sex-based biological factors may influence the clinical expression of PTS. For instance, Mallet et al. (2021) proposed that hormonal differences and immune system variability between genders could contribute to differential susceptibility. Specifically, heightened inflammatory responses or distinct patterns of nerve vulnerability in females may explain the increased C5 involvement observed in this cohort. These findings warrant further investigation into gender-specific immune responses and anatomical variations that may modulate disease severity and presentation (Fazio et al., 2022).

The evaluation of muscle edema, fat infiltration, and atrophy provides critical insights into the pathophysiology of PTS and its impact on shoulder function. Notably, the presence of *edema* in the subscapularis and deltoid muscles reflects an acute inflammatory response, particularly in muscles innervated by the C5 and C6 roots. A statistically significant gender difference in subscapularis edema ($p = 0.013$), with greater prevalence in females, suggests that lower muscle mass and hormonal influences - such as estrogen-mediated immune modulation - may contribute to increased inflammatory susceptibility (Mallet et al., 2021; Fazio et al., 2022). These findings highlight the potential need for gender-specific early interventions to mitigate inflammation and preserve function. The deltoid muscle, essential for arm abduction and innervated by the axillary nerve, also showed frequent edema, underscoring its vulnerability in PTS. The correlation between deltoid edema and axillary nerve involvement aligns with prior research demonstrating that brachial plexus pathology leads to muscle inflammation and functional impairment (Juel et al., 2014; Beghi et al., 2017). Consistent with clinical findings, the rotator cuff

muscles - particularly the supraspinatus and infraspinatus - exhibited high rates of Grade 1 edema (29.4% and 27.5%, respectively). Recent studies (Fazio et al., 2022; Gouveia et al., 2019) have emphasized the association between infraspinatus edema and acute pain in PTS. In this cohort, a statistically significant correlation was observed between infraspinatus edema and reported pain ($p = 0.018$), suggesting that mild edema in this muscle may serve as an early marker of inflammation and symptom onset. Excluding Grade 0 findings, the presence of mild to moderate edema (Grades 1 and 2) across multiple muscles - particularly the trapezius and infraspinatus - indicates a broader pattern of muscle involvement associated with pain and functional limitation. These results are consistent with previous studies (Juel et al., 2014; van Alfen & van Engelen, 2006), which highlight the relationship between muscle inflammation and the severity of clinical symptoms in PTS. The statistical significance of these findings reinforces the role of muscle edema not only as a structural marker but also as a clinically relevant indicator of functional impairment. Given the potential for bilateral muscle inflammation, even in predominantly unilateral cases, clinicians should monitor both sides of the body. Bilateral involvement may lead to more severe disability and necessitate more comprehensive treatment strategies.

The analysis of *fat infiltration* patterns in patients with PTS provides important insights into the chronic phase of the disease, particularly in relation to long-standing nerve injury. Fat infiltration, especially in the infraspinatus muscle reflects ongoing neuromuscular degeneration and impaired reinnervation. These findings are consistent with previous studies demonstrating that prolonged denervation in PTS leads to progressive muscle atrophy and fat replacement, particularly in muscles critical to shoulder mechanics, such as those of the rotator cuff (Kline et al., 2019; Mallet et al., 2021). In general, fat infiltration was minimal across most shoulder girdle and upper limb muscles, with the majority of cases classified as Grade 0. This aligns with the understanding that early-stage PTS is primarily characterized by inflammation and edema, rather than fatty degeneration (Juel et al., 2014; van Alfen & van Engelen, 2006). However, the supraspinatus muscle emerged as an exception, showing higher rates of fat infiltration that were significantly associated with pain. This observation is supported by Gouveia et al. (2019) and Kline et al. (2022), who identified the supraspinatus as one of the earliest and most frequently affected muscles in PTS, likely due to its anatomical role and its innervation by the C5 root. In contrast, most other muscles - including those of the arm and posterior shoulder - exhibited little to no fat infiltration, suggesting that muscle degeneration in PTS is often localized and progresses gradually. Fazio et al. (2022) similarly reported that while certain muscles, such as the infraspinatus and trapezius, may show signs of degeneration, the overall muscular condition remains relatively preserved in many patients, particularly in the early stages of the disease. Recent studies have emphasized the diagnostic value of identifying fat infiltration patterns using high-resolution MRI. As noted by van Eijk et al. (2023), the extent of fat infiltration can provide valuable information about the chronicity and severity of nerve damage. The supraspinatus, due to its functional importance and vulnerability, is considered a key muscle to monitor. Its higher infiltration rates have been shown to correlate with pain intensity, reinforcing its role as a clinical and imaging biomarker (Kline et al., 2022). Interestingly, the current analysis also revealed a left-side predominance of fat infiltration in the infraspinatus muscle. This asymmetry is consistent with

findings by Gouveia et al. (2019), who reported that PTS often presents with unilateral or asymmetrical muscle involvement, frequently affecting the dominant side. Although the underlying mechanisms remain unclear, such asymmetry may reflect differences in mechanical load, vascular supply, or immune response. Kline et al. (2019) further highlighted the utility of early MRI in detecting asymmetrical fat infiltration and muscle atrophy, which are critical for monitoring disease progression and guiding rehabilitation. While the present sample may not be large enough to confirm statistically significant gender or age-related differences, the observed patterns underscore the chronic nature of PTS, and the importance of individualized rehabilitation strategies aimed at preserving muscle function and mitigating long-term deficits.

The analysis of muscle *atrophy* across limb-girdle and rotator cuff muscle groups in patients with PTS reveals several clinically relevant trends. Notably, atrophy was most prevalent in the supraspinatus muscle, particularly among older patients. This observation aligns with findings from Kline et al. (2022), who reported that age-related physiological changes - such as reduced regenerative capacity and altered muscle metabolism - may exacerbate the effects of chronic denervation, leading to more pronounced atrophy in older individuals (Juel et al., 2021; Mallet et al., 2021). Within the rotator cuff, the supraspinatus muscle exhibited the highest rate of atrophy, affecting 41.2% of the PTS cohort. This is consistent with its known anatomical vulnerability and functional role in shoulder abduction (van Eijk et al., 2023). A statistically significant difference in atrophy prevalence was observed between patients reporting pain (66.7%) and those without pain (30.6%), with a p-value of 0.028. This suggests a potential link between pain and muscle degeneration, supporting previous findings by Gouveia et al. (2019), who proposed that inflammatory processes associated with pain may accelerate muscle breakdown in the early stages of PTS. Moderate atrophy rates were also observed in the infraspinatus (29.4%) and subscapularis (25.5%) muscles. However, no statistically significant differences were found between patients with and without pain in these muscles. This aligns with prior studies (Fazio et al., 2022) suggesting that the relationship between pain and atrophy may vary across muscle groups. For instance, van Alfen & van Engelen (2006) noted that atrophy in the infraspinatus and subscapularis may develop more gradually and may not always correlate with acute pain or immediate functional impairment. Overall, while muscle atrophy was observed across multiple muscle groups, the supraspinatus was the only muscle to show a statistically significant association with pain. This highlights the complex and muscle-specific nature of atrophy in PTS. The findings suggest that pain may serve as a predictor of muscle degeneration in some cases, but not universally across all affected muscles. These results echo conclusions from recent literature (Gouveia et al., 2019; Mallet et al., 2021), which emphasize the need for further research into the interplay between pain, functional impairment, and muscle atrophy in PTS. Understanding these relationships is essential for developing targeted rehabilitation protocols and improving long-term outcomes for patients with chronic nerve injury.

Consistent with prior research (van Alfen & van Engelen, 2021; Fazio et al., 2022), our findings support the notion that peripheral nerve injury in PTS often results in a disproportionate pain experience, which does not always

correlate with the extent of structural damage observed on imaging. EMG and MRI assessments revealed a high prevalence of nerve root involvement - particularly at the C5 and C6 levels - across the 51-patient cohort. This aligns with previous studies identifying these roots as the most commonly affected in PTS (Juel et al., 2014; Kline et al., 2022). However, despite the frequency of nerve root involvement, no statistically significant associations were found between specific root involvement and the presence of pain or functional impairment. For example, while 72.2% of patients with pain showed C5 involvement, this was not significantly different from the 80% of pain-free patients who also exhibited C5 pathology. Similar patterns were observed for C6, C7, and C8 roots, suggesting that pain and dysfunction are not directly proportional to the degree or location of nerve damage. These findings are consistent with the work of van Eijk et al. (2023) and Gouveia et al. (2019), who proposed that pain in PTS is likely mediated by both peripheral and central mechanisms. This includes factors such as individual pain sensitivity, immune response variability, and psychosocial influences, which may modulate the perception and impact of nerve injury. As van Alfen (2022) and Kline et al. (2022) have noted, variability in pain intensity may also reflect differences in nerve regeneration capacity and the involvement of adjacent non-neural structures - such as muscle and connective tissue - that are not always captured by conventional imaging or EMG.

The absence of a clear correlation between nerve root involvement and clinical symptoms underscores the complexity of PTS and the limitations of relying solely on structural or electrophysiological findings for diagnosis and management. Individual differences in pain thresholds, compensatory mechanisms, and symptom chronicity likely contribute to the observed variability in clinical presentation.

MRI analysis provided further insight into the relationship between muscle alterations and clinical symptoms in PTS, such *pain*. Notably, the presence of edema - particularly in the trapezius and infraspinatus muscles - was significantly associated with pain, suggesting that even mild edema may reflect an underlying inflammatory response contributing to pain perception. Conversely, the absence of edema in other muscle groups suggests a more localized pathological process, reinforcing the importance of targeted imaging assessments focused on muscles most likely to reflect clinical symptomatology. Muscle atrophy findings added another layer of complexity. While the supraspinatus muscle showed a statistically significant difference in atrophy rates between patients with and without pain, other muscles did not demonstrate similar correlations. This variability suggests that the relationship between muscle atrophy and clinical symptoms is not uniform across all muscle groups in PTS. These findings highlight the need for further investigation into the mechanisms driving muscle degeneration, which may occur independently of pain or functional impairment.

Our analysis also explored the distribution of *neurogenic impairment* and its correlations. Among patients with EMG-confirmed neurogenic impairment, 41.5% reported right-sided involvement, compared to 40% in those without impairment ($p = 1.000$). Similarly, left-sided involvement was reported by 39% of impaired patients and 40% of non-impaired patients ($p = 1.000$). Bilateral involvement was nearly identical between groups (19.5% vs. 20%), indicating no statistically significant differences in laterality. When examining specific nerve roots, EMG

findings showed C5 involvement in 75.6% of patients with neurogenic impairment and 70% of those without (p = 0.701). For C6, involvement was noted in 82.9% of impaired patients and 80% of non-impaired patients (p = 1.000). Similar non-significant trends were observed for C7 and C8, suggesting that while nerve root involvement is common, it does not significantly differ between patients with and without neurogenic impairment. MRI findings mirrored these patterns. For the C5 root, abnormalities were observed in 41.5% of impaired patients and 30% of non-impaired patients (p = 0.721). At C6, abnormalities were present in 65.9% of impaired patients versus 50% of non-impaired patients (p = 0.470). Again, similar trends were noted for C7 and C8, with no statistically significant differences. These findings underscore the complexity of PTS, where structural and neurophysiological abnormalities do not always correlate with clinical symptoms such as pain or functional impairment. The lack of significant associations between nerve root involvement and symptom presentation suggests that additional factors that may play a critical role in shaping the clinical picture.

This reinforces the need for a multidimensional diagnostic approach that integrates imaging, electrophysiology, and clinical evaluation to accurately assess disease severity and guide personalized treatment strategies.

The integration of EMG findings and MRI observations offers valuable insights into the neuromuscular alterations associated with PTS, particularly when focusing on three key parameters: edema, fat infiltration, and muscle atrophy.

- Edema, often indicative of acute inflammation or early muscle damage, was more frequently observed in patients with EMG-confirmed neurogenic impairment. For example, in the trapezius muscle, Grade 1 edema was present in 14.6% of patients with neurogenic impairment, while no edema was detected in the non-impaired group. Similar patterns were observed in the supraspinatus and infraspinatus muscles, where higher grades of edema were more prevalent among those with neurogenic findings. These results suggest a potential link between nerve dysfunction and localized muscle inflammation, reinforcing the role of MRI in detecting early pathological changes.

- Muscle atrophy, a hallmark of chronic denervation, was also evaluated. The deltoid muscle showed a higher incidence of atrophy in patients with neurogenic impairment (24.4%) compared to those without (10%). However, across most muscle groups, these differences did not reach statistical significance. This suggests that while atrophy is a common feature in PTS, its presence may not be solely attributable to neurogenic impairment, and other factors - such as disease duration, muscle-specific vulnerability, and compensatory mechanisms - may influence its development.

These findings underscore the complexity of PTS pathophysiology. Although trends in muscle changes are evident in relation to nerve involvement, the absence of consistent statistical significance highlights the variability in clinical presentation. This variability necessitates a personalized approach to diagnosis and treatment.

Given the high prevalence of nerve root involvement and the inconsistent correlation with pain and functional impairment, individualized management strategies are essential. Advanced imaging techniques, such as high-resolution MRI, should be employed not only to confirm nerve involvement but also to assess the extent of muscle changes and guide targeted interventions.

7.1.2 Quantitative results

This study highlights the value of quantitative MRI parameters as non-invasive biomarkers for assessing and monitoring nerve damage in PTS. Consistent with recent findings by Kline et al. (2023) and Fazio et al. (2022), our results confirm that MRI-based quantification of nerve root morphology offers a powerful tool for early detection and longitudinal tracking of disease progression. Analyzing the ROI measurements, we observed a statistically significant increase in nerve root diameter among PTS patients compared to healthy controls ($F = 104.76$, $p < 0.001$). This finding strongly supports previous work by van Alfen et al. (2018) and van Eijk et al. (2023), which identified nerve root swelling as a hallmark of PTS-related pathology. The enlargement likely reflects underlying inflammatory or traumatic processes affecting the brachial plexus. The observed increase in CSA across C5-C8 nerve roots in PTS patients supports the presence of nerve root enlargement, a hallmark of inflammation or injury. The larger CSA values in pathological roots suggest localized edema or inflammatory swelling, potentially associated with Wallerian degeneration - a process involving axonal breakdown and myelin clearance following nerve injury. This mechanism has been well-documented in neurodegenerative conditions such as ALS (Gerevini et al., 2016), where similar patterns of nerve root enlargement and signal changes have been observed. Importantly, this increase in diameter was symmetrical, with no significant differences between right and left sides, suggesting a systemic rather than localized pattern of nerve involvement. This observation aligns with Kline et al. (2022), who reported bilateral structural changes despite predominantly unilateral clinical symptoms. Further analysis of AR revealed significantly larger values in PTS patients compared to controls ($F = 32.13$, $p < 0.001$), reinforcing the presence of structural nerve alterations. These findings are consistent with earlier studies (e.g., van Alfen & van Engelen, 2020), which noted morphological changes in nerve roots during the acute and subacute phases of PTS, likely due to edema and inflammation. T2 signal intensity, a sensitive marker of tissue composition and inflammation, was also significantly elevated in PTS patients ($F = 24.92$, $p < 0.001$). This increase was consistent across all nerve roots and both sides of the body, further supporting the presence of diffuse inflammatory activity. These results are in line with studies by Moser et al. (2021), Fazio et al. (2022), and Weninger et al. (2020), who demonstrated that T2 hyperintensity correlates with acute nerve injury and may serve as a useful indicator of disease stage.

The subgroup analysis comparing pathological and non-pathological nerve roots within the PTS cohort ($n = 412$ roots) revealed a significant difference in nerve root diameter, with pathological roots exhibiting markedly larger dimensions. This finding corroborates previous work by van Alfen et al. (2021), which described structural enlargement in affected roots due to edema, inflammation, or demyelination. On the contrary, the comparative

analysis of nerve root areas revealed no statistically significant overall difference between pathological and non-pathological roots within the PTS cohort ($F(1,51) = 2.97$, $p = 0.0847$). However, a significant interaction effect was observed between pathology status and specific nerve root levels ($F(1,51) = 19.04$, $p = 0.001$), indicating that certain roots - particularly C6, C7, and C8 - exhibited significantly larger areas when pathological. These findings are consistent with previous studies (Moser et al., 2021; Gouveia et al., 2019), which identified C6 and C7 as especially vulnerable to injury in PTS, likely due to their anatomical positioning and biomechanical exposure. In addition, T2 signal intensity (AR, MED) did not differ significantly between pathological and non-pathological roots within the PTS group. This suggests that while morphological changes such as increased diameter and area are evident, T2 signal intensity may not reliably distinguish between affected and unaffected roots. This observation aligns with findings by Fazio et al. (2023), who noted that T2 hyperintensity may not always correlate with the degree of nerve damage, particularly in chronic stages where fat infiltration predominates overactive inflammation. These results imply that while structural metrics (e.g., CSA and AR) are valuable for identifying nerve involvement, T2 signal intensity alone may not be sufficient to differentiate stages of nerve pathology. Longitudinal studies are needed to clarify the temporal dynamics between structural changes, T2 signal alterations, and clinical symptoms. The findings of this study also have significant implications for the longitudinal monitoring of patients with neurodegenerative or inflammatory nerve conditions. The ability to measure CSA and T2 signal intensity over time provides clinicians with a method to track the progression of the disease. For example, in patients with an early diagnosis of PTS or a similar condition, repeated imaging could reveal changes in nerve root size or signal intensity, allowing for adjustments in treatment strategies based on objective data. As noted by Gerevini et al. (2016), the progressive increase in T2 signal intensity in ALS patients was closely associated with worsening clinical symptoms. Similarly, in brachial plexopathies, an increase in T2 signal intensity over time could signal a worsening of the inflammatory process, while a reduction in CSA might indicate chronic atrophy or irreversible nerve damage. By utilizing these quantitative markers, clinicians can better predict disease outcomes and offer timely interventions to mitigate nerve damage and improve patient quality of life.

In terms of therapeutic implications, the ability to measure nerve root changes quantitatively could influence the timing and choice of interventions. For instance, patients with significantly elevated T2 values might benefit from anti-inflammatory treatments or immunomodulatory therapies aimed at reducing nerve inflammation. Conversely, patients with reduced CSA, indicating chronic nerve atrophy, may require physical therapy focused on muscle strengthening and rehabilitation to compensate for the loss of nerve function.

Conclusion

7.2 Conclusion

This study offers an evaluation of the multifactorial nature of PTS, highlighting significant structural changes in nerve roots and adjacent musculature - edema, fat infiltration, and atrophy - and their relationship to clinical

symptoms such as pain, muscle weakness, and functional impairment at EMG. Through the integration of advanced imaging modalities, particularly MRI and EMG, we presented the critical role of these tools in the detection, characterization, and longitudinal monitoring of PTS.

Our findings confirm that PTS predominantly affects middle-aged males, with a mean age of diagnosis. This demographic trend suggests that age-related physiological changes, including hormonal fluctuations and immune modulation, may contribute to disease susceptibility and progression. As PTS remains a relatively rare and often underdiagnosed condition, larger, more diverse cohorts and longitudinal studies are needed to establish clearer patterns and validate these initial observations. Such variations could be attributed to the due sample size and to anatomical factors, such as smaller muscle size or differing biomechanical loading patterns in females, or immune-mediated mechanisms that influence the inflammatory response differently by gender.

Pain emerged as the most frequently reported initial symptom, underscoring its diagnostic value in the early stages of the disease and its potential role in guiding timely intervention to prevent downstream neuromuscular deterioration.

PTS was predominantly unilateral in presentation, with bilateral involvement being rare and typically associated with more severe or systemic disease. The C6 nerve root was the most frequently affected, consistent with its anatomical vulnerability within the brachial plexus.

MRI and EMG findings were instrumental in identifying both structural and functional impairments. Edema in muscles such as the trapezius and infraspinatus was significantly associated with pain, suggesting a close link between inflammation and symptom severity. The supraspinatus muscle, which exhibited the highest prevalence of atrophy, particularly in older patients, reflects the cumulative impact of chronic denervation and age-related muscle degeneration. Fat infiltration, especially in the infraspinatus, further underscores the chronic nature of PTS-related muscle damage. The association between fat infiltration and pain in the supraspinatus highlights the complex interplay between nerve injury, inflammation, and muscle remodeling. These findings reinforce the importance of early intervention to mitigate long-term structural and functional decline.

Regarding the quantitative MRI parameters - specifically CSA and T2 signal intensity - proved to be valuable in assessing the extent of nerve root involvement. The observed increases in CSA and T2 signal intensity in PTS patients compared to healthy controls reflect underlying inflammation and structural nerve damage. These metrics not only enhance diagnostic accuracy but also serve as objective markers for tracking disease progression in correlation with clinic and EMG.

From a clinical perspective, these findings underscore the importance of individualized management strategies that integrate imaging data with patient-reported symptoms and demographic variables such as age and gender. A personalized, multimodal approach - combining MRI, EMG, and comprehensive clinical evaluation - has the potential to optimize therapeutic outcomes and significantly enhance quality of life for individuals affected by PTS. This study establishes a foundational framework for future research aimed at refining diagnostic criteria

and developing targeted, evidence-based treatment protocols. By synthesizing structural, functional, and clinical data, we advocate for a more nuanced and effective model of care - one that emphasizes early detection, personalized intervention, and long-term preservation of neuromuscular function.

7.3 Study Limitations

While this study offers valuable insights into the morphological and signal alterations of the brachial plexus in PTS, several limitations must be acknowledged across both qualitative and quantitative analyses.

A primary limitation lies in the retrospective design, which resulted in variability in MRI image quality. As imaging data were collected from existing clinical records, not all scans met the high-resolution standards required for detailed analysis. This inconsistency may have affected the accuracy of qualitative assessments - such as evaluating edema or atrophy - and limited the reliability of nerve root evaluations. Standardized imaging protocols are essential for ensuring consistency, which retrospective studies often cannot guarantee.

Another significant limitation is the manual delineation of ROIs for quantitative measurements of CSA and T2 signal intensity. Despite efforts to standardize the process, manual ROI selection introduces operator-dependent variability, potentially affecting measurement precision and reproducibility. Future studies would benefit from automated or semi-automated ROI methods to minimize subjectivity and improve consistency.

Additionally, the lack of blinding to patients' clinical histories may have introduced bias in both image interpretation and data analysis. Knowledge of which nerve roots were affected could have influenced the evaluators' judgments, underscoring the importance of blinding in clinical research to enhance objectivity.

The absence of inter-operator consensus further contributed to variability in both qualitative and quantitative assessments. Differences in interpretation and measurement technique can lead to inconsistencies, reducing the overall validity of the findings. To address this, the study implemented a standardized protocol for quantitative measurements - specifically, measuring 15 mm (±2 mm) from the spinal foramen - and used a scoring system for evaluating edema and fat infiltration. Operator training and calibration were also conducted at the outset to mitigate variability.

An important limitation of this study is the absence of established reference data for the specific quantitative measurements performed - particularly CSA and T2 signal intensity along the brachial nerve roots at approximately 15 mm from the spinal foramen. The lack of normative values for this anatomical region in healthy individuals complicates the interpretation of results, as it limits the ability to define clear thresholds for pathological changes.

Another constraint is the limited sample size and the use of different MRI systems over the study period (2019-2024). While the newer MRI scanner provided higher-resolution images and more consistent data, it was only available for a subset of patients, potentially introducing selection bias. Additionally, the 3D Cube STIR sequence used for quantitative analysis, although effective for visualizing nerve roots, is sensitive to motion artifacts and requires longer acquisition times. This may have compromised image quality in patients experiencing pain or discomfort during scanning, affecting measurement accuracy. The reliance on a single

imaging protocol also limits comparability with studies using alternative MRI sequences.

The inconsistent use of contrast agents across the cohort represents another limitation. Contrast-enhanced imaging is valuable for detecting subtle inflammatory changes and distinguishing nerve pathology from other conditions. The absence of contrast in some cases may have reduced sensitivity, particularly in early-stage disease, and introduced variability in the detection of pathological features.

Methodologically, the comparison between PTS patients and healthy controls was affected by unequal group sizes, which may have introduced bias in the estimation of fixed and random effects. Although baseline demographic characteristics were statistically comparable, the potential for selection bias and unmeasured confounding cannot be excluded. More detailed patient profiling would strengthen future analyses.

To build on these findings, future studies should aim to include larger, more diverse cohorts and adopt prospective, multicenter designs with multiple blinded measurements of radiologists with large expertise. Standardized imaging protocols, consistent use of contrast agents, and the integration of automated measurement tools will be essential for improving data quality and comparability. Longitudinal studies tracking CSA and T2 signal intensity over time, ideally in conjunction with clinical and biochemical markers, could provide deeper insights into disease progression and therapeutic response. Such efforts will be critical for refining diagnostic criteria and developing targeted, evidence-based interventions for PTS.

7.4 Potential Future Applications

MRI is already a cornerstone in the diagnosis of various neuropathies, but ongoing technological advancements are poised to significantly expand its clinical utility. These future applications are not merely extensions of current practices - they represent transformative opportunities for earlier diagnosis, more precise treatment planning, and deeper understanding of peripheral nerve disorders.

Quantitative MRI is expected to play a central role in the future of neuropathy diagnostics. Automated, AI-powered tools could standardize measurements of nerve CSA, edema, and T2 relaxation times, reducing operator variability and improving diagnostic accuracy. These metrics would also enable clinicians to monitor disease progression and treatment response with greater precision.

The integration of machine learning (ML) and artificial intelligence (AI) with MRI holds significant promise. By analyzing large imaging datasets, ML algorithms could detect subtle patterns predictive of neuropathy onset or progression - patterns that may be imperceptible to the human eye. This could enable earlier intervention and more personalized treatment strategies.

AKNOWLEDMENTS

I would like to express my heartfelt gratitude to my supervisors for their unwavering support, guidance, and expertise throughout my PhD journey. In particular, I am deeply thankful to Prof. Cavaletti, whose mentorship during these transformative years has been invaluable. His insights and encouragement have provided me with the tools needed to navigate the complexities of my research during all these years.

I sincerely extend my sincere appreciation to my co-tutor, Prof. Gerevini. Her collaborative spirit and critical feedback, rooted in her extensive expertise in neuroimaging, have significantly enriched my work each time I had the opportunity to learn from her. The willingness to share her long-life knowledge and experience has been instrumental in shaping the direction of my research.

A special acknowledgment goes to the dedicated team at Papa Giovanni XXIII Hospital in Bergamo. The commitment to excellence and collaborative efforts have greatly enhanced the quality of this project. Thank you for your tireless daily work, especially in facilitating data collection and, for your continuous encouragement throughout the research process and your availability to teach me and support me learning from the basics.

Additionally, I would like to express my gratitude to Prof. Moresco, whose initial guidance and support were pivotal in allowing me to enter this esteemed program. The belief in my potential from the very beginning motivated me to pursue this academic path, and I am grateful for the opportunities that have emerged from it.

Finally, I want to thank Sanofi Italy for the opportunity.

This journey would not have been possible without the contributions of these remarkable individuals and teams, and I am genuinely appreciative of each role played in my work. Thank you all for being part of this academic and professional adventure.

REFERENCES

Abresch R.T., Jensen M.P., Carter G.T. (2001). Health-Related Quality of Life in Peripheral Neuropathy, in Physical medicine and rehabilitation clinics of North America, volume 12, pp. 461-472.

Agarwal A., ChandraA A., Jaipal U. et al., (2019). Can imaging be the new yardstick for diagnosing peripheral neuropathy? A comparison between high resolution ultrasound and MR neurography with an approach to diagnosis, in Insights imaging, volume 10.

Al Hinai R., Kelly L., O'Connor M., Berman H. (2024). Unraveling the mysteries of parsonage turner syndrome: A journey towards optimal management. A systematic review, in Journal of hand and microsurgery.

Arnold R., Pianta T.J., Issar T., Kirby A., et al. (20229. Peripheral neuropathy: an important contributor to physical limitation and morbidity in stages 3 and 4 chronic kidney disease, Nephrology Dialysis Transplantation, volume 37, pp. 713–719.

Attal N., Bouhassira D., Colvin L. (2023). Advances and challenges in neuropathic pain: a narrative review and future directions, in British journal of anaesthesia, volume 131, pp. 79-92.

Ayeni E.A., Aldossary A.M., Ayejoto D.A. et al., (2022). Neurodegenerative Diseases: Implications of Environmental and Climatic Influences on Neurotransmitters and Neuronal Hormones Activities, in International journal of environmental research and public health, volume 19.

Bae E.H., Greenwald M.K., Schwartz A.G. (2021). Chemotherapy-Induced Peripheral Neuropathy: Mechanisms and Therapeutic Avenues, in Neurotherapeutics, volume 18, pp. 2384-2396.

Beghi, E., Kurland, L. T., Mulder, D. W., & Nicolosi, A. (1985). Brachial plexus neuropathy in the population of Rochester, Minnesota, 1970-1981. Annals of Neurology, volume 18, pp. 320-323.

Bercovich E., Javitt M.C. (2018). Medical Imaging: From Roentgen to the Digital Revolution, and Beyond, in Rambam Maimonides medical journal, volume 9.

Birnkrant, D. J., Bushby, K., Bann, C. M., Apkon, S. D., Blackwell, A., Brumbaugh, D. et al (2018). Diagnosis and management of Duchenne muscular dystrophy, part 1: diagnosis, and neuromuscular, rehabilitation, endocrine, and gastrointestinal and nutritional management. The Lancet. Neurology, volume 17, pp. 251–267.

Bornet P., Norris D.G. (2020). Medical Imaging: From Roentgen to the Digital Revolution, and Beyond, in BJR, volume 93.

Bowley, M. P., & Chad, D. A. (2019). Clinical neurophysiology of demyelinating polyneuropathy. Clinical Neurophysiology: Diseases and Disorders, pp. 241–268.

Brown, J. M., Radmanesh, A., Ceban, E., Lane, M., & Behrens, T. E. (2020). Longitudinal imaging markers in multiple sclerosis: Impact of new T2 lesion count and atrophy measurements on disability progression. Neuroimage Clinical, volume 25.

Cassandrini D., Trovato R., Rubegni A., Lenzi S. et al., (2017). Congenital myopathies: clinical phenotypes and new diagnostic tools, in Italiano Journal of pediatrics, volume 43.

Chen Y., Haacke E.M., Li J. (2019). Peripheral nerve magnetic resonance imaging, in F1000 Research, volume 8.

Chhabra A., Andreisek G., Soldatos T., Wang K.C. et al., (2011). MR Neurography: Past, Present, and Future, in AJR, volume 197.

Dalakas M. C. (2015). Inflammatory muscle diseases. The New England journal of medicine, volume 372, pp. 1734–1747.

Davoudi, M., Rezaei, P., Rajaeiramsheh, F. et al. (2021). Predicting the quality of life based on pain dimensions and psychiatric symptoms in patients with Painful diabetic neuropathy: a cross-sectional prevalence study in Iranian patients. Health Qual Life Outcomes, volume 19.

Deenen, J. C. W., Horlings, C. G. C., Verschuuren, J. J. G. M., Verbeek, A. L. M., & van Engelen, B. G. M. (2015). The Epidemiology of Neuromuscular Disorders: A Comprehensive Overview of the Literature. Journal of Neuromuscular Diseases, volume 2, pp. 73–85.

Dratch L., Azage M., Baldwin A. et al., (2024). Genetic testing in adults with neurologic disorders: Indications, approach, and clinical impacts, in Journal of Neurology, volume 271, pp. 733-747.

Esteva, A., Kuprel, B., Novoa, R. A., Ko, J., Swetter, S. M., Blau, H. M., & Thrun, S. (2017). Dermatologist- level classification of skin cancer with deep neural networks. Nature, volume 542, pp. 115-118.

Feinberg, J. H., & Radecki, J. (2010). Parsonage-Turner syndrome. HSS Journal, volume 6, pp. 199-205. Finsterer J. (2020). Update Review about Metabolic Myopathies, in Life, volume 10.

Fralish Z., Lotz E.M., Chavez T. et al., (2021). Neuromuscular Development and Disease: Learning From in vitro and in vivo Models, in Frontiers in cell and developmental biology, volume 9.

Gasparotti, R., Padua, L., Briani, C. et al. (2017). New technologies for the assessment of neuropathies. Nat Rev Neurology, volume 13, pp. 203–216.

Gerevini S., Agosta F., Riva N. et al., (2016). MR Imaging of Brachial Plexus and Limb-Girdle Muscles in Patients with

Amyotrophic Lateral Sclerosis, in Neuroradiology, volume 0, pp. 1-9.

Gilcrease-Garcia B.M., Deshmukh S.W., Parson M.S. (2020). Anatomy, Imaging, and Pathologic Conditions of the Brachial Plexus, in Radiographics : a review publication of the Radiological Society of North America, volume (6), pp. 1686–1714.

Hadden, R. D., Cornblath, D. R., Hughes, R. A., Zielasek, J., Hartung, H. P., Toyka, K. V., & Swan, A. V. (1998). Electrophysiological classification of Guillain-Barré syndrome: clinical associations and outcome. Plasma Exchange/Sandoglobulin Guillain-Barré Syndrome Trial Group. Annals of neurology, volume 44, pp. 780–788.

Hammi C., Yeung B. (2022) Neuropatia, in StatPearl Publishing.

Heydemann A. (2018). Skeletal Muscle Metabolism in Duchenne and Becker Muscular Dystrophy— Implications for Therapies, in Nutrients, volume 10.

Katona, I., & Weis, J. (2018). Diseases of the peripheral nerves. Neuropathology, pp. 453–474.

Koenig, M., Beggs, A. H., Moyer, M., Scherpf, S., Heindrich, K., Bettecken, T. et. al. (1989). The molecular basis for Duchenne versus Becker muscular dystrophy: correlation of severity with type of deletion. American journal of human genetics, volume 45, pp. 498–506.

Kollmer J., Bendszus M. (2021). Magnetic Resonance Neurography: Improved Diagnosis of Peripheral Neuropathies, in Neurotherapeutics, volume 18, pp. 2368-2383.

Lehmann H.C., Wunderlich G., Fink G.R., Sommer C. (2020). Diagnosis of peripheral neuropathy, in Neurological research and practice, volume 2.

Litjens, G., Kooi, T., Bejnordi, B. E., Setio, A. A. A., Ciompi, F., Ghafoorian, M., van der Laak, J. A. W. M., van Ginneken, B., & Sánchez, C. I. (2017). A survey on deep learning in medical image analysis. Medical Image Analysis, volume 42, pp. 60–88.

Lohrke J., Frenzel T., Endrikat J., et al., (2016). 25 Years of Contrast-Enhanced MRI: Developments, Current Challenges and Future Perspectives, in Springer, volume 33, pp. 1-28.

Lundervold, A. S., & Lundervold, A. (2019). An overview of deep learning in medical imaging focusing on MRI. Zeitschrift für Medizinische Physik, volume 22, pp. 102-127.

Markl M, Schnell S, Wu C, Bollache E, Jarvis K, Barker AJ, Robinson JD, Rigsby CK. Advanced flow MRI: emerging techniques and applications. Clin Radiol. 2016, volume 71, pp. 779-95.

Meneses do Rego A.C., Araujo-Filho I. (2024). Parsonage-Turner Syndrome: An update, in World journal of advanced research and reviews, volume 23, pp. 2882-2889.

Mercuri, E., et al. (2007). "Muscle MRI in the evaluation of muscular dystrophies: a new scoring system."

Neuromuscular Disorders, 17(8), 593-599.

Milner CS, Kannan K, Iyer VG, Thirkannad SM (2016). Parsonage-Turner Syndrome: Clinical and Epidemiological Features From a Hand Surgeon's Perspective. Hand (N Y).Mogil, J. (2009). Animal models of pain: progress and challenges. Nat Rev Neurosciences, volume 10, pp. 283–294.

Nagy H., Veerapaneni K.D. (2023). Myopathy, StatPearls.

Nave, K.-A., Sereda, M. W., & Ehrenreich, H. (2007). Mechanisms of Disease: inherited demyelinating neuropathies—from basic to clinical research. Nature Clinical Practice Neurology, volume 3, 453–464.

Pacifico P., Coy-Dibley J.S., Millero R.J., Menichella D.M. (2023). Peripheral mechanisms of peripheral neuropathic pain, in

Frontiers in molecular neuroscience, volume 16.

Ranzenberger, L. R., Das, J. M., & Snyder, T. (2023). Diffusion Tensor Imaging. In StatPearls. StatPearls Publishing.

Ravenscroft G., Bryson-Richardson R.J., Nowak K.J., Laing N.G., (2018). Recent advances in understanding congenital myopathies, in F1000 Research, volume 7.

Reede, R. D., Jensen, T. S., Campbell, J. N., Cruccu, G., Dostrovsky, J. O., Griffin, J. W., Hansson, P., Hughes, R., Nurmikko, T., & Serra, J. (2008). Neuropathic pain: redefinition and a grading system for clinical and research purposes. Neurology, volume 70, pp. 1630–1635.

Scalf RE, Wenger DE, Frick MA, Mandrekar JN, Adkins MC. MRI findings of 26 patients with Parsonage-Turner syndrome. AJR Am J Roentgenol. 2007 Jul;189(1):W39-44. doi: 10.2214/AJR.06.1136. PMID: 17579134.

Schirinzi E., Ricci G., Torri F., Mancuso M., Siciliano G. (2024). Biomolecules of Muscle Fatigue in Metabolic Myopathies, in Biomolecules, volume 14.

Shinu P., Morsy M.A., Nair A.B. et. al. (2022). Novel Therapies for the Treatment of Neuropathic Pain: Potential and Pitfalls, in journal of clinical medicine, volume 11.

Shkodra M., Caraceni A. (2022). Treatment of Neuropathic Pain Directly Due to Cancer: An Update, in Cancers, volume 14.

Solbiati, M., Franzoni, S., Ognibeni, G., Filosto, M., & Scalvini, A. (2018). Predictors of rehabilitation outcome in post-stroke patients: A multi-center retrospective study. Journal of Rehabilitation Medicine, volume 50, pp. 758-764.

Su X., Kong X., Liu D. et al., (2019). Multimodal magnetic resonance imaging of peripheral nerves: establishment and validation of brachial and lumbosacral plexi

Tae W.S., Ham B.J., Pyun S.B., Kang S.H., Kim B.J. (2018). Current Clinical Applications of Diffusion-Tensor Imaging in Neurological Disorders, in Journal of clinical neurology, volume 14, pp. 129-140

Toth, C., Lander, S., Wiebe, S., & Zochodne, D. W. (2019). The importance of inflammation in neural repair. Journal of Neuroinflammation, volume 16.

Tsairis, P., Dyck, P. J., & Mulder, D. W. (1972). Natural history of brachial plexus neuropathy: report on 99 patients. Archives of Neurology, volume 27, pp. 109-117.

Tulba D., Popescu B.O., Manole E., Baicus C. (2021). Immune Axonal Neuropathies Associated With Systemic Autoimmune Rheumatic Diseases, in Frontiers in pharmacology, volume 12.

Upadhyaya, Vaishali & Upadhyaya, Divya & Bansal, Richa & Pandey, Tarun & Pandey, AshokKumar. (2019). MR neurography in Parsonage-Turner syndrome. Indian Journal of Radiology and Imaging. 29. 264.

Van Alfen, N., & Van Engelen, B. G. M. (2006). The clinical spectrum of neuralgic amyotrophy in 246 cases. Brain, volume 129, pp. 438-450.

Van Been E.J.R., Huhl C., Anzai Y. et al., (2018). Value of MRI in Medicine: More Than Just Another Test?, in Journal of Magn. Reason. Imaging, volume 49, pp. 14-25.

Van Snick E, Valgaeren B, Claikens B. Parsonage-Turner Syndrome. J Belg Soc Radiol. 2023 Apr 28;107(1):33. doi: 10.5334/jbsr.3088. PMID: 37124325; PMCID: PMC10143934.

Vaskovic J. (2023). MRI: the basics, in Radiological Anatomy, march 2023.

Viard, A., Eustache, F., & Segobin, S. (2021). History of Magnetic Resonance Imaging: A Trip Down Memory Lane. Neuroscience,

volume 3.

Washsner J., Gale E.M., Rodriguez A., Caravan P., (2019). Chemistry of MRI Contrast Agents: Current Challenges and New Frontiers, in Chem. Rev., volume 119, pp. 957-1057.

Yang S.H., Chang C., Liano Z.X. (2019). Polymyositis and dermatomyositis – challenges in diagnosis and management, in Journal of transation autoimmunity, volume 2.

Zatz M., Passos-Bueno M.R., Vainzof M. (2016). Neuromuscular disorders: genes, genetic counseling and therapeutic trials, in Genetics and molecular biology, volume 39, pp. 339-348.

Zis, P., Sarrigiannis, P. G., Rao, D. G., Hewamadduma, C., & Hadjivassiliou, M. (2016). Chronic idiopathic axonal polyneuropathy: a systematic review. Journal of Neurology, volume 263, pp. 1903–1910.

LIST OF TABLES

Table 1 – Patients' Characteristics

No. of patients	51
Gender, n (%)	
Female	10 (19.6)
Male	41 (80.4)
Age, mean (SD)	51.9 ± 15.9
Race, n (%)	
Caucasian	49 (96.1)
Middle Eastern	2 (3.9)
Side, n (%)	
Right	21 (41.2)
Left	20 (39.2)
Both	10 (19.6)
Clinical Onset, n (%)	
Pain	36 (70.6)
Functional Impairment	27 (52.9)
EMG, n (%)	
EMG Neurogenic Impairment	41 (80.4)
EMG Denervation Activity	10 (19.6)
EMG Bilateral Pess	1 (2.0)
EMG Paralysis	1 (2.0)
EMG Absence of electrical activity	1 (2.0)
EMG Motor Unit remodelling	3 (5.9)
MRI Onset, n (%)	
Aspecific	2 (4.0)
Inflammatory	46 (92.0)
Trauma	2 (4.0)

Table 2 – Demographic Characteristics

	Total	**Healthy Control Subjects**	**Patients with Disease (PTS)**
No. of Subjects	76	25	51
Age at MRI imaging* (years)	50.0 ± 16.6 (14-83) [52, 39-62]	46.5±18.1 (18-83) [46, 32-56]	51.9± 15.9 (14-78) [53, 46-63]
Gender, n(%)			
Female	18 (23.7)	7 (28.0)	10 (19.6)
Male	58 (76.3)	18 (72.0)	41 (80.4)

Note - * Results are reported as means ± standard deviation, with the range in round brackets. Results in squared brackets are median and interquartile range.

Table 3 – Side of Nerve Roots per Gender and Age Range

		Gender			**Age Range**		
	Overall (n = 51)	**Female (n = 10)**	**Male (n = 41)**	**p-value**	**< 55 years (n = 27)**	**≥ 55 years (n = 24)**	**p-value**
Side							

Right	21	(41.2)	5	(50.0)	16	(39.0)	0.816	10	(37.0)	11	(45.8)	0.510
Left	20	(39.2)	4	(40.0)	16	(39.0)		10	(37.0)	10	(41.7)	
Both	10	(19.6)	1	(10.0)	9	(22.0)		7	(25.9)	3	(12.5)	
Uni vs. Bilateral												
Monolateral	41	(80.4)	9	(90.0)	32	(78.0)	0.664	20	(74.1)	21	(87.5)	0.300
Bilateral	10	(19.6)	1	(10.0)	9	(22.0)		7	(25.9)	3	(12.5)	

Note: Results are reported as relative frequencies and percentages, sample size = 51 cases.

Table 4 – Nerve Roots

				Gender					**Age Range**			
	Overall		**Female**		**Male**		**p-value**	**< 55 years**		**≥ 55 years**		**p-value**
Right												
C5	9	(29.0)	4	(66.7)	5	(20.0)	0.043	5	(29.4)	4	(28.6)	1.000
C6	19	(61.3)	4	(66.7)	15	(60.0)	1.000	10	(58.8)	9	(64.3)	1.000
C7	13	(41.9)	3	(50.0)	10	(40.0)	0.676	7	(41.2)	6	(42.9)	1.000
C8	15	(48.4)	3	(50.0)	12	(48.0)	1.000	10	(58.8)	5	(35.7)	0.285
T1	4	(12.9)	1	(16.7)	3	(12.0)	1.000	2	(11.8)	2	(14.3)	1.000
Left												
C5	13	(43.3)	3	(60.0)	10	(40.0)	0.628	5	(29.4)	8	(61.5)	0.138
C6	17	(56.7)	3	(60.0)	14	(56.0)	1.000	7	(41.2)	10	(76.9)	0.071
C7	13	(43.3)	2	(40.0)	11	(44.0)	1.000	8	(47.1)	5	(38.5)	0.721
C8	10	(33.3)	2	(40.0)	8	(32.0)	1.000	7	(41.2)	3	(23.1)	0.440
T1	2	(6.7)	1	(20.0)	1	(4.0)	0.310	1	(5.9)	1	(7.7)	1.000

Note: Results are reported as relative frequencies and percentages; sample size of 51 patients with PTS.

Table 5 – Nerve Trunk

				Gender					**Age Range**			
	Overall		**Female**		**Male**		**p-value**	**< 55 years**		**≥ 55 years**		**p-value**
Right												
Upper Primary Trunk	7	(20.6)	1	(16.7)	6	(21.4)	1.000	3	(16.7)	4	(25.0)	0.681
Middle Primary Trunk	1	(3.2)	0	(0.0)	1	(4.0)	1.000	1	(5.9)	0	(0.0)	1.000
Lower Primary Trunk	4	(12.9)	1	(16.7)	3	(12.0)	1.000	4	(23.5)	0	(0.0)	0.107
Left												
Upper Primary Trunk	4	(13.3)	0	(0.0)	4	(16.0)	1.000	2	(11.8)	2	(15.4)	1.000
Middle Primary Trunk	4	(13.3)	0	(0.0)	4	(16.0)	1.000	2	(11.8)	2	(15.4)	1.000
Lower Primary Trunk	3	(10.0)	0	(0.0)	3	(12.0)	1.000	2	(11.8)	1	(7.7)	1.000

Note: Results are reported as relative frequencies and percentages; sample size of 51 patients with PTS.

Table 6 - Edema

				Gender					**Age Range**			
	Overall		**Female**		**Male**		**p-value**	**< 55 years**		**≥ 55 years**		**p-value**
Right												
Shoulder Girdle Muscles												
Pectoralis Major Muscle	1	(3.2)	0	(0.0)	1	(4.0)	1.000	0	(0.0)	1	(7.1)	0.452
Pectoralis Minor Muscle	1	(3.2)	0	(0.0)	1	(4.0)	1.000	0	(0.0)	1	(7.1)	0.452

Subclavious Muscle	0	(0.0)	0	(0.0)	0	(0.0)	N/A	0	(0.0)	0	(0.0)	N/A
Serratus Anterior Muscle	4	(12.9)	1	(16.7)	3	(12.0)	1.000	1	(5.9)	3	(21.4)	0.304
Deltoid Muscle	6	(19.4)	2	(33.3)	4	(16.0)	0.567	1	(5.9)	5	(35.7)	0.067
Shoulder Girdle Posterio Muscle												
Trapezius Muscle	3	(9.7)	1	(16.7)	2	(8.0)	0.488	2	(11.8)	1	(7.1)	1.000
Latissum Dorsi Muscle	0	(0.0)	0	(0.0)	0	(0.0)	N/A	0	(0.0)	0	(0.0)	N/A
Levator Scapula Muscle	2	(6.5)	0	(0.0)	2	(8.0)	1.000	2	(11.8)	0	(0.0)	0.488
Rhomboid Major Muscle	1	(3.2)	1	(16.7)	0	(0.0)	0.194	0	(0.0)	1	(7.1)	0.452
Rhomboid Minor Muscle	1	(3.2)	0	(0.0)	1	(4.0)	1.000	1	(5.9)	0	(0.0)	1.000
Teres Major Muscle	1	(3.2)	1	(16.7)	0	(0.0)	0.194	0	(0.0)	1	(7.1)	0.452
Teres Minor Muscle	3	(9.7)	1	(16.7)	2	(8.0)	0.488	2	(11.8)	1	(7.1)	1.000
Rotation Cuff Muscle												
Supraspinatus Muscle	13	(41.9)	3	(50.0)	10	(40.0)	0.676	7	(41.2)	6	(42.9)	1.000
Infraspinatus Muscle	13	(41.9)	3	(50.0)	10	(40.0)	0.676	6	(35.3)	7	(50.0)	0.481
Subscapularis Muscle	11	(35.5)	5	(83.3)	6	(24.0)	0.013	5	(29.4)	6	(42.9)	0.477
Arm Posterior Muscle												
Triceps Muscle	4	(12.5)	1	(16.7)	3	(11.5)	1.000	2	(11.1)	2	(14.3)	1.000
Anconeus Muscle	0	(0.0)	0	(0.0)	0	(0.0)	N/A	0	(0.0)	0	(0.0)	N/A
Arm Anterior Muscle												
Brachialis Muscle	0	(0.0)	0	(0.0)	0	(0.0)	N/A	0	(0.0)	0	(0.0)	N/A
Coracobrachialis Muscle	0	(0.0)	0	(0.0)	0	(0.0)	N/A	0	(0.0)	0	(0.0)	N/A
Neck Lateral Muscle												
Scalene Muscle Ant	0	(0.0)	0	(0.0)	0	(0.0)	N/A	0	(0.0)	0	(0.0)	N/A
Scalene Muscle Med	0	(0.0)	0	(0.0)	0	(0.0)	N/A	0	(0.0)	0	(0.0)	N/A
Scalene Muscle Post	0	(0.0)	0	(0.0)	0	(0.0)	N/A	0	(0.0)	0	(0.0)	N/A
Left												
Shoulder Girdle Muscles												
Pectoralis Major Muscle	1	(3.3)	0	(0.0)	1	(4.0)	1.000	1	(5.9)	0	(0.0)	1.000
Pectoralis Minor Muscle	1	(3.3)	0	(0.0)	1	(4.0)	1.000	1	(5.9)	0	(0.0)	1.000
Subclavious Muscle	1	(3.3)	0	(0.0)	1	(4.0)	1.000	1	(5.9)	0	(0.0)	1.000
Serratus Anterior Muscle	1	(3.3)	0	(0.0)	1	(4.0)	1.000	1	(5.9)	0	(0.0)	1.000
Deltoid Muscle	10	(31.3)	2	(33.3)	8	(30.8)	1.000	7	(38.9)	3	(21.4)	0.446
Shoulder Girdle Posterio Muscle												
Trapezius Muscle	4	(13.3)	1	(20.0)	3	(12.0)	0.538	3	(17.6)	1	(7.7)	0.613
Latissum Dorsi Muscle	0	(0.0)	0	(0.0)	0	(0.0)	N/A	0	(0.0)	0	(0.0)	N/A
Levator Scapula Muscle	1	(3.3)	0	(0.0)	1	(4.0)	1.000	1	(5.9)	0	(0.0)	1.000
Rhomboid Major Muscle	2	(6.7)	1	(20.0)	1	(4.0)	0.310	1	(5.9)	1	(7.7)	1.000
Rhomboid Minor Muscle	0	(0.0)	0	(0.0)	0	(0.0)	N/A	0	(0.0)	0	(0.0)	N/A
Teres Major Muscle	1	(3.3)	0	(0.0)	1	(4.0)	1.000	0	(0.0)	1	(7.7)	0.433
Teres Minor Muscle	1	(3.3)	0	(0.0)	1	(4.0)	1.000	1	(5.9)	0	(0.0)	1.000
Rotation Cuff Muscle												
Supraspinatus Muscle	12	(40.0)	2	(40.0)	10	(40.0)	1.000	7	(41.2)	5	(38.5)	1.000
Infraspinatus Muscle	10	(33.3)	2	(40.0)	8	(32.0)	1.000	6	(35.3)	4	(30.8)	1.000
Subscapularis Muscle	4	(13.3)	0	(0.0)	4	(16.0)	1.000	1	(5.9)	3	(23.1)	0.290
Arm Posterior Muscle												
Triceps Muscle	2	(6.7)	0	(0.0)	2	(8.0)	1.000	1	(5.9)	1	(7.7)	1.000

Anconeus Muscle	0	(0.0)	0	(0.0)	0	(0.0)	N/A	0	(0.0)	0	(0.0)	N/A
Arm Anterior Muscle												
Brachialis Muscle	0	(0.0)	0	(0.0)	0	(0.0)	N/A	0	(0.0)	0	(0.0)	N/A
Coracobrachialis Muscle	0	(0.0)	0	(0.0)	0	(0.0)	N/A	0	(0.0)	0	(0.0)	N/A
Neck Lateral Muscle												
Scalene Muscle Ant	0	(0.0)	0	(0.0)	0	(0.0)	N/A	0	(0.0)	0	(0.0)	N/A
Scalene Muscle Med	0	(0.0)	0	(0.0)	0	(0.0)	N/A	0	(0.0)	0	(0.0)	N/A
Scalene Muscle Post	0	(0.0)	0	(0.0)	0	(0.0)	N/A	0	(0.0)	0	(0.0)	N/A

Table 7 – Fat Infiltration

	Overall		Gender				Age Range				
			Female		Male	p-value	< 55 years		≥ 55 years		p-value
Right											
Shoulder Girdle Muscles											
Pectoralis Major Muscle	1	(3.2)	0	(0.0)	1	(4.0)	1.000	1	(5.9)	0	(0.0)	1.000
Pectoralis Minor Muscle	1	(3.2)	0	(0.0)	1	(4.0)	1.000	1	(5.9)	0	(0.0)	1.000
Subclavious Muscle	1	(3.2)	0	(0.0)	1	(4.0)	1.000	1	(5.9)	0	(0.0)	1.000
Serratus Anterior Muscle	3	(9.7)	1	(16.7)	2	(8.0)	0.488	2	(11.8)	1	(7.1)	1.000
Deltoid Muscle	5	(16.1)	1	(16.7)	4	(16.0)	1.000	3	(17.6)	2	(14.3)	1.000
Shoulder Girdle Posterio Muscle											
Trapezius Muscle	1	(3.2)	1	(16.7)	0	(0.0)	0.194	0	(0.0)	1	(7.1)	0.452
Latissum Dorsi Muscle	0	(0.0)	0	(0.0)	0	(0.0)	N/A	0	(0.0)	0	(0.0)	N/A
Levator Scapula Muscle	0	(0.0)	0	(0.0)	0	(0.0)	N/A	0	(0.0)	0	(0.0)	N/A
Rhomboid Major Muscle	1	(3.2)	0	(0.0)	1	(4.0)	1.000	1	(5.9)	0	(0.0)	1.000
Rhomboid Minor Muscle	0	(0.0)	0	(0.0)	0	(0.0)	N/A	0	(0.0)	0	(0.0)	N/A
Teres Major Muscle	0	(0.0)	0	(0.0)	0	(0.0)	N/A	0	(0.0)	0	(0.0)	N/A
Teres Minor Muscle	2	(6.5)	1	(16.7)	1	(4.0)	0.355	0	(0.0)	2	(14.3)	0.196
Rotation Cuff Muscle											
Supraspinatus Muscle	6	(19.4)	2	(33.3)	4	(16.0)	0.567	2	(11.8)	4	(28.6)	0.370
Infraspinatus Muscle	5	(16.1)	1	(16.7)	4	(16.0)	1.000	3	(17.6)	2	(14.3)	1.000
Subscapularis Muscle	5	(16.1)	2	(33.3)	3	(12.0)	0.241	1	(5.9)	4	(28.6)	0.148
Arm Posterior Muscle											
Triceps Muscle	0	(0.0)	0	(0.0)	0	(0.0)	N/A	0	(0.0)	0	(0.0)	N/A
Anconeus Muscle	0	(0.0)	0	(0.0)	0	(0.0)	N/A	0	(0.0)	0	(0.0)	N/A
Arm Anterior Muscle											
Brachialis Muscle	0	(0.0)	0	(0.0)	0	(0.0)	N/A	0	(0.0)	0	(0.0)	N/A
Coracobrachialis Muscle	0	(0.0)	0	(0.0)	0	(0.0)	N/A	0	(0.0)	0	(0.0)	N/A
Neck Lateral Muscle											
Scalene Muscle Ant	0	(0.0)	0	(0.0)	0	(0.0)	N/A	0	(0.0)	0	(0.0)	N/A
Scalene Muscle Med	0	(0.0)	0	(0.0)	0	(0.0)	N/A	0	(0.0)	0	(0.0)	N/A
Scalene Muscle Post	0	(0.0)	0	(0.0)	0	(0.0)	N/A	0	(0.0)	0	(0.0)	N/A
Left											
Shoulder Girdle Muscles											
Pectoralis Major Muscle	2	(6.7)	1	(20.0)	1	(4.0)	0.310	1	(5.9)	1	(7.7)	1.000
Pectoralis Minor Muscle	2	(6.7)	1	(20.0)	1	(4.0)	0.310	1	(5.9)	1	(7.7)	1.000
Subclavious Muscle	2	(6.5)	0	(0.0)	2	(7.7)	1.000	1	(5.9)	1	(7.1)	1.000
Serratus Anterior Muscle	3	(9.7)	1	(20.0)	2	(7.7)	0.422	1	(5.9)	2	(14.3)	0.576
Deltoid Muscle	4	(13.3)	2	(40.0)	2	(8.0)	0.119	2	(11.8)	2	(15.4)	1.000
Shoulder Girdle Posterio Muscle											
Trapezius Muscle	1	(3.3)	0	(0.0)	1	(4.0)	1.000	0	(0.0)	1	(7.7)	0.433
Latissum Dorsi Muscle	0	(0.0)	0	(0.0)	0	(0.0)	N/A	0	(0.0)	0	(0.0)	N/A
Levator Scapula Muscle	0	(0.0)	0	(0.0)	0	(0.0)	N/A	0	(0.0)	0	(0.0)	N/A
Rhomboid Major Muscle	1	(3.3)	1	(20.0)	0	(0.0)	0.167	1	(5.9)	0	(0.0)	1.000
Rhomboid Minor Muscle	0	(0.0)	0	(0.0)	0	(0.0)	N/A	0	(0.0)	0	(0.0)	N/A

Teres Major Muscle	0	(0.0)	0	(0.0)	0	(0.0)	N/A	0	(0.0)	0	(0.0)	N/A
Teres Minor Muscle	1	(3.3)	0	(0.0)	1	(4.0)	1.000	0	(0.0)	1	(7.7)	0.433
Rotation Cuff Muscle												
Supraspinatus Muscle	9	(30.0)	3	(60.0)	6	(24.0)	0.143	3	(17.6)	6	(46.2)	0.123
Infraspinatus Muscle	12	(38.7)	3	(60.0)	9	(34.6)	0.350	4	(22.2)	8	(61.5)	0.060
Subscapularis Muscle	5	(16.7)	1	(20.0)	4	(16.0)	1.000	1	(5.9)	4	(30.8)	0.138
Arm Posterior Muscle												
Triceps Muscle	1	(3.3)	0	(0.0)	1	(4.0)	1.000	1	(5.9)	0	(0.0)	1.000
Anconeus Muscle	0	(0.0)	0	(0.0)	0	(0.0)	N/A	0	(0.0)	0	(0.0)	N/A
Arm Anterior Muscle												
Brachialis Muscle	0	(0.0)	0	(0.0)	0	(0.0)	N/A	0	(0.0)	0	(0.0)	N/A
Coracobrachialis Muscle	0	(0.0)	0	(0.0)	0	(0.0)	N/A	0	(0.0)	0	(0.0)	N/A
Neck Lateral Muscle												
Scalene Muscle Ant	0	(0.0)	0	(0.0)	0	(0.0)	N/A	0	(0.0)	0	(0.0)	N/A
Scalene Muscle Med	0	(0.0)	0	(0.0)	0	(0.0)	N/A	0	(0.0)	0	(0.0)	N/A
Scalene Muscle Post	0	(0.0)	0	(0.0)	0	(0.0)	N/A	0	(0.0)	0	(0.0)	N/A

Table 8 - Atrophy

			Gender				Age Range				
	Overall		Female		Male	p-value	< 55 years		≥ 55 years		p-value
Right											
Shoulder Girdle Muscles											
Pectoralis Major Muscle	0	(0.0)	0	(0.0)	0	(0.0)	N/A	0	(0.0)	0	(0.0)	N/A
Pectoralis Minor Muscle	0	(0.0)	0	(0.0)	0	(0.0)	N/A	0	(0.0)	0	(0.0)	N/A
Subclavious Muscle	0	(0.0)	0	(0.0)	0	(0.0)	N/A	0	(0.0)	0	(0.0)	N/A
Serratus Anterior Muscle	1	(3.2)	1	(16.7)	0	(0.0)	0.194	0	(0.0)	1	(7.1)	0.452
Deltoid Muscle	4	(12.5)	0	(0.0)	4	(15.4)	0.566	2	(11.1)	2	(14.3)	1.000
Shoulder Girdle Posterio Muscle											
Trapezius Muscle	0	(0.0)	0	(0.0)	0	(0.0)	N/A	0	(0.0)	0	(0.0)	N/A
Latissum Dorsi Muscle	0	(0.0)	0	(0.0)	0	(0.0)	N/A	0	(0.0)	0	(0.0)	N/A
Levator Scapula Muscle	0	(0.0)	0	(0.0)	0	(0.0)	N/A	0	(0.0)	0	(0.0)	N/A
Rhomboid Major Muscle	0	(0.0)	0	(0.0)	0	(0.0)	N/A	0	(0.0)	0	(0.0)	N/A
Rhomboid Minor Muscle	0	(0.0)	0	(0.0)	0	(0.0)	N/A	0	(0.0)	0	(0.0)	N/A
Teres Major Muscle	0	(0.0)	0	(0.0)	0	(0.0)	N/A	0	(0.0)	0	(0.0)	N/A
Teres Minor Muscle	0	(0.0)	0	(0.0)	0	(0.0)	N/A	0	(0.0)	0	(0.0)	N/A
Rotation Cuff Muscle											
Supraspinatus Muscle	8	(25.0)	2	(33.3)	6	(23.1)	0.625	3	(16.7)	5	(35.7)	0.252
Infraspinatus Muscle	4	(12.9)	0	(0.0)	4	(16.0)	0.561	1	(5.9)	3	(21.4)	0.304
Subscapularis Muscle	5	(16.1)	2	(33.3)	3	(12.0)	0.241	1	(5.9)	4	(28.6)	0.148
Arm Posterior Muscle											
Triceps Muscle	2	(6.5)	0	(0.0)	2	(8.0)	1.000	1	(5.9)	1	(7.1)	1.000
Anconeus Muscle	0	(0.0)	0	(0.0)	0	(0.0)	N/A	0	(0.0)	0	(0.0)	N/A
Arm Anterior Muscle											
Brachialis Muscle	1	(3.2)	0	(0.0)	1	(4.0)	1.000	0	(0.0)	1	(7.1)	0.452
Coracobrachialis Muscle	0	(0.0)	0	(0.0)	0	(0.0)	N/A	0	(0.0)	0	(0.0)	N/A
Neck Lateral Muscle											
Scalene Muscle Ant	0	(0.0)	0	(0.0)	0	(0.0)	N/A	0	(0.0)	0	(0.0)	N/A
Scalene Muscle Med	0	(0.0)	0	(0.0)	0	(0.0)	N/A	0	(0.0)	0	(0.0)	N/A
Scalene Muscle Post	0	(0.0)	0	(0.0)	0	(0.0)	N/A	0	(0.0)	0	(0.0)	N/A
Left											
Shoulder Girdle Muscles											
Pectoralis Major Muscle	1	(3.3)	0	(0.0)	1	(4.0)	1.000	0	(0.0)	1	(7.7)	0.433
Pectoralis Minor Muscle	1	(3.3)	0	(0.0)	1	(4.0)	1.000	0	(0.0)	1	(7.7)	0.433
Subclavious Muscle	0	(0.0)	0	(0.0)	0	(0.0)	N/A	0	(0.0)	0	(0.0)	N/A
Serratus Anterior Muscle	1	(3.3)	0	(0.0)	1	(4.0)	1.000	0	(0.0)	1	(7.7)	0.433
Deltoid Muscle	2	(6.7)	0	(0.0)	2	(8.0)	1.000	0	(0.0)	2	(15.4)	0.179
Shoulder Girdle Posterio Muscle											
Trapezius Muscle	1	(3.3)	0	(0.0)	1	(4.0)	1.000	1	(5.9)	0	(0.0)	1.000
Latissum Dorsi Muscle	0	(0.0)	0	(0.0)	0	(0.0)	N/A	0	(0.0)	0	(0.0)	N/A
Levator Scapula Muscle	2	(6.7)	1	(20.0)	1	(4.0)	0.310	1	(5.9)	1	(7.7)	1.000
Rhomboid Major Muscle	0	(0.0)	0	(0.0)	0	(0.0)	N/A	0	(0.0)	0	(0.0)	N/A
Rhomboid Minor Muscle	0	(0.0)	0	(0.0)	0	(0.0)	N/A	0	(0.0)	0	(0.0)	N/A

Teres Major Muscle	1	(3.3)	0	(0.0)	1	(4.0)	1.000	0	(0.0)	1	(7.7)	0.433
Teres Minor Muscle	1	(3.3)	0	(0.0)	1	(4.0)	1.000	0	(0.0)	1	(7.7)	0.433
Rotation Cuff Muscle												
Supraspinatus Muscle	6	(20.0)	1	(20.0)	5	(20.0)	1.000	1	(5.9)	5	(38.5)	0.061
Infraspinatus Muscle	6	(20.0)	1	(20.0)	5	(20.0)	1.000	1	(5.9)	5	(38.5)	0.061
Subscapularis Muscle	3	(10.0)	0	(0.0)	3	(12.0)	1.000	0	(0.0)	3	(23.1)	0.070
Arm Posterior Muscle												
Triceps Muscle	0	(0.0)	0	(0.0)	0	(0.0)	N/A	0	(0.0)	0	(0.0)	N/A
Anconeus Muscle	0	(0.0)	0	(0.0)	0	(0.0)	N/A	0	(0.0)	0	(0.0)	N/A
Arm Anterior Muscle												
Brachialis Muscle	0	(0.0)	0	(0.0)	0	(0.0)	N/A	0	(0.0)	0	(0.0)	N/A
Coracobrachialis Muscle	0	(0.0)	0	(0.0)	0	(0.0)	N/A	0	(0.0)	0	(0.0)	N/A
Neck Lateral Muscle												
Scalene Muscle Ant	1	(3.3)	0	(0.0)	1	(4.0)	1.000	0	(0.0)	1	(7.7)	0.433
Scalene Muscle Med	1	(3.3)	0	(0.0)	1	(4.0)	1.000	0	(0.0)	1	(7.7)	0.433
Scalene Muscle Post	1	(3.3)	0	(0.0)	1	(4.0)	1.000	0	(0.0)	1	(7.7)	0.433

Table 9 – Nerve Involvement at EMG and MRI respectively

		EMG			
		C5	**C6**	**C7**	**C8**
MRI	**C5**	18	16	8	4
	C6	25	28	14	6
	C7	17	19	11	5
	C8	14	16	11	9

Table 10 – Nerve Characteristics by EMG and MRI, at Clinics

	Total	**Pain (n = 36)**	**No Pain (n = 15)**	**p-value**	**Functional Impairment (n = 27)**	**No Functional Impairment (n = 24)**	**p-value**
Side							
Right	21 (41.2)	17 (47.2)	4 (26.7)	0.079	14 (51.9)	7 (29.2)	0.273
Left	20 (39.2)	15 (41.7)	5 (33.3)		9 (33.3)	11 (45.8)	
Both	10 (19.6)	4 (11.1)	6 (40)		4 (14.8)	6 (25)	
EMG C5	38 (74.5)	26 (72.2)	12 (80)	0.730	20 (74.1)	18 (75)	1.000
EMG C6	42 (82.4)	30 (83.3)	12 (80)	1.000	22 (81.5)	20 (83.3)	1.000
EMG C7	23 (45.1)	15 (41.7)	8 (53.3)	0.542	11 (40.7)	12 (50)	0.580
EMG C8	12 (23.5)	10 (27.8)	2 (13.3)	0.470	6 (22.2)	6 (25)	1.000
MRI C5	20 (39.2)	14 (38.9)	6 (40)	1.000	10 (37)	10 (41.7)	0.780
MRI C6	32 (62.7)	25 (69.4)	7 (46.7)	0.203	18 (66.7)	14 (58.3)	0.575
MRI C7	22 (43.1)	16 (44.4)	6 (40)	1.000	13 (48.1)	9 (37.5)	0.573
MRI C8	20 (39.2)	16 (44.4)	4 (26.7)	0.348	11 (40.7)	9 (37.5)	1.000

Note: Results are reported as relative frequencies and percentages, sample size of 51 patients.

Table 11 - Edema

	Total	**Pain (n = 36)**	**No Pain (n = 15)**	**p-value**	**Functional Impairment (n = 27)**	**No Functional Impairment (n = 24)**	**p-value**

Shoulder Girdle Muscles							
Pectoralis Major Muscle							
Grade 0	49 (96.1)	34 (94.4)	15 (100)	1.000	25 (92.6)	24 (100)	1.000
Grade 1	1 (2)	1 (2.8)	0 (0)		1 (3.7)	0 (0)	
Grade 2	1 (2)	1 (2.8)	0 (0)		1 (3.7)	0 (0)	
Grade 3	0 (0)	0 (0)	0 (0)		0 (0)	0 (0)	
Grade 4	0 (0)	0 (0)	0 (0)		0 (0)	0 (0)	
Pectorali Minor Muscle							
Grade 0	49 (96.1)	34 (94.4)	15 (100)	1.000	25 (92.6)	24 (100)	1.000
Grade 1	1 (2)	1 (2.8)	0 (0)		1 (3.7)	0 (0)	
Grade 2	1 (2)	1 (2.8)	0 (0)		1 (3.7)	0 (0)	
Grade 3	0 (0)	0 (0)	0 (0)		0 (0)	0 (0)	
Grade 4	0 (0)	0 (0)	0 (0)		0 (0)	0 (0)	
Subclavius Muscle							
Grade 0	50 (98)	35 (97.2)	15 (100)	1.000	26 (96.3)	24 (100)	1.000
Grade 1	0 (0)	0 (0)	0 (0)		0 (0)	0 (0)	
Grade 2	1 (2)	1 (2.8)	0 (0)		1 (3.7)	0 (0)	
Grade 3	0 (0)	0 (0)	0 (0)		0 (0)	0 (0)	
Grade 4	0 (0)	0 (0)	0 (0)		0 (0)	0 (0)	
Serratus Anterior Muscle							
Grade 0	44 (86.3)	30 (83.3)	14 (93.3)	0.756	22 (81.5)	22 (91.7)	0.671
Grade 1	6 (11.8)	5 (13.9)	1 (6.7)		4 (14.8)	2 (8.3)	
Grade 2	1 (2)	1 (2.8)	0 (0)		1 (3.7)	0 (0)	
Grade 3	0 (0)	0 (0)	0 (0)		0 (0)	0 (0)	
Grade 4	0 (0)	0 (0)	0 (0)		0 (0)	0 (0)	
Deltoid Muscle							
Grade 0	31 (60.8)	23 (63.9)	8 (53.3)	0.749	15 (55.6)	16 (66.7)	0.447
Grade 1	12 (23.5)	8 (22.2)	4 (26.7)		6 (22.2)	6 (25)	
Grade 2	8 (15.7)	5 (13.9)	3 (20)		6 (22.2)	2 (8.3)	
Grade 3	0 (0)	0 (0)	0 (0)		0 (0)	0 (0)	
Grade 4	0 (0)	0 (0)	0 (0)		0 (0)	0 (0)	
Shoulder Girdle Posterior Muscle							
Trapezius Muscle							
Grade 0	42 (82.4)	32 (88.9)	10 (66.7)	0.026	24 (88.9)	18 (75)	0.129
Grade 1	6 (11.8)	4 (11.1)	2 (13.3)		1 (3.7)	5 (20.8)	
Grade 2	3 (5.9)	0 (0)	3 (20)		2 (7.4)	1 (4.2)	
Grade 3	0 (0)	0 (0)	0 (0)		0 (0)	0 (0)	
Grade 4	0 (0)	0 (0)	0 (0)		0 (0)	0 (0)	
Latissimus dorsi muscle							
Grade 0	51 (100)	36 (100)	15 (100)	NA	27 (100)	24 (100)	NA
Grade 1	0 (0)	0 (0)	0 (0)		0 (0)	0 (0)	

Grade 2	0 (0)	0 (0)	0 (0)		0 (0)	0 (0)	
Grade 3	0 (0)	0 (0)	0 (0)		0 (0)	0 (0)	
Grade 4	0 (0)	0 (0)	0 (0)		0 (0)	0 (0)	
Levator Scapula Muscle							
Grade 0	50 (98)	35 (97.2)	15 (100)	1.000	27 (100)	23 (95.8)	0.471
Grade 1	0 (0)	0 (0)	0 (0)		0 (0)	0 (0)	
Grade 2	1 (2)	1 (2.8)	0 (0)		0 (0)	1 (4.2)	
Grade 3	0 (0)	0 (0)	0 (0)		0 (0)	0 (0)	
Grade 4	0 (0)	0 (0)	0 (0)		0 (0)	0 (0)	
Rhomboid Major Muscle							
Grade 0	48 (94.1)	35 (97.2)	13 (86.7)	0.203	26 (96.3)	22 (91.7)	0.595
Grade 1	3 (5.9)	1 (2.8)	2 (13.3)		1 (3.7)	2 (8.3)	
Grade 2	0 (0)	0 (0)	0 (0)		0 (0)	0 (0)	
Grade 3	0 (0)	0 (0)	0 (0)		0 (0)	0 (0)	
Grade 4	0 (0)	0 (0)	0 (0)		0 (0)	0 (0)	
Rhomboid Minor Muscle							
Grade 0	49 (96.1)	35 (97.2)	14 (93.3)	0.506	25 (92.6)	24 (100)	0.492
Grade 1	2 (3.9)	1 (2.8)	1 (6.7)		2 (7.4)	0 (0)	
Grade 2	0 (0)	0 (0)	0 (0)		0 (0)	0 (0)	
Grade 3	0 (0)	0 (0)	0 (0)		0 (0)	0 (0)	
Grade 4	0 (0)	0 (0)	0 (0)		0 (0)	0 (0)	
Teres Major Muscle							
Grade 0	48 (94.1)	34 (94.4)	14 (93.3)	0.355	25 (92.6)	23 (95.8)	1.000
Grade 1	2 (3.9)	2 (5.6)	0 (0)		1 (3.7)	1 (4.2)	
Grade 2	1 (2)	0 (0)	1 (6.7)		1 (3.7)	0 (0)	
Grade 3	0 (0)	0 (0)	0 (0)		0 (0)	0 (0)	
Grade 4	0 (0)	0 (0)	0 (0)		0 (0)	0 (0)	
Teres Minor Muscle							
Grade 0	47 (92.2)	34 (94.4)	13 (86.7)	0.443	25 (92.6)	22 (91.7)	0.789
Grade 1	3 (5.9)	2 (5.6)	1 (6.7)		1 (3.7)	2 (8.3)	
Grade 2	1 (2)	0 (0)	1 (6.7)		1 (3.7)	0 (0)	
Grade 3	0 (0)	0 (0)	0 (0)		0 (0)	0 (0)	
Grade 4	0 (0)	0 (0)	0 (0)		0 (0)	0 (0)	
Rotation Cuff Muscle							
Supraspinatus Muscle							
Grade 0	25 (49)	21 (58.3)	4 (26.7)	0.121	14 (51.9)	11 (45.8)	0.628
Grade 1	15 (29.4)	9 (25)	6 (40)		6 (22.2)	9 (37.5)	
Grade 2	10 (19.6)	5 (13.9)	5 (33.3)		6 (22.2)	4 (16.7)	
Grade 3	1 (2)	1 (2.8)	0 (0)		1 (3.7)	0 (0)	
Grade 4	0 (0)	0 (0)	0 (0)		0 (0)	0 (0)	
Infraspinatus Muscle							

Grade 0	28 (54.9)	24 (66.7)	4 (26.7)	0.018	15 (55.6)	13 (54.2)	0.736
Grade 1	14 (27.5)	8 (22.2)	6 (40)		6 (22.2)	8 (33.3)	
Grade 2	8 (15.7)	3 (8.3)	5 (33.3)		5 (18.5)	3 (12.5)	
Grade 3	1 (2)	1 (2.8)	0 (0)		1 (3.7)	0 (0)	
Grade 4	0 (0)	0 (0)	0 (0)		0 (0)	0 (0)	
Subscapularis Muscle							
Grade 0	36 (70.6)	27 (75)	9 (60)	0.429	17 (63)	19 (79.2)	0.411
Grade 1	13 (25.5)	8 (22.2)	5 (33.3)		9 (33.3)	4 (16.7)	
Grade 2	2 (3.9)	1 (2.8)	1 (6.7)		1 (3.7)	1 (4.2)	
Grade 3	0 (0)	0 (0)	0 (0)		0 (0)	0 (0)	
Grade 4	0 (0)	0 (0)	0 (0)		0 (0)	0 (0)	
Arm Posterior Muscle							
Triceps Muscle							
Grade 0	44 (86.3)	31 (86.1)	13 (86.7)	0.308	24 (88.9)	20 (83.3)	0.402
Grade 1	6 (11.8)	5 (13.9)	1 (6.7)		2 (7.4)	4 (16.7)	
Grade 2	1 (2)	0 (0)	1 (6.7)		1 (3.7)	0 (0)	
Grade 3	0 (0)	0 (0)	0 (0)		0 (0)	0 (0)	
Grade 4	0 (0)	0 (0)	0 (0)		0 (0)	0 (0)	
Anconeus Muscle							
Grade 0	51 (100)	36 (100)	15 (100)	NA	27 (100)	24 (100)	NA
Grade 1	0 (0)	0 (0)	0 (0)		0 (0)	0 (0)	
Grade 2	0 (0)	0 (0)	0 (0)		0 (0)	0 (0)	
Grade 3	0 (0)	0 (0)	0 (0)		0 (0)	0 (0)	
Grade 4	0 (0)	0 (0)	0 (0)		0 (0)	0 (0)	
Arm Anterior Muscle							
Brachialis Muscle							
Grade 0	51 (100)	36 (100)	15 (100)	NA	27 (100)	24 (100)	NA
Grade 1	0 (0)	0 (0)	0 (0)		0 (0)	0 (0)	
Grade 2	0 (0)	0 (0)	0 (0)		0 (0)	0 (0)	
Grade 3	0 (0)	0 (0)	0 (0)		0 (0)	0 (0)	
Grade 4	0 (0)	0 (0)	0 (0)		0 (0)	0 (0)	
Coracobrachialis Muscle							
Grade 0	51 (100)	36 (100)	15 (100)	NA	27 (100)	24 (100)	NA
Grade 1	0 (0)	0 (0)	0 (0)		0 (0)	0 (0)	
Grade 2	0 (0)	0 (0)	0 (0)		0 (0)	0 (0)	
Grade 3	0 (0)	0 (0)	0 (0)		0 (0)	0 (0)	
Grade 4	0 (0)	0 (0)	0 (0)		0 (0)	0 (0)	
Neck Lateral Muscle							
Scalene Muscle Ant							
Grade 0	50 (98)	36 (100)	14 (93.3)	0.294	26 (96.3)	24 (100)	1.000
Grade 1	0 (0)	0 (0)	0 (0)		0 (0)	0 (0)	

Grade 2	1 (2)	0 (0)	1 (6.7)		1 (3.7)	0 (0)	
Grade 3	0 (0)	0 (0)	0 (0)		0 (0)	0 (0)	
Grade 4	0 (0)	0 (0)	0 (0)		0 (0)	0 (0)	
Scalene Muscle Med							
Grade 0	51 (100)	36 (100)	15 (100)	NA	27 (100)	24 (100)	NA
Grade 1	0 (0)	0 (0)	0 (0)		0 (0)	0 (0)	
Grade 2	0 (0)	0 (0)	0 (0)		0 (0)	0 (0)	
Grade 3	0 (0)	0 (0)	0 (0)		0 (0)	0 (0)	
Grade 4	0 (0)	0 (0)	0 (0)		0 (0)	0 (0)	
Scalene Muscle Post							
Grade 0	51 (100)	36 (100)	15 (100)	NA	27 (100)	24 (100)	NA
Grade 1	0 (0)	0 (0)	0 (0)		0 (0)	0 (0)	
Grade 2	0 (0)	0 (0)	0 (0)		0 (0)	0 (0)	
Grade 3	0 (0)	0 (0)	0 (0)		0 (0)	0 (0)	
Grade 4	0 (0)	0 (0)	0 (0)		0 (0)	0 (0)	

Note: Results are reported as relative frequencies and percentages. N/A: Statistical Test Not Applicable

Table 12 – Fat Infiltration

	Total	Pain (n = 36)	No Pain (n = 15)	p-value	Functional Impairment (n = 27)	No Functional Impairment (n = 24)	p-value
Shoulder Girdle Muscles							
Pectoralis Major Muscle							
Grade 0	49 (96.1)	35 (97.2)	14 (93.3)	0.506	26 (96.3)	23 (95.8)	1.000
Grade 1	0 (0)	0 (0)	0 (0)		0 (0)	0 (0)	
Grade 2A	2 (3.9)	1 (2.8)	1 (6.7)		1 (3.7)	1 (4.2)	
Grade 2B	0 (0)	0 (0)	0 (0)		0 (0)	0 (0)	
Grade 3	0 (0)	0 (0)	0 (0)		0 (0)	0 (0)	
Grade 4	0 (0)	0 (0)	0 (0)		0 (0)	0 (0)	
Pectorali Minor Muscle							
Grade 0	49 (96.1)	35 (97.2)	14 (93.3)	0.506	26 (96.3)	23 (95.8)	1.000
Grade 1	0 (0)	0 (0)	0 (0)		0 (0)	0 (0)	
Grade 2A	2 (3.9)	1 (2.8)	1 (6.7)		1 (3.7)	1 (4.2)	
Grade 2B	0 (0)	0 (0)	0 (0)		0 (0)	0 (0)	
Grade 3	0 (0)	0 (0)	0 (0)		0 (0)	0 (0)	
Grade 4	0 (0)	0 (0)	0 (0)		0 (0)	0 (0)	
Subclavius Muscle							
Grade 0	50 (98)	35 (97.2)	15 (100)	1.000	26 (96.3)	24 (100)	1.000
Grade 1	0 (0)	0 (0)	0 (0)		0 (0)	0 (0)	
Grade 2A	1 (2)	1 (2.8)	0 (0)		1 (3.7)	0 (0)	
Grade 2B	0 (0)	0 (0)	0 (0)		0 (0)	0 (0)	
Grade 3	0 (0)	0 (0)	0 (0)		0 (0)	0 (0)	
Grade 4	0 (0)	0 (0)	0 (0)		0 (0)	0 (0)	
Serratus Anterior Muscle							
Grade 0	48 (94.1)	34 (94.4)	14 (93.3)	1.000	25 (92.6)	23 (95.8)	1.000
Grade 1	0 (0)	0 (0)	0 (0)		0 (0)	0 (0)	
Grade 2A	3 (5.9)	2 (5.6)	1 (6.7)		2 (7.4)	1 (4.2)	
Grade 2B	0 (0)	0 (0)	0 (0)		0 (0)	0 (0)	
Grade 3	0 (0)	0 (0)	0 (0)		0 (0)	0 (0)	
Grade 4	0 (0)	0 (0)	0 (0)		0 (0)	0 (0)	
Deltoid Muscle							
Grade 0	41 (80.4)	31 (86.1)	10 (66.7)	0.218	20 (74.1)	21 (87.5)	0.523
Grade 1	4 (7.8)	2 (5.6)	2 (13.3)		3 (11.1)	1 (4.2)	
Grade 2A	6 (11.8)	3 (8.3)	3 (20)		4 (14.8)	2 (8.3)	
Grade 2B	0 (0)	0 (0)	0 (0)		0 (0)	0 (0)	
Grade 3	0 (0)	0 (0)	0 (0)		0 (0)	0 (0)	
Grade 4	0 (0)	0 (0)	0 (0)		0 (0)	0 (0)	
Shoulder Girdle Posterior Muscle							
Trapezius Muscle							
Grade 0	48 (94.1)	35 (97.2)	13 (86.7)	0.203	26 (96.3)	22 (91.7)	0.595

Grade 1	3 (5.9)	1 (2.8)	2 (13.3)		1 (3.7)	2 (8.3)	
Grade 2A	0 (0)	0 (0)	0 (0)		0 (0)	0 (0)	
Grade 2B	0 (0)	0 (0)	0 (0)		0 (0)	0 (0)	
Grade 3	0 (0)	0 (0)	0 (0)		0 (0)	0 (0)	
Grade 4	0 (0)	0 (0)	0 (0)		0 (0)	0 (0)	
Latissimus dorsi muscle							
Grade 0	51 (100)	36 (100)	15 (100)	NA	27 (100)	24 (100)	NA
Grade 1	0 (0)	0 (0)	0 (0)		0 (0)	0 (0)	
Grade 2A	0 (0)	0 (0)	0 (0)		0 (0)	0 (0)	
Grade 2B	0 (0)	0 (0)	0 (0)		0 (0)	0 (0)	
Grade 3	0 (0)	0 (0)	0 (0)		0 (0)	0 (0)	
Grade 4	0 (0)	0 (0)	0 (0)		0 (0)	0 (0)	
Levator Scapula Muscle							
Grade 0	51 (100)	36 (100)	15 (100)	NA	27 (100)	24 (100)	NA
Grade 1	0 (0)	0 (0)	0 (0)		0 (0)	0 (0)	
Grade 2A	0 (0)	0 (0)	0 (0)		0 (0)	0 (0)	
Grade 2B	0 (0)	0 (0)	0 (0)		0 (0)	0 (0)	
Grade 3	0 (0)	0 (0)	0 (0)		0 (0)	0 (0)	
Grade 4	0 (0)	0 (0)	0 (0)		0 (0)	0 (0)	
Rhomboid Major Muscle							
Grade 0	49 (96.1)	35 (97.2)	14 (93.3)	0.506	25 (92.6)	24 (100)	1.000
Grade 1	1 (2)	0 (0)	1 (6.7)		1 (3.7)	0 (0)	
Grade 2A	1 (2)	1 (2.8)	0 (0)		1 (3.7)	0 (0)	
Grade 2B	0 (0)	0 (0)	0 (0)		0 (0)	0 (0)	
Grade 3	0 (0)	0 (0)	0 (0)		0 (0)	0 (0)	
Grade 4	0 (0)	0 (0)	0 (0)		0 (0)	0 (0)	
Rhomboid Minor Muscle							
Grade 0	50 (98)	36 (100)	14 (93.3)	0.294	26 (96.3)	24 (100)	1.000
Grade 1	1 (2)	0 (0)	1 (6.7)		1 (3.7)	0 (0)	
Grade 2A	0 (0)	0 (0)	0 (0)		0 (0)	0 (0)	
Grade 2B	0 (0)	0 (0)	0 (0)		0 (0)	0 (0)	
Grade 3	0 (0)	0 (0)	0 (0)		0 (0)	0 (0)	
Grade 4	0 (0)	0 (0)	0 (0)		0 (0)	0 (0)	
Teres Major Muscle							
Grade 0	51 (100)	36 (100)	15 (100)	NA	27 (100)	24 (100)	NA
Grade 1	0 (0)	0 (0)	0 (0)		0 (0)	0 (0)	
Grade 2A	0 (0)	0 (0)	0 (0)		0 (0)	0 (0)	
Grade 2B	0 (0)	0 (0)	0 (0)		0 (0)	0 (0)	
Grade 3	0 (0)	0 (0)	0 (0)		0 (0)	0 (0)	
Grade 4	0 (0)	0 (0)	0 (0)		0 (0)	0 (0)	
Teres Minor Muscle							

Grade 0	49 (96.1)	35 (97.2)	14 (93.3)	0.506	26 (96.3)	23 (95.8)	1.000
Grade 1	2 (3.9)	1 (2.8)	1 (6.7)		1 (3.7)	1 (4.2)	
Grade 2A	0 (0)	0 (0)	0 (0)		0 (0)	0 (0)	
Grade 2B	0 (0)	0 (0)	0 (0)		0 (0)	0 (0)	
Grade 3	0 (0)	0 (0)	0 (0)		0 (0)	0 (0)	
Grade 4	0 (0)	0 (0)	0 (0)		0 (0)	0 (0)	
Rotation Cuff Muscle							
Supraspinatus Muscle							
Grade 0	35 (68.6)	30 (83.3)	5 (33.3)	0.001	18 (66.7)	17 (70.8)	0.511
Grade 1	11 (21.6)	4 (11.1)	7 (46.7)		7 (25.9)	4 (16.7)	
Grade 2A	3 (5.9)	2 (5.6)	1 (6.7)		2 (7.4)	1 (4.2)	
Grade 2B	2 (3.9)	0 (0)	2 (13.3)		0 (0)	2 (8.3)	
Grade 3	0 (0)	0 (0)	0 (0)		0 (0)	0 (0)	
Grade 4	0 (0)	0 (0)	0 (0)		0 (0)	0 (0)	
Infraspinatus Muscle							
Grade 0	34 (66.7)	27 (75)	7 (46.7)	0.128	18 (66.7)	16 (66.7)	0.827
Grade 1	8 (15.7)	4 (11.1)	4 (26.7)		4 (14.8)	4 (16.7)	
Grade 2A	6 (11.8)	4 (11.1)	2 (13.3)		4 (14.8)	2 (8.3)	
Grade 2B	3 (5.9)	1 (2.8)	2 (13.3)		1 (3.7)	2 (8.3)	
Grade 3	0 (0)	0 (0)	0 (0)		0 (0)	0 (0)	
Grade 4	0 (0)	0 (0)	0 (0)		0 (0)	0 (0)	
Subscapularis Muscle							
Grade 0	38 (74.5)	30 (83.3)	8 (53.3)	0.095	21 (77.8)	17 (70.8)	0.647
Grade 1	8 (15.7)	4 (11.1)	4 (26.7)		4 (14.8)	4 (16.7)	
Grade 2A	3 (5.9)	1 (2.8)	2 (13.3)		2 (7.4)	1 (4.2)	
Grade 2B	2 (3.9)	1 (2.8)	1 (6.7)		0 (0)	2 (8.3)	
Grade 3	0 (0)	0 (0)	0 (0)		0 (0)	0 (0)	
Grade 4	0 (0)	0 (0)	0 (0)		0 (0)	0 (0)	
Arm Posterior Muscle							
Triceps Muscle							
Grade 0	51 (100)	36 (100)	15 (100)	NA	27 (100)	24 (100)	NA
Grade 1	0 (0)	0 (0)	0 (0)		0 (0)	0 (0)	
Grade 2A	0 (0)	0 (0)	0 (0)		0 (0)	0 (0)	
Grade 2B	0 (0)	0 (0)	0 (0)		0 (0)	0 (0)	
Grade 3	0 (0)	0 (0)	0 (0)		0 (0)	0 (0)	
Grade 4	0 (0)	0 (0)	0 (0)		0 (0)	0 (0)	
Anconeus Muscle							
Grade 0	51 (100)	36 (100)	15 (100)	NA	27 (100)	24 (100)	NA
Grade 1	0 (0)	0 (0)	0 (0)		0 (0)	0 (0)	
Grade 2A	0 (0)	0 (0)	0 (0)		0 (0)	0 (0)	
Grade 2B	0 (0)	0 (0)	0 (0)		0 (0)	0 (0)	

Grade 3	0 (0)	0 (0)	0 (0)		0 (0)	0 (0)	
Grade 4	0 (0)	0 (0)	0 (0)		0 (0)	0 (0)	
Arm Anterior Muscle							
Brachialis Muscle							
Grade 0	51 (100)	36 (100)	15 (100)	NA	27 (100)	24 (100)	NA
Grade 1	0 (0)	0 (0)	0 (0)		0 (0)	0 (0)	
Grade 2A	0 (0)	0 (0)	0 (0)		0 (0)	0 (0)	
Grade 2B	0 (0)	0 (0)	0 (0)		0 (0)	0 (0)	
Grade 3	0 (0)	0 (0)	0 (0)		0 (0)	0 (0)	
Grade 4	0 (0)	0 (0)	0 (0)		0 (0)	0 (0)	
Coracobrachialis Muscle							
Grade 0	51 (100)	36 (100)	15 (100)	NA	27 (100)	24 (100)	NA
Grade 1	0 (0)	0 (0)	0 (0)		0 (0)	0 (0)	
Grade 2A	0 (0)	0 (0)	0 (0)		0 (0)	0 (0)	
Grade 2B	0 (0)	0 (0)	0 (0)		0 (0)	0 (0)	
Grade 3	0 (0)	0 (0)	0 (0)		0 (0)	0 (0)	
Grade 4	0 (0)	0 (0)	0 (0)		0 (0)	0 (0)	
Neck Lateral Muscle							
Scalene Muscle Ant							
Grade 0	51 (100)	36 (100)	15 (100)	NA	27 (100)	24 (100)	NA
Grade 1	0 (0)	0 (0)	0 (0)		0 (0)	0 (0)	
Grade 2A	0 (0)	0 (0)	0 (0)		0 (0)	0 (0)	
Grade 2B	0 (0)	0 (0)	0 (0)		0 (0)	0 (0)	
Grade 3	0 (0)	0 (0)	0 (0)		0 (0)	0 (0)	
Grade 4	0 (0)	0 (0)	0 (0)		0 (0)	0 (0)	
Scalene Muscle Med							
Grade 0	51 (100)	36 (100)	15 (100)	NA	27 (100)	24 (100)	NA
Grade 1	0 (0)	0 (0)	0 (0)		0 (0)	0 (0)	
Grade 2A	0 (0)	0 (0)	0 (0)		0 (0)	0 (0)	
Grade 2B	0 (0)	0 (0)	0 (0)		0 (0)	0 (0)	
Grade 3	0 (0)	0 (0)	0 (0)		0 (0)	0 (0)	
Grade 4	0 (0)	0 (0)	0 (0)		0 (0)	0 (0)	
Scalene Muscle Post							
Grade 0	51 (100)	36 (100)	15 (100)	NA	27 (100)	24 (100)	NA
Grade 1	0 (0)	0 (0)	0 (0)		0 (0)	0 (0)	
Grade 2A	0 (0)	0 (0)	0 (0)		0 (0)	0 (0)	
Grade 2B	0 (0)	0 (0)	0 (0)		0 (0)	0 (0)	
Grade 3	0 (0)	0 (0)	0 (0)		0 (0)	0 (0)	
Grade 4	0 (0)	0 (0)	0 (0)		0 (0)	0 (0)	

Note: Results are reported as relative frequencies and percentages. N/A: Statistical Test Not Applicable

Table 13 - Atrophy

	Total	Pain (n = 36)	No Pain (n = 15)	p-value	Functional Impairment (n = 27)	No Functional Impairment (n = 24)	p-value
Shoulder Girdle Muscles							
Pectoralis Major Muscle	4 (7.8)	3 (8.3)	1 (6.7)	1.000	2 (7.4)	2 (8.3)	1.000
Pectoralis Minor Muscle	4 (7.8)	3 (8.3)	1 (6.7)	1.000	2 (7.4)	2 (8.3)	1.000
Subclavious Muscle	1 (2)	1 (2.8)	0 (0)	1.000	1 (3.7)	0 (0)	1.000
Serratus Anterior Muscle	4 (7.8)	4 (11.1)	0 (0)	0.307	3 (11.1)	1 (4.2)	0.612
Deltoid Muscle	11 (21.6)	7 (19.4)	4 (26.7)	0.711	8 (29.6)	3 (12.5)	0.182
Shoulder Girdle Posterio Muscle							
Trapezius Muscle	3 (5.9)	2 (5.6)	1 (6.7)	1.000	2 (7.4)	1 (4.2)	1.000
Latissum Dorsi Muscle	0 (0)	0 (0)	0 (0)	NA	0 (0)	0 (0)	NA
Levator Scapula Muscle	2 (3.9)	0 (0)	2 (13.3)	0.082	1 (3.7)	1 (4.2)	1.000
Rhomboid Major Muscle	0 (0)	0 (0)	0 (0)	NA	0 (0)	0 (0)	NA
Rhomboid Minor Muscle	0 (0)	0 (0)	0 (0)	NA	0 (0)	0 (0)	NA
Teres Major Muscle	2 (3.9)	2 (5.6)	0 (0)	1.000	2 (7.4)	0 (0)	0.492
Teres Minor Muscle	2 (3.9)	1 (2.8)	1 (6.7)	0.506	2 (7.4)	0 (0)	0.492
Rotation Cuff Muscle							
Supraspinatus Muscle	21 (41.2)	11 (30.6)	10 (66.7)	0.028	12 (44.4)	9 (37.5)	0.777
Infraspinatus Muscle	15 (29.4)	8 (22.2)	7 (46.7)	0.101	8 (29.6)	7 (29.2)	1.000
Subscapularis Muscle	13 (25.5)	7 (19.4)	6 (40)	0.164	8 (29.6)	5 (20.8)	0.534
Arm Posterior Muscle							
Triceps Muscle	2 (3.9)	2 (5.6)	0 (0)	1.000	1 (3.7)	1 (4.2)	1.000
Anconeus Muscle	0 (0)	0 (0)	0 (0)	NA	0 (0)	0 (0)	NA
Arm Anterior Muscle							
Brachialis Muscle	1 (2)	0 (0)	1 (6.7)	0.294	1 (3.7)	0 (0)	1.000
Coracobrachialis Muscle	0 (0)	0 (0)	0 (0)	NA	0 (0)	0 (0)	NA
Neck Lateral Muscle							
Scalene Muscle Ant	1 (2)	0 (0)	1 (6.7)	0.294	0 (0)	1 (4.2)	0.471
Scalene Muscle Med	1 (2)	0 (0)	1 (6.7)	0.294	0 (0)	1 (4.2)	0.471
Scalene Muscle Post	1 (2)	0 (0)	1 (6.7)	0.294	0 (0)	1 (4.2)	0.471

Note: Results are reported as relative frequencies and percentages. N/A: Statistical Test Not Applicable

Table14 – Nerve characteristics by EMG Findings

	EMG Neurogenic Impairment			EMG Denervation Activity		
	Yes (n = 41)	No (n = 10)	p-value	Yes (n = 41)	No (n = 10)	p-value
Side						
Right	17 (41.5)	4 (40)	1.000	5 (50)	16 (39)	0.816
Left	16 (39)	4 (40)		4 (40)	16 (39)	
Both	8 (19.5)	2 (20)		1 (10)	9 (22)	
EMG C5	31 (75.6)	7 (70)	0.701	7 (70)	31 (75.6)	0.701
EMG C6	34 (82.9)	8 (80)	1.000	9 (90)	33 (80.5)	0.667

EMG C7	19 (46.3)	4 (40)	1.000	7 (70)	16 (39)	0.154
EMG C8	11 (26.8)	1 (10)	0.417	4 (40)	8 (19.5)	0.218
MRI C5	17 (41.5)	3 (30)	0.721	2 (20)	18 (43.9)	0.280
MRI C6	27 (65.9)	5 (50)	0.470	5 (50)	27 (65.9)	0.470
MRI C7	19 (46.3)	3 (30)	0.483	4 (40)	18 (43.9)	1.000
MRI C8	18 (43.9)	2 (20)	0.280	4 (40)	16 (39)	1.000

Note: Results are reported as relative frequencies and percentages. N/A: Statistical Test Not Applicable

Table 15 - Edema

	EMG Neurogenic Impairment			**EMG Denervation Activity**		
	Yes (n = 41)	No (n = 10)	p-value	Yes (n = 41)	No (n = 10)	p-value
Shoulder Girdle Muscles						
Pectoralis Major Muscle						
Grade 0	39 (95.1)	10 (100)	1.000	10 (100)	39 (95.1)	1.000
Grade 1	1 (2.4)	0 (0)		0 (0)	1 (2.4)	
Grade 2	1 (2.4)	0 (0)		0 (0)	1 (2.4)	
Grade 3	0 (0)	0 (0)		0 (0)	0 (0)	
Grade 4	0 (0)	0 (0)		0 (0)	0 (0)	
Pectorali Minor Muscle						
Grade 0	39 (95.1)	10 (100)	1.000	10 (100)	39 (95.1)	1.000
Grade 1	1 (2.4)	0 (0)		0 (0)	1 (2.4)	
Grade 2	1 (2.4)	0 (0)		0 (0)	1 (2.4)	
Grade 3	0 (0)	0 (0)		0 (0)	0 (0)	
Grade 4	0 (0)	0 (0)		0 (0)	0 (0)	
Subclavius Muscle						
Grade 0	40 (97.6)	10 (100)	1.000	10 (100)	40 (97.6)	1.000
Grade 1	0 (0)	0 (0)		0 (0)	0 (0)	
Grade 2	1 (2.4)	0 (0)		0 (0)	1 (2.4)	
Grade 3	0 (0)	0 (0)		0 (0)	0 (0)	
Grade 4	0 (0)	0 (0)		0 (0)	0 (0)	
Serratus Anterior Muscle						
Grade 0	36 (87.8)	8 (80)	0.667	9 (90)	35 (85.4)	1.000
Grade 1	4 (9.8)	2 (20)		1 (10)	5 (12.2)	
Grade 2	1 (2.4)	0 (0)		0 (0)	1 (2.4)	
Grade 3	0 (0)	0 (0)		0 (0)	0 (0)	
Grade 4	0 (0)	0 (0)		0 (0)	0 (0)	
Deltoid Muscle						
Grade 0	25 (61)	6 (60)	0.785	5 (50)	26 (63.4)	0.683
Grade 1	9 (22)	3 (30)		3 (30)	9 (22)	
Grade 2	7 (17.1)	1 (10)		2 (20)	6 (14.6)	
Grade 3	0 (0)	0 (0)		0 (0)	0 (0)	

Grade 4	0 (0)	0 (0)		0 (0)	0 (0)	
Shoulder Girdle Posterior Muscle						
Trapezius Muscle						
Grade 0	32 (78)	10 (100)	0.486	8 (80)	34 (82.9)	0.091
Grade 1	6 (14.6)	0 (0)		0 (0)	6 (14.6)	
Grade 2	3 (7.3)	0 (0)		2 (20)	1 (2.4)	
Grade 3	0 (0)	0 (0)		0 (0)	0 (0)	
Grade 4	0 (0)	0 (0)		0 (0)	0 (0)	
Latissimus dorsi muscle						
Grade 0	41 (100)		NA	10 (100)		NA
Grade 1	0 (0)	0 (0)		0 (0)	0 (0)	
Grade 2	0 (0)	0 (0)		0 (0)	0 (0)	
Grade 3	0 (0)	0 (0)		0 (0)	0 (0)	
Grade 4	0 (0)	0 (0)		0 (0)	0 (0)	
Levator Scapula Muscle						
Grade 0	40 (97.6)	10 (100)	1.000	10 (100)	40 (97.6)	1.000
Grade 1	0 (0)	0 (0)		0 (0)	0 (0)	
Grade 2	1 (2.4)	0 (0)		0 (0)	1 (2.4)	
Grade 3	0 (0)	0 (0)		0 (0)	0 (0)	
Grade 4	0 (0)	0 (0)		0 (0)	0 (0)	
Rhomboid Major Muscle						
Grade 0	39 (95.1)	9 (90)	0.488	9 (90)	39 (95.1)	0.488
Grade 1	2 (4.9)	1 (10)		1 (10)	2 (4.9)	
Grade 2	0 (0)	0 (0)		0 (0)	0 (0)	
Grade 3	0 (0)	0 (0)		0 (0)	0 (0)	
Grade 4	0 (0)	0 (0)		0 (0)	0 (0)	
Rhomboid Minor Muscle						
Grade 0	40 (97.6)	9 (90)	0.357	9 (90)	40 (97.6)	0.357
Grade 1	1 (2.4)	1 (10)		1 (10)	1 (2.4)	
Grade 2	0 (0)	0 (0)		0 (0)	0 (0)	
Grade 3	0 (0)	0 (0)		0 (0)	0 (0)	
Grade 4	0 (0)	0 (0)		0 (0)	0 (0)	
Teres Major Muscle						
Grade 0	38 (92.7)	10 (100)	1.000	9 (90)	39 (95.1)	0.226
Grade 1	2 (4.9)	0 (0)		0 (0)	2 (4.9)	
Grade 2	1 (2.4)	0 (0)		1 (10)	0 (0)	
Grade 3	0 (0)	0 (0)		0 (0)	0 (0)	
Grade 4	0 (0)	0 (0)		0 (0)	0 (0)	
Teres Minor Muscle						
Grade 0	37 (90.2)	10 (100)	1.000	10 (100)	37 (90.2)	1.000
Grade 1	3 (7.3)	0 (0)		0 (0)	3 (7.3)	

Grade 2	1 (2.4)	0 (0)		0 (0)	1 (2.4)	
Grade 3	0 (0)	0 (0)		0 (0)	0 (0)	
Grade 4	0 (0)	0 (0)		0 (0)	0 (0)	
Rotation Cuff Muscle						
Supraspinatus Muscle						
Grade 0	21 (51.2)	4 (40)	0.367	5 (50)	20 (48.8)	0.726
Grade 1	12 (29.3)	3 (30)		4 (40)	11 (26.8)	
Grade 2	8 (19.5)	2 (20)		1 (10)	9 (22)	
Grade 3	0 (0)	1 (10)		0 (0)	1 (2.4)	
Grade 4	0 (0)	0 (0)		0 (0)	0 (0)	
Infraspinatus Muscle						
Grade 0	23 (56.1)	5 (50)	0.273	5 (50)	23 (56.1)	0.693
Grade 1	12 (29.3)	2 (20)		4 (40)	10 (24.4)	
Grade 2	6 (14.6)	2 (20)		1 (10)	7 (17.1)	
Grade 3	0 (0)	1 (10)		0 (0)	1 (2.4)	
Grade 4	0 (0)	0 (0)		0 (0)	0 (0)	
Subscapularis Muscle						
Grade 0	29 (70.7)	7 (70)	0.519	8 (80)	28 (68.3)	0.813
Grade 1	11 (26.8)	2 (20)		2 (20)	11 (26.8)	
Grade 2	1 (2.4)	1 (10)		0 (0)	2 (4.9)	
Grade 3	0 (0)	0 (0)		0 (0)	0 (0)	
Grade 4	0 (0)	0 (0)		0 (0)	0 (0)	
Arm Posterior Muscle						
Triceps Muscle						
Grade 0	36 (87.8)	8 (80)	0.667	7 (70)	37 (90.2)	0.066
Grade 1	4 (9.8)	2 (20)		2 (20)	4 (9.8)	
Grade 2	1 (2.4)	0 (0)		1 (10)	0 (0)	
Grade 3	0 (0)	0 (0)		0 (0)	0 (0)	
Grade 4	0 (0)	0 (0)		0 (0)	0 (0)	
Anconeus Muscle						
Grade 0	41 (100)	10 (100)	NA	10 (100)	41 (100)	NA
Grade 1	0 (0)	0 (0)		0 (0)	0 (0)	
Grade 2	0 (0)	0 (0)		0 (0)	0 (0)	
Grade 3	0 (0)	0 (0)		0 (0)	0 (0)	
Grade 4	0 (0)	0 (0)		0 (0)	0 (0)	
Arm Anterior Muscle						
Brachialis Muscle						
Grade 0	41 (100)	10 (100)	NA	10 (100)	41 (100)	NA
Grade 1	0 (0)	0 (0)		0 (0)	0 (0)	
Grade 2	0 (0)	0 (0)		0 (0)	0 (0)	
Grade 3	0 (0)	0 (0)		0 (0)	0 (0)	

Grade 4	0 (0)	0 (0)		0 (0)	0 (0)	
Coracobrachialis Muscle						
Grade 0	41 (100)	10 (100)	NA	10 (100)	41 (100)	NA
Grade 1	0 (0)	0 (0)		0 (0)	0 (0)	
Grade 2	0 (0)	0 (0)		0 (0)	0 (0)	
Grade 3	0 (0)	0 (0)		0 (0)	0 (0)	
Grade 4	0 (0)	0 (0)		0 (0)	0 (0)	
Neck Lateral Muscle						
Scalene Muscle Ant						
Grade 0	40 (97.6)	10 (100)	1.000	9 (90)	41 (100)	0.196
Grade 1	0 (0)	0 (0)		0 (0)	0 (0)	
Grade 2	1 (2.4)	0 (0)		1 (10)	0 (0)	
Grade 3	0 (0)	0 (0)		0 (0)	0 (0)	
Grade 4	0 (0)	0 (0)		0 (0)	0 (0)	
Scalene Muscle Med						
Grade 0	41 (100)	10 (100)	NA	10 (100)	41 (100)	NA
Grade 1	0 (0)	0 (0)		0 (0)	0 (0)	
Grade 2	0 (0)	0 (0)		0 (0)	0 (0)	
Grade 3	0 (0)	0 (0)		0 (0)	0 (0)	
Grade 4	0 (0)	0 (0)		0 (0)	0 (0)	
Scalene Muscle Post						
Grade 0	41 (100)	10 (100)	NA	10 (100)	41 (100)	NA
Grade 1	0 (0)	0 (0)		0 (0)	0 (0)	
Grade 2	0 (0)	0 (0)		0 (0)	0 (0)	
Grade 3	0 (0)	0 (0)		0 (0)	0 (0)	
Grade 4	0 (0)	0 (0)		0 (0)	0 (0)	

Note: Results are reported as relative frequencies and percentages. N/A: Statistical Test Not Applicable

Table 16 – Fat Infiltration

	EMG Neurogenic Impairment			EMG Denervation Activity		
	Yes (n = 41)	**No (n = 10)**	**p-value**	**Yes (n = 41)**	**No (n = 10)**	**p-value**
Shoulder Girdle Muscles						
Pectoralis Major Muscle						
Grade 0	39 (95.1)	10 (100)	1.000	10 (100)	39 (95.1)	1.000
Grade 1	0 (0)	0 (0)		0 (0)	0 (0)	
Grade 2A	2 (4.9)	0 (0)		0 (0)	2 (4.9)	
Grade 2B	0 (0)	0 (0)		0 (0)	0 (0)	
Grade 3	0 (0)	0 (0)		0 (0)	0 (0)	
Grade 4	0 (0)	0 (0)		0 (0)	0 (0)	
Pectorali Minor Muscle						
Grade 0	39 (95.1)	10 (100)	1.000	10 (100)	39 (95.1)	1.000
Grade 1	0 (0)	0 (0)		0 (0)	0 (0)	
Grade 2A	2 (4.9)	0 (0)		0 (0)	2 (4.9)	
Grade 2B	0 (0)	0 (0)		0 (0)	0 (0)	
Grade 3	0 (0)	0 (0)		0 (0)	0 (0)	
Grade 4	0 (0)	0 (0)		0 (0)	0 (0)	
Subclavius Muscle						
Grade 0	40 (97.6)	10 (100)	1.000	10 (100)	40 (97.6)	1.000
Grade 1	0 (0)	0 (0)		0 (0)	0 (0)	
Grade 2A	1 (2.4)	0 (0)		0 (0)	1 (2.4)	
Grade 2B	0 (0)	0 (0)		0 (0)	0 (0)	
Grade 3	0 (0)	0 (0)		0 (0)	0 (0)	
Grade 4	0 (0)	0 (0)		0 (0)	0 (0)	
Serratus Anterior Muscle						
Grade 0	38 (92.7)	10 (100)	1.000	10 (100)	38 (92.7)	1.000
Grade 1	0 (0)	0 (0)		0 (0)	0 (0)	
Grade 2A	3 (7.3)	0 (0)		0 (0)	3 (7.3)	
Grade 2B	0 (0)	0 (0)		0 (0)	0 (0)	
Grade 3	0 (0)	0 (0)		0 (0)	0 (0)	
Grade 4	0 (0)	0 (0)		0 (0)	0 (0)	
Deltoid Muscle						
Grade 0	32 (78)	9 (90)	0.544	9 (90)	32 (78)	0.544
Grade 1	3 (7.3)	1 (10)		1 (10)	3 (7.3)	
Grade 2A	6 (14.6)	0 (0)		0 (0)	6 (14.6)	
Grade 2B	0 (0)	0 (0)		0 (0)	0 (0)	
Grade 3	0 (0)	0 (0)		0 (0)	0 (0)	
Grade 4	0 (0)	0 (0)		0 (0)	0 (0)	
Shoulder Girdle Posterior Muscle						
Trapezius Muscle						

Grade 0	38 (92.7)	10 (100)	1.000	9 (90)	39 (95.1)	0.488
Grade 1	3 (7.3)	0 (0)		1 (10)	2 (4.9)	
Grade 2A	0 (0)	0 (0)		0 (0)	0 (0)	
Grade 2B	0 (0)	0 (0)		0 (0)	0 (0)	
Grade 3	0 (0)	0 (0)		0 (0)	0 (0)	
Grade 4	0 (0)	0 (0)		0 (0)	0 (0)	
Latissimus dorsi muscle						
Grade 0	41 (100)	10 (100)	NA	10 (100)	41 (100)	NA
Grade 1	0 (0)	0 (0)		0 (0)	0 (0)	
Grade 2A	0 (0)	0 (0)		0 (0)	0 (0)	
Grade 2B	0 (0)	0 (0)		0 (0)	0 (0)	
Grade 3	0 (0)	0 (0)		0 (0)	0 (0)	
Grade 4	0 (0)	0 (0)		0 (0)	0 (0)	
Levator Scapula Muscle						
Grade 0	41 (100)	10 (100)	NA	10 (100)	41 (100)	NA
Grade 1	0 (0)	0 (0)		0 (0)	0 (0)	
Grade 2A	0 (0)	0 (0)		0 (0)	0 (0)	
Grade 2B	0 (0)	0 (0)		0 (0)	0 (0)	
Grade 3	0 (0)	0 (0)		0 (0)	0 (0)	
Grade 4	0 (0)	0 (0)		0 (0)	0 (0)	
Rhomboid Major Muscle						
Grade 0	40 (97.6)	9 (90)	0.357	9 (90)	40 (97.6)	0.357
Grade 1	0 (0)	1 (10)		1 (10)	0 (0)	
Grade 2A	1 (2.4)	0 (0)		0 (0)	1 (2.4)	
Grade 2B	0 (0)	0 (0)		0 (0)	0 (0)	
Grade 3	0 (0)	0 (0)		0 (0)	0 (0)	
Grade 4	0 (0)	0 (0)		0 (0)	0 (0)	
Rhomboid Minor Muscle						
Grade 0	41 (100)	9 (90)	0.196	9 (90)	41 (100)	0.196
Grade 1	0 (0)	1 (10)		1 (10)	0 (0)	
Grade 2A	0 (0)	0 (0)		0 (0)	0 (0)	
Grade 2B	0 (0)	0 (0)		0 (0)	0 (0)	
Grade 3	0 (0)	0 (0)		0 (0)	0 (0)	
Grade 4	0 (0)	0 (0)		0 (0)	0 (0)	
Teres Major Muscle						
Grade 0	41 (100)	10 (100)	NA	10 (100)	41 (100)	NA
Grade 1	0 (0)	0 (0)		0 (0)	0 (0)	
Grade 2A	0 (0)	0 (0)		0 (0)	0 (0)	
Grade 2B	0 (0)	0 (0)		0 (0)	0 (0)	
Grade 3	0 (0)	0 (0)		0 (0)	0 (0)	
Grade 4	0 (0)	0 (0)		0 (0)	0 (0)	

Teres Minor Muscle						
Grade 0	39 (95.1)	10 (100)	1.000	10 (100)	39 (95.1)	1.000
Grade 1	2 (4.9)	0 (0)		0 (0)	2 (4.9)	
Grade 2A	0 (0)	0 (0)		0 (0)	0 (0)	
Grade 2B	0 (0)	0 (0)		0 (0)	0 (0)	
Grade 3	0 (0)	0 (0)		0 (0)	0 (0)	
Grade 4	0 (0)	0 (0)		0 (0)	0 (0)	
Rotation Cuff Muscle						
Supraspinatus Muscle						
Grade 0	28 (68.3)	7 (70)	0.541	6 (60)	29 (70.7)	0.483
Grade 1	9 (22)	2 (20)		3 (30)	8 (19.5)	
Grade 2A	3 (7.3)	0 (0)		0 (0)	3 (7.3)	
Grade 2B	1 (2.4)	1 (10)		1 (10)	1 (2.4)	
Grade 3	0 (0)	0 (0)		0 (0)	0 (0)	
Grade 4	0 (0)	0 (0)		0 (0)	0 (0)	
Infraspinatus Muscle						
Grade 0	28 (68.3)	6 (60)	0.121	6 (60)	28 (68.3)	0.121
Grade 1	6 (14.6)	2 (20)		2 (20)	6 (14.6)	
Grade 2A	6 (14.6)	0 (0)		0 (0)	6 (14.6)	
Grade 2B	1 (2.4)	2 (20)		2 (20)	1 (2.4)	
Grade 3	0 (0)	0 (0)		0 (0)	0 (0)	
Grade 4	0 (0)	0 (0)		0 (0)	0 (0)	
Subscapularis Muscle						
Grade 0	30 (73.2)	8 (80)	0.616	7 (70)	31 (75.6)	0.555
Grade 1	7 (17.1)	1 (10)		3 (30)	5 (12.2)	
Grade 2A	3 (7.3)	0 (0)		0 (0)	3 (7.3)	
Grade 2B	1 (2.4)	1 (10)		0 (0)	2 (4.9)	
Grade 3	0 (0)	0 (0)		0 (0)	0 (0)	
Grade 4	0 (0)	0 (0)		0 (0)	0 (0)	
Arm Posterior Muscle						
Triceps Muscle						
Grade 0	41 (100)	10 (100)	NA	10 (100)	41 (100)	NA
Grade 1	0 (0)	0 (0)		0 (0)	0 (0)	
Grade 2A	0 (0)	0 (0)		0 (0)	0 (0)	
Grade 2B	0 (0)	0 (0)		0 (0)	0 (0)	
Grade 3	0 (0)	0 (0)		0 (0)	0 (0)	
Grade 4	0 (0)	0 (0)		0 (0)	0 (0)	
Anconeus Muscle						
Grade 0	41 (100)	10 (100)	NA	10 (100)	41 (100)	NA
Grade 1	0 (0)	0 (0)		0 (0)	0 (0)	
Grade 2A	0 (0)	0 (0)		0 (0)	0 (0)	

Grade 2B	0 (0)	0 (0)		0 (0)	0 (0)	
Grade 3	0 (0)	0 (0)		0 (0)	0 (0)	
Grade 4	0 (0)	0 (0)		0 (0)	0 (0)	
Arm Anterior Muscle						
Brachialis Muscle						
Grade 0	41 (100)	10 (100)	NA	10 (100)	41 (100)	NA
Grade 1	0 (0)	0 (0)		0 (0)	0 (0)	
Grade 2A	0 (0)	0 (0)		0 (0)	0 (0)	
Grade 2B	0 (0)	0 (0)		0 (0)	0 (0)	
Grade 3	0 (0)	0 (0)		0 (0)	0 (0)	
Grade 4	0 (0)	0 (0)		0 (0)	0 (0)	
Coracobrachialis Muscle						
Grade 0	41 (100)	10 (100)	NA	10 (100)	41 (100)	NA
Grade 1	0 (0)	0 (0)		0 (0)	0 (0)	
Grade 2A	0 (0)	0 (0)		0 (0)	0 (0)	
Grade 2B	0 (0)	0 (0)		0 (0)	0 (0)	
Grade 3	0 (0)	0 (0)		0 (0)	0 (0)	
Grade 4	0 (0)	0 (0)		0 (0)	0 (0)	
Neck Lateral Muscle						
Scalene Muscle Ant						
Grade 0	41 (100)	10 (100)	NA	10 (100)	41 (100)	NA
Grade 1	0 (0)	0 (0)		0 (0)	0 (0)	
Grade 2A	0 (0)	0 (0)		0 (0)	0 (0)	
Grade 2B	0 (0)	0 (0)		0 (0)	0 (0)	
Grade 3	0 (0)	0 (0)		0 (0)	0 (0)	
Grade 4	0 (0)	0 (0)		0 (0)	0 (0)	
Scalene Muscle Med						
Grade 0	41 (100)	10 (100)	NA	10 (100)	41 (100)	NA
Grade 1	0 (0)	0 (0)		0 (0)	0 (0)	
Grade 2A	0 (0)	0 (0)		0 (0)	0 (0)	
Grade 2B	0 (0)	0 (0)		0 (0)	0 (0)	
Grade 3	0 (0)	0 (0)		0 (0)	0 (0)	
Grade 4	0 (0)	0 (0)		0 (0)	0 (0)	
Scalene Muscle Post						
Grade 0	41 (100)	10 (100)	NA	10 (100)	41 (100)	NA
Grade 1	0 (0)	0 (0)		0 (0)	0 (0)	
Grade 2A	0 (0)	0 (0)		0 (0)	0 (0)	
Grade 2B	0 (0)	0 (0)		0 (0)	0 (0)	
Grade 3	0 (0)	0 (0)		0 (0)	0 (0)	
Grade 4	0 (0)	0 (0)		0 (0)	0 (0)	

Note: Results are reported as relative frequencies and percentages. N/A: Statistical Test Not Applicable

Table 17- Atrophy

	EMG Neurogenic Impairment			EMG Denervation Activity		
	Yes (n = 41)	No (n = 10)	p-value	Yes (n = 41)	No (n = 10)	p-value
Shoulder Girdle Muscles						
Pectoralis Major Muscle	3 (7.3)	1 (10)	1.000	0 (0)	4 (9.8)	0.573
Pectoralis Minor Muscle	3 (7.3)	1 (10)	1.000	0 (0)	4 (9.8)	0.573
Subclavious Muscle	1 (2.4)	0 (0)	1.000	0 (0)	1 (2.4)	1.000
Serratus Anterior Muscle	4 (9.8)	0 (0)	0.573	0 (0)	4 (9.8)	0.573
Deltoid Muscle	10 (24.4)	1 (10)	0.428	1 (10)	10 (24.4)	0.428
Shoulder Girdle Posterio Muscle						
Trapezius Muscle	2 (4.9)	1 (10)	0.488	0 (0)	3 (7.3)	1.000
Latissum Dorsi Muscle	0 (0)	0 (0)	NA	0 (0)	0 (0)	NA
Levator Scapula Muscle	1 (2.4)	1 (10)	0.357	0 (0)	2 (4.9)	1.000
Rhomboid Major Muscle	0 (0)	0 (0)	NA	0 (0)	0 (0)	NA
Rhomboid Minor Muscle	0 (0)	0 (0)	NA	0 (0)	0 (0)	NA
Teres Major Muscle	1 (2.4)	1 (10)	0.357	0 (0)	2 (4.9)	1.000
Teres Minor Muscle	1 (2.4)	1 (10)	0.357	0 (0)	2 (4.9)	0.357
Rotation Cuff Muscle						
Supraspinatus Muscle	17 (41.5)	4 (40)	1.000	4 (40)	17 (41.5)	1.000
Infraspinatus Muscle	10 (24.4)	5 (50)	0.135	3 (30)	12 (29.3)	1.000
Subscapularis Muscle	10 (24.4)	3 (30)	0.701	3 (30)	10 (24.4)	0.701
Arm Posterior Muscle						
Triceps Muscle	1 (2.4)	1 (10)	0.357	2 (20)	0 (0)	0.035
Anconeus Muscle	0 (0)	0 (0)	NA	0 (0)	0 (0)	NA
Arm Anterior Muscle						
Brachialis Muscle	1 (2.4)	0 (0)	1.000	0 (0)	1 (2.4)	1.000
Coracobrachialis Muscle	0 (0)	0 (0)	NA	0 (0)	0 (0)	NA
Neck Lateral Muscle						
Scalene Muscle Ant	0 (0)	1 (10)	0.196	0 (0)	1 (2.4)	1.000
Scalene Muscle Med	0 (0)	1 (10)	0.196	0 (0)	1 (2.4)	1.000
Scalene Muscle Post	0 (0)	1 (10)	0.196	0 (0)	1 (2.4)	1.000

Note: Results are reported as relative frequencies and percentages. N/A: Statistical Test Not Applicable

Table 18 – Brachial Nerve Root Diameter, Area and Signal Intensity – Control vs. PTS*

		Total (n = 76)			Healthy Subjects (CTL) (n = 25)			Patients with PTS (PTS) (n = 51)		
		CSA (mm)	AR (mm^2)	MED	CSA (mm)	AR (mm^2)	MED	CSA (mm)	AR (mm^2)	MED
C5	Right	3.3±0.9 (2-5.4) [3,2.7-3.7]	17.9±7.5 (9.7-40.8) [15.4,12.6-21.3]	151.5±68.3 (68-387) [138,104-158.5]	2.8±0.4 (2-3.4) [2.9,2.4-3]	14.4±3.3 (9.7-22.3) [14.4,11.7-16.3]	131±41.8 (68-215) [123,101-153]	4.4±0.7 (3.2-5.4) [4.5,3.9-5.1]	25.9±8.3 (15.1-40.8) [24.6,19-29.8]	197.9±93.4 (86-387) [153,137-283]
	Left	3.2±0.8 (1.9-4.9) [3.1,2.6-3.9]	15.7±5.7 (7.2-35.5) [13.8,11.9-18.4]	148±59.4 (52-365) [141,106.5-178]	2.7±0.4 (1.9-3.3) [2.7,2.4-3]	12.8±2.6 (7.2-19.8) [12.8,11.7-13.8]	129.4±42.1 (52-213) [124,100-161]	4.1±0.7 (2.7-4.9) [4.2,3.5-4.7]	20.5±6.3 (11.5-35.5) [19.5,17-22.1]	178.9±71.6 (102-365) [164,117-215]
C6	Right	3.9±0.9 (2.3-5.6) [3.6,3-4.6]	24.6±9.8 (9-49.1) [21.7,17.3-31.2]	183.4±60.4 (94-370) [175,139-212]	3.2±0.5 (2.3-4.4) [3.3,2.9-3.5]	18.6±4.8 (9.9-31.2) [18.5,15.2-20.5]	167.6±44.6 (99-280) [156,133-201]	4.7±0.7 (3.2-5.6) [4.9,4.2-5.2]	32.1±9.1 (9-49.1) [31.5,27.2-38.7]	203.2±72 (94-370) [180,161.5-256.5]

	Left	3.6±0.8 (2.1-5.3) [3.4,3-4]	21.8±8.5 (8.5-45.7) [20.4,15.3-25.9]	181.9±57.2 (81.3-325) [182.5,132-220.5]	3.1±0.4 (2.1-4) [3.1,2.8-3.3]	17.5±4.6 (8.5-25.6) [16.5,14.7-20.6]	175.2±54.5 (81.3-275) [170,131-211]	4.3±0.7 (3.3-5.3) [4.1,3.7-4.9]	27.4±9.3 (11.2-45.7) [28.2,18.6-34]	190.7±61 (87-325) [194,146-239]
C7	Right	3.7±1 (2-6.4) [3.3,3-4.3]	24.3±10.6 (10.1-54.4) [22.9,14.7-31]	189.4±61 (85-348) [187,148-211]	3.1±0.5 (2-4.9) [3,2.9-3.2]	19.1±6.4 (10.1-31.7) [20.3,13.3-23.3]	172.4±46.7 (101-316) [173,136-205]	4.8±0.8 (3.3-6.4) [4.7,4.2-5.5]	34.3±10.1 (17.3-54.4) [34.2,27.7-37.4]	222.2±73.1 (85-348) [216,170-276]
	Left	3.8±1 (2.1-6.1) [3.6,3-4.5]	23.7±9 (10-44.2) [24,16.4-29]	188.4±52.8 (87-297) [183,150-222]	3.2±0.6 (2.1-4.5) [3.1,2.8-3.5]	19.2±6.3 (10-31.4) [18.7,14.1-25.7]	177.4±48.2 (87-285) [181,144-204]	4.8±0.6 (3.7-6.1) [4.9,4.4-5.2]	31.7±7.3 (19-44.2) [32.2,26.2-36.7]	208±56.6 (114-297) [203.5,163-250]
C8	Right	3.7±0.9 (2.1-5.6) [3.7,3-4.5]	25.6±9.7 (10.7-49.8) [25,17.2-31.1]	186.2±63.3 (72-309) [184,136-245]	3.2±0.6 (2.1-4.2) [3.2,2.9-3.6]	20.5±5.9 (10.7-32.9) [19,16.1-25.4]	174.5±63.1 (72-300) [172,117-219]	4.7±0.5 (3.8-5.6) [4.7,4.5-4.9]	34.6±8.5 (19.6-49.8) [34.2,28.3-41.1]	207.2±60.3 (130-309) [203,155-245]
	Left	3.7±1 (2.2-6.4) [3.3,3.1-4.5]	24.5±10 (10.7-50.5) [22.3,18.1-31.9]	185.8±61.8 (88-366) [180,137-217]	3.2±0.4 (2.2-3.9) [3.1,3-3.4]	20±6.2 (10.7-36.2) [19.5,15.3-22.3]	172.9±47.3 (88-253) [165,137-206]	4.9±0.9 (3.2-6.4) [4.9,4.5-5.5]	34±9.9 (16.9-50.5) [34.8,26.1-39.8]	212.5±80.4 (116-366) [186,149-289.5]

* Results are reported as means ± standard deviation, with the range in round brackets. Results in squared brackets are median and interquartile range.

Table 19 – Brachial Nerve Root Diameter, Areas and T2 Signal Intensity – Comparison between pathological and non-pathological nerve roots in patients with PTS*

		Total Nerve Roots (n = 412)			Non-Pathological Nerve Roots (no PTS) (n = 290)			Pathological Nerve Roots (PTS) (n = 122)		
		CSA (mm)	AR (mm^2)	MED	CSA (mm)	AR (mm^2)	MED	CSA (mm)	AR (mm^2)	MED
C5	Right	4±0.8 (2.4-5.6) [3.9,3.4-4.5]	21.3±7.9 (7.9-40.8) [20,15.6-26.6]	178.5±77.4 (66-387) [158,121-209]	3.8±0.7 (2.4-5.6) [3.9,3.4-4.3]	20±7.3 (7.9-38.7) [19.5,14.6-25.2]	173±72.7 (66-375) [164,120-197]	4.4±0.7 (3.2-5.4) [4.5,3.9-5.1]	25.9±8.3 (15.1-40.8) [24.6,19-29.8]	197.9±93.4 (86-387) [153,137-283]
	Left	3.9±0.6 (2.4-5.3) [4,3.5-4.3]	20.7±6.2 (7.3-35.5) [20.3,17-23.5]	169.6±55.6 (77-365) [158,127-211]	3.9±0.6 (2.4-5.3) [3.9,3.5-4.2]	20.7±6.3 (7.3-32.8) [20.3,16.3-25.3]	165.7±48.8 (77-261) [150,127-211]	4.1±0.7 (2.7-4.9) [4.3,3.6-4.7]	20.5±6.1 (11.5-35.5) [20.1,17.1-21.8]	178±69.3 (102-365) [164,128.5-205]
C6	Right	4.3±0.8 (2.6-7) [4.3,3.8-4.8]	26.9±9.5 (9-49.1) [26.1,20.9-31.8]	203.4±69.6 (94-426) [198,154-240]	4.1±0.8 (2.6-7) [4.1,3.4-4.5]	23.3±8.1 (11.3-47.7) [22.6,18-27.5]	203.6±69.2 (97-426) [199,151-225]	4.7±0.7 (3.2-5.6) [4.9,4.2-5.2]	32.1±9.1 (9-49.1) [31.4,27.1-38.7]	203.2±72 (94-370) [180,161.5-256.5]
	Left	4.2±0.6 (2.9-5.9) [4.3,3.8-4.5]	25±8.3 (10.9-45.7) [23.8,18.6-31.6]	200.8±69.2 (26.2-409) [191,159-239]	4.2±0.7 (2.9-5.9) [4.3,4-4.5]	23.2±7.3 (10.9-37) [22.8,18.2-28.9]	212.6±67.3 (106-409) [191,168-271]	4.3±0.7 (3.3-5.3) [4.3,3.7-4.9]	27.7±9.1 (11.2-45.7) [29.2,20.4-33.5]	182.5±69.8 (26.2-325) [186,134.5-231.5]
C7	Right	4.3±0.8 (2.7-6.4) [4.3,3.9-4.8]	28.3±9.2 (12-54.4) [28,20.3-34.2]	220.1±67.2 (85-406) [215,177-268]	4.1±0.7 (2.7-5.7) [4.1,3.7-4.5]	26.2±7.9 (12-45.2) [25.6,19.5-32]	219.4±66 (90-406) [214,179-258]	4.8±0.8 (3.3-6.4) [4.7,4.2-5.5]	34.3±10.1 (17.3-54.4) [34.2,27.7-37.4]	222.2±73.1 (85-348) [216,170-276]
	Left	4.4±1 (2.9-8.8) [4.3,3.8-4.5]	26.4±7.3 (12.3-47.2) [26.2,21.8-30.3]	208±63.3 (50.5-415) [200,163-247]	4.2±1 (2.9-8.8) [4,3.8-4.4]	24.3±6.4 (12.3-47.2) [23.4,21.2-27.3]	212.4±61.6 (135-415) [199,170-243]	4.8±0.6 (3.7-6.1) [4.8,4.4-5.2]	31.3±7.1 (19-44.2) [30.6,26.2-36.7]	197.5±68.1 (50.5-297) [201,150-250]
C8	Right	4.4±0.6 (3.2-6) [4.3,3.9-4.8]	30.1±8.6 (16.2-49.8) [28.4,22.4-37.3]	220.5±75.5 (103-440) [203.5,163-276]	4.3±0.6 (3.2-6) [4.2,3.9-4.6]	28.3±8.1 (16.2-45) [27.1,21.8-35.2]	225.7±80.8 (103-440) [204,163.5-281.5]	4.7±0.5 (3.8-5.6) [4.7,4.5-4.9]	34.6±8.5 (19.6-49.8) [34.2,28.3-41.1]	207.2±60.3 (130-309) [203,155-245]
	Left	4.3±0.8 (2.8-6.4) [4.3,3.8-4.7]	27.5±9.8 (12.7-51.1) [26.1,20.5-34.5]	213.9±68.1 (98-409) [196,169-257]	4.1±0.6 (2.8-5.7) [4.2,3.7-4.3]	24.9±8.1 (12.7-51.1) [24.8,18.6-29.2]	215.7±65.4 (98-409) [203,175-253]	5±1 (3.2-6.4) [5,4.5-5.6]	35.2±10.5 (16.9-50.5) [35,26.6-42.1]	208.5±78.3 (116-366) [180,161-284]

* Results are reported as means ± standard deviation, with the range in round brackets. Results in squared brackets are median and interquartile range.